Engineered adhesion peptides for functionalization of natural surfaces, polymers, and metal alloys

Von der Fakultät für Mathematik, Informatik und Naturwissenschaften der RWTH Aachen University zur Erlangung des akademischen Grades einer Doktorin der Naturwissenschaften genehmigte Dissertation

vorgelegt von

Lina Apitius (geb. Weber)

Master of Science (M.Sc.) Biotechnologie

aus Mettingen, NRW

Berichter:

Univ.-Prof. Dr. rer. nat. Ulrich Schwaneberg

Univ.-Prof. Dr. rer. nat. Andrij Pich

Tag der mündlichen Prüfung:

18.01.2019

Alice laughed. 'There's no use trying,' she said. 'One can't believe impossible things.'

'I daresay you haven't had much practice,' said the Queen. 'When I was your age, I always did it for half-an-hour a day. Why, sometimes I've believed as many as six impossible things before breakfast.'

Lewis Carroll (1865) *Alice's Adventures in Wonderland*

I. Publications and Patents

Publications

Apitius L, Buschmann S, Schönauer D, Bergs C, Pich A, Jakob F, and Schwaneberg U (2019). Biadhesive peptides for assembling of bare-metal implants and compound loaded micro-containers. → Submitted to Macromolecular Bioscience

Apitius L, Rübsam K, Jakesch C, Jakob F, and Schwaneberg U (2019). Ultra-high-throughput screening system for directed polymer binding peptide evolution. → Submitted to Biotechnology and Bioengineering

Islam* S & **Apitius* L**, Jakob F, and Schwaneberg U (2019). "Targeting microplastic particles in the void of diluted suspensions." Environment International 123: 428-435.
*shared first authorship

Rübsam* K & **Weber* L**, Jakob F, and Schwaneberg U (2018). "Directed evolution of polypropylene and polystyrene binding peptides." Biotechnol Bioeng 115(2): 321-330.
*shared first authorship

Patents

Mussmann N, Wieland S, Degering C, Zimmermann W, Wei R, Jakob F, Islam S, Schwaneberg U, **Weber L**, Rübsam R, Eidener J, Haarmann T, Lorenz P, Schwerdtfeger R. 2018. Mittel erhaltend PolyesteraseI. DE 2018P35186

Schwaneberg U, Sözer S, Mertens M, Davari MD, Jakob F, Islam S, **Weber L**. 2018. Fusion Peptides or Proteins, their Use, and Systems and Kits based thereupon, for the Separation and/or Detection of Plastics, particularly of Microplastics. EP18178726.8.

Publications in collaboration projects

Schwinges P, Pariyar S, Jakob F, Rahimi M, **Apitius L**, Noga G, Hunsche M, Schmitt L, Langenbach C, Schwaneberg S, and Conrath C (2018). A bifunctional dermaseptin-thanatin dipeptide functionalizes crop surface for sustainable pest management. → Submitted to RSC Green Chemistry

Pariyar S, Jakob F, **Apitius L**, Schwaneberg U, Hunsche M, and Noga G (2018). Anchor peptides as innovative adjuvants reduce rain wash-off, but do not impair photosynthetic activity or cause oxidative damage in apple leaves. → Submitted to ActaHort IHC2018

Frauenkron-Machedjou VJ, Fulton A, Zhao J, **Weber L**, Jaeger KE, Schwaneberg U, and Zhu L (2018). Exploring the full natural diversity of single amino acid exchange reveals that 40–60% of BSLA positions improve organic solvents resistance. Bioresour. Bioprocess. (2018) 5: 2.

II. Table of contents

III Abstract

Plastics or synthetic organic polymers have been produced in large scale since the 1950´s. Until today, roughly 8300 million metric tons of virgin plastics have been produced for an uncountable number of applications. Despite favorable bulk properties, the surface characteristics of polymers are often not ideal for intended applications (e.g., wettability, anti-static, anti-fouling, and bio-compatibility) and are mainly engineered by physical or chemical means. UV-radiation, flame/plasma or wet-chemical treatments often generate large volumes of toxic waste or safety hazard.

Anchor peptides enable a biological surface functionalization at very high densities (monolayers) of peptides. By the use of anchor peptides multiple functionalities (e.g., NH_2^-, COOH- or OH-groups) can be introduced simultaneously. Anchor peptides are highly diverse in length, secondary structure, binding affinity as well as binding strength. In order to identify suitable target binder, a general anchor peptide platform was established using the fluorescent eGFP as reporter protein in binding studies. Identified binders need to perform under application conditions, therefore, anchor peptides have to be adapted by directed peptide evolution. Anchor peptides are very short in length (12-100 amino acids) and conventional diversity generation is challenging due to a low mutational rate of existing methods. To overcome this drawback, a Peptide-Polymer *evo*lution protocol (PeP*evo* protocol) was established. The anchor peptide Tachystatin A2 was randomized by epPCR employing a very high mutation frequency (59 mutations/kb) and was evolved for improved polystyrene binding strength. The fusion partner eGFP was used to quantify peptide binding in a micro-titer plate-based fluorescent assay. Therefore, the key performance parameters protein concentration, standard deviation and selection pressure were optimized. The anionic surfactant sodium dodecylbenzenesulfonate (LAS; 0.5 mM) was applied as selection pressure to identify improved polystyrene-binding Tachystatin A2 variants. Finally, the PeP*evo* protocol yielded an up to six-fold stronger polystyrene-binder in the presence of 0.5 mM LAS in one round of directed evolution.

One bottleneck of directed evolution is the screening throughput that is needed to analyze a meaningful amount of generated peptide diversity. An *E. coli* cell surface display technology for the engineering of anchor peptides was development, that enabled screening of large libraries (>10^6). The polypropylene-binding peptide LCI was fused as a

passenger peptide to the cell-surface presented esterase A. LCI immobilized the *E. coli* cells on polypropylene beads and improved binding variants were enriched from culture broth. In a semi-rational approach, five LCI positions were saturated simultaneously. One round of directed evolution yielded an up to twelve-fold stronger polypropylene binder in the presence of 0.125 mM LAS.

The usage of polymers for medical applications (e.g., stents or catheters) is often hampered by a low bio-compatibility. Medical implants often cause severe infections in patients and are therefore often coated with drug- or antibiotic-releasing systems. The versatility of anchor peptides facilitates the generation of biadhesive peptides that bind chemically and structurally different surfaces whereby the biadhesive peptide functions as a glue. A biadhesive peptide was generated that was composed of one stainless steel binding anchor peptide and one polycaprolactone binding anchor peptide. The generated biadhesive peptide Dermaseptin S1-Domain Z-LCI immobilized antibiotic-loaded polycaprolactone micro-containers on stainless steel surfaces, enabling the construction of drug eluting bare-metal stents. The antimicrobial activity of kanamycin-releasing polycaprolactone coated stainless steel wires was confirmed by growth inhibition of *E. coli* cells.

Microplastics lingering in the environment are of increasing concern for human health. Enzymatic degradation of microplastic particles such as polyurethane is a promising strategy to convert plastic waste into carbon dioxide, monomers, and valuable compounds. A fusion protein composed of the polyester-polyurethane degrading cutinase Tcur1278 and the anchor peptide Tachystatin A2 was generated. Tachystatin A2 directed the enzyme (Tcur1278) to polyester-polyurethane nanoparticles. The anchor peptide enhanced the degradation kinetics and reduced the degradation half-life of the polymer significantly (both up to six-fold) in highly diluted suspensions at ambient temperature. The utilization of tunable anchor peptides enables a targeted microplastic degradation e.g., in wastewater treatment plants.

1 Introduction

1.1 Surface engineering of polymers

Polymers are mainly selected for a given application due to their favorable bulk properties like thermal stability, mechanical strength or solvent resistance, even though the surface characteristics are not ideal for the intended application (Penn and Wang 1994). Therefore, polymer surfaces are often engineered. Physical, chemical or biological treatments modify polymer surfaces (see Figure 1) by the introduction of functional groups to prepare substrates with controllable structures adjusting surface properties (e.g., adsorption, adhesion, wettability, anti-static, friction or interaction with biological environment) (Chen and McCarthy 1998). Surface engineering finds numerous applications in automotive, electronic, biomedical, power, and construction industries (Farris, Pozzoli et al. 2010). Chemical functionalization techniques include a modification of the chemistry of a target material (e.g., organic/ inorganic coatings, bio-functionalization or biomimetic modification) whereby physical functionalization techniques alter the surface properties only (Clauser, Gester et al. 2016). However, most of the surface engineering approaches are expensive, restricted to batch processing, safety hazards, or generating large volumes of solvent waste (Fabbri and Messori 2017).

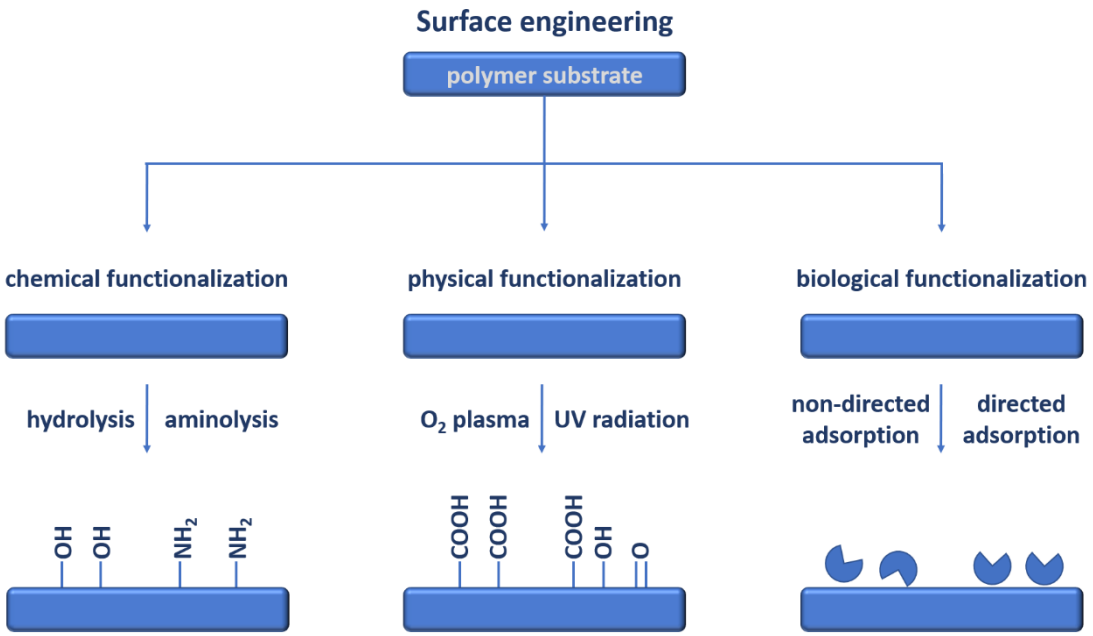

Figure 1: Engineering of polymer surfaces. Surfaces can be engineered by chemical, physical or biological treatments to introduce desired functional groups.

1.1.1 Chemical surface engineering

Functional coatings must satisfy several requirements, including a tight adhesion to the targeted substrate as well as desired mechanical properties. Many coatings have been designed with scratch and wear resistance, tunable hydrophobicity or lipophobicity, antibacterial or antifouling properties, antistatic properties, and chemical resistance. In order to produce coatings with a high suitability, the temperature range of applied coating techniques have to match the low temperature range to which polymers can be exposed without physical deformation or chemical degradation (Fabbri and Messori 2017). Chemical surface treatment techniques involve a careful control of the surface chemical environment or the addition of specific chemical species for the modification of targeted surfaces (Wei, Xu et al. 2009).

Chemical vapor deposition (CVD) a commonly used processes to coat metallic or ceramic compounds, but can also be applied for the functionalization of polymers. Plenty of CVD processes exist, such as atmospheric pressure CVD, metal-organic CVD, low pressure CVD, laser- or photo- CVD, chemical vapor infiltration or plasma-assisted CVD (Makhlouf 2011). Monomers that are delivered to the surface through the vapor phase undergo a simultaneous polymerization and form thin films. CVD enables a coating of insoluble polymers like polytetrafluoroethylene (PTFE), since macromolecules do not need to be dissolved and therefore prevents solvent damage to the substrate. In CVD, de-wetting and surface tension effects are negligible and CVD coatings can be applied to any geometry of target substrate. This enables the application of CVD for numerous substrates (e.g., organic, inorganic, rigid, flexible, planar, three-dimensional, dense, or porous) (Asatekin, Barr et al. 2010).

The **sol–gel process** is a wet-chemical technique to obtain inorganic and hybrid organic-inorganic polymers (Kloskowski, Pilarczyk et al. 2010). The process is carried out at room temperature and allows the synthesis of multifunctional coatings, such as scratch and wear resistant coatings, antibacterial coatings, antistatic coatings, hydrophobic and oleophobic coatings or coatings with improved adhesion and wettability (Schottner 2001). Polymers synthesized by sol-gel processes can be physically immobilized on a carrier (Allabashi, Arkas et al. 2007), as well as in monolithic sorbents (Yu, Geng et al. 2008). Polymers with various shapes (e.g., porous structures, thin fibers, dense powders and thin films) can be functionalized applying a sol-gel process. A sol-gel process is based on the

hydrolysis of suitable precursors (e.g., tetramethoxysilane (TEOS) or metal alkoxides $M(OR)_x$) and a subsequent condensation reaction releasing water or an alcohol. Alkoxyl groups are substituted by hydroxyl groups. A condensation of partially hydrolyzed alkoxides follows the substitution reaction. A sol is constituted by an increase in polymer chain length and a formation of nanoparticles in a liquid phase. Agglomeration of sol particles are formed due to van der Waals forces or hydrogen bonds between the polymer chains. A three dimensional network, the so-called gel is formed. Gel systems applied for materials synthesis are commonly based on covalent interactions leading to an irreversible gelation (Ruckenstein and Rao 1986, Kloskowski, Pilarczyk et al. 2010).

Hydrolysis requires an excess of water and/or the use of an acidic or alkaline hydrolysis catalyst (acetic acid or NaOH). In an alkaline hydrolysis reaction, the polymer substrate becomes negatively charged and the electrostatic potential increases with degree of conversion, whereas in an acidic hydrolysis reaction, interactions between functional acid and amide groups enable a formation of intramolecular imide groups (Moens and Smets 1957). Poly(lactic-co-glycolic acid) (PLGA) is used as a scaffold in soft tissue engineering (e.g., breast reconstruction) and can be functionalized by acidic hydrolysis. Acidic hydrolysis allows an introduction of carboxylic acid functional groups on the surface of thin PLGA films with minimal erosion (Croll, O'Connor et al. 2004). Alkali hydrolysis was applied, for instance, to modify polyesters such as polycaprolactone (PCL) (Sun and Önneby 2006).

Aminolysis is a commonly applied method to introduce primary and secondary amine groups to the surface of ester-containing polymers (e.g., PLGA or polymethyl methacrylate (PMMA)) (Croll, O'Connor et al. 2004, Xu, He et al. 2006). An aminolysis reaction is a nucleophilic substitution at the carbonyl carbon forming a tetrahedral intermediate formation. Thereby the NH_2 group can be introduced by reversible addition−fragmentation chain transfer (RAFT) polymerization (Xu, He et al. 2006). Subsequently, functional moieties can be introduced to these active sites (“conjugated to” or “grafted from”) (Zhu, Mao et al. 2013). Employing aminolysis of the RAFT-end groups and simultaneous thiol-ene reactions, polymers like PMMA were bio-functionalized with a methacrylate-modified mannose or a maleimide-modified biotin (Boyer, Granville et al. 2009).

Ultraviolet (UV)-curable coatings are light induced polymerizations of liquid polymers into crosslinked solid polymer films (Sangermano, Roppolo et al. 2015). Solvent-free UV-curing methods are eco-efficient and thus reduce significantly the usage of volatile organic compounds in industrial plastic coating applications (Schwalm, 2007; Bhattacharya, 2006). UV-curable monomers and oligomers are mainly acrylic, methacrylic, epoxy, and thiol-ene based (Fabbri and Messori 2017). UV-curable coatings find numerous applications in automotive gloss-coatings, flooring varnish, scratch resistant coatings, flexible electronics, conductive coatings, light-emitting diodes, lasers, fluorescence sensors, display devices and in heterogeneous photo-catalysis (Sangermano, Roppolo et al. 2015). A UV-curing process is based on the interaction of UV light with a photo-initiator generating radical or cationic species. This leads to a chain-growth polymerization or cationic ring opening polymerization (Sangermano, Roppolo et al. 2015). “Bottom-up” or “top-down” approaches are applied as UV-curing methods. In “bottom-up” approaches free surface is available, whereas in “top-down” approaches the accessibility of free surface is constrained (Cho, Lee et al. 2015).

1.1.2 Physical surface engineering

Inert polymers like polyethylene (PE), polypropylene (PP) and polystyrene (PS) have quite low surface energies and need to be treated prior to processes in industry (Chan 1999). Physical forces (e.g., corona discharge, flame treatment, plasma-assisted coating, vapor based coatings, radiation-induced surface modification, and self-assembled monolayers) are applied to introduce oxygen-containing functional groups on to polymer surfaces (Fabbri and Messori 2017).

Corona discharge treatment of plastic films is utilized to increase the surface adhesion and wettability of a polymer surface by oxidation and introduction of OH and COOH groups. In corona discharge treatments, a high voltage is applied across electrodes ionizing the surrounding air. An atmospheric pressure plasma is formed that is called a corona discharge (Chan 1999). The polymer particle energies are around 10 electron-volts (eV), which is higher than the energies of typical covalent bonds (carbon-carbon bonds: 2.54 eV and carbon-hydrogen bonds: 3.79 eV). This energy allows the formation of free radicals on the treated surface (Carley James and Kitze 1980). The set-up for corona

discharge treatments is very simple and cost-effective, but the applications are limited for 3-D structures and fibrous materials like woven fabrics.

Corona discharge treatment and **flame treatment** are the most extensively used methods for surface activation of polyolefin substrates. The flame treatment technique can be applied for modifying film surfaces as well as tridimensional objects (Farris, Pozzoli et al. 2010) and enhances the adhesion properties of polymers before coatings are applied. During combustion, a fuel (e.g., hydrocarbon) and an oxidant (e.g., oxygen in the air) produce heat and a flame. Chemical species migrate within the flame resulting in a subsonic wave forming many active radical species (Glassman and Yetter 2008, Farris, Pozzoli et al. 2010)

Plasma-assisted coating methods are typically performed utilizing oxygen, ammonia, or air derived plasma to introduce carboxyl groups (C-O, C=O, and COOH) or amine groups on the targeted polymer surface. Oxygen-plasma is used to increase the surface energy of polymers, whereas fluorine-plasma treatment is used to decrease the surface energy improving chemical inertness of the polymer. A cross-linking of functional groups at a polymer surface is introduced by a treatment with an inert-gas plasma (Fabbri and Messori 2017). The destruction of polymers during treatment is prevented by the use of non-thermal or cold plasmas for surface modification (Desmet, Morent et al. 2009). Thin-film coatings supplied by plasma treatments can enhance biocompatibility or controlled drug release (Yoshida, Hagiwara et al. 2013).

Radiation-induced surface modification uses a radiation source to emit energy travelling through media and space. The radiation is emitted from atoms (electrons dropping to lower energy levels) and is divided into ionizing and non-ionizing radiation (Jaganathan, Balaji et al. 2015). Several types of radiation are used to functionalize polymer surfaces (e.g., γ-Irradiation, UV-irradiation, laser-induced surface modifications, and ion beam based processes) (Fabbri and Messori 2017). The treatment of polymers with high-energy irradiation can lead to a recombination (cross-linking) or degradation of the polymer (cleavage of polymer chains). Higher-energy radiation is therefore not recommended for the modification of most biodegradable polymers (Bailey, Geurts et al. 2013).

In biological environments the material performance for a specific application is dependent on its surface properties and on the required chemical, physical, biological,

and mechanical properties (Alves, Pinto et al. 2011). Often **grafting** technologies are used to introduce functional properties to a given surface (e.g., polymer brushes) (Milner 1991). A formation of polymer brushes on a surface is achieved by either "grafting to" or "grafting from" approaches (Raynor, Capadona et al. 2009). Therefore, the surface of a polymer has to be activated; for instance, the surface of a thermoplastic polyurethane (TPU) can either be activated by plasma or by ultra-violet (UV) irradiation (Alves, Pinto et al. 2011). Inert gas plasma introduces non-functional radicals that react, if subjected to the atmosphere or to O_2, to peroxides and hydroperoxides (Fabbri and Messori 2017). A limitation of "grafting to" technologies is a steric hindrance of the polymer chain. Already attached chains might block the access for available binding sites on the surface. Consequently, polymer chains are often forming thinly packed layers on the surface. In "grafting from" approaches functional chain growth polymerizations are initiated from functional groups on a surface, resulting in a higher density of polymer chains on a substrate (Raynor, Capadona et al. 2009).

Vapor based coatings, like physical vapor deposition (PVD), involve atom-by-atom or molecule-by-molecule transfer of material under vacuum conditions, whereby the precursors are deposited in solid form to the vapor phase (e.g., metallization of polymer packaging films) (Wei, Xu et al. 2009). PVDs are alternatives for wet chemical deposited coatings (Selvakumar and Barshilia 2012) and have been used to generate solar selective coatings (Makhlouf 2011) and for the functionalization of textiles (corrosion-resistant and wear-resistant coatings) (Wei, Xu et al. 2009). One frequently used PVD technology in industry is sputtering. During the sputtering process, energetic ions bomb atoms from a solid target material. These released atoms condense on the substrate and form a thin layer (Tanaka, Kasahara et al. 2000).

Self-assembled monolayers (SAM) are traditionally used to engineer inorganic surfaces. SAMs are applied for bioengineering, biomaterials, and biomimetics in cases where a deformability and a degree of mechanical flexibility of the support is needed (e.g., implantable biomaterials) (Chaudhury 1995, Fabbri and Messori 2017). A SAM is formed by functional organic molecules, in solution or vapor phase, that adsorb and spontaneously organize into a single layer on a surface support (Raynor, Capadona et al. 2009). The generation of SAMs (on a PE support) is performed in four steps (Chaudhury 1995). Polar functionalities are introduced onto the PE surface by plasma oxidation. A thin

silicate layer is formed onto this oxidized surface by adsorption and hydrolysis of $SiCl_4$. Monolayer films are formed on the silicate-coated PE surface by exposure to a vapor of alkyltrichlorosilanes. If required, functionalities such as amine, ethylene oxide, carboxylic acid, and sulphonate groups can be introduced in a free radical process (Chaudhury 1995).

1.1.3 Biological surface engineering

The application of polymers as biomaterials requires an improved biocompatibility and the possibility of interactions with complex biological environments (Fabbri and Messori 2017). Therefore, many natural materials have been introduced onto polymer surfaces (e.g., chitosan, gelatin, collagen, alginate, cell-recognizing peptides and proteins). Coating technologies are based on adsorption, entanglements, or covalent linkages (Sun and Önneby 2006). Biocompatible materials need either to repulse biological materials (platelets or bacteria; applies for catheters and blood tubes) or improve adhesion and proliferation (fibroblasts or endothelial cells; applies for wound healing and tissue regeneration) (Balaji, Jaganathan et al. 2015). The prevention of toxic chemicals as well as a usage of ecofriendly substances made biological methods a versatile tool for the improvement of biocompatibility of polymers. (Fabbri and Messori 2017).

Coatings with bio-polymers such as poly- or oligosaccharides are investigated to develop bio-based "green" environmentally friendly materials (e.g., poly-/ oligosaccharides-based block copolymers (BCP)). Poly-/oligosaccharidic blocks introduce hydroxyl groups to the BCP and enable an interaction with further molecules (e.g., 4,4'-bipyridine and 1-aminopyrene) that can be used for photonic and memory devices (Noronha, Otsuka et al. 2017). Hybrid BCPs find further applications in antifouling and antibacterial coatings, drug delivery (Lo, Chen et al. 2009) and biosensors (Ayyub, Sekowski et al. 2011).

In marine environment, antifouling coatings are widely applied. Surface properties of materials are modified in non-biocidal ways to minimize adsorption and adhesion. The hydrophilic coatings are produced by the introduction of carbohydrates. Carbohydrates are more stable to oxidation than ethylene glycols, expanding the life time of coatings. SAMs of mono-and disaccharides formed on gold surfaces reduced fouling from protein solutions (Ederth, Ekblad et al. 2011). Polymer and stainless steel surfaces can be functionalized with lactose by aryldiazonium chemistry to reduced adhesion of fouling

promoters in a marine environment. These carbohydrates coatings can be easily applied from aqueous solutions via spray or dip coating (Myles, Haberlin et al. 2018).

Protein coatings are utilized to modulate physical and functional surface properties by the introduction of film-forming biopolymers (proteins) that can be combined with plasticizers or other components. Many mechanisms, such as formation of covalent bonds (disulfide bonds or cross-linking), electrostatic, hydrophobic, or ionic interactions are involved in film formation. These mechanisms are dependent on pH, salt addition, heating, enzymatic action or drying effects (Chiralt, González-Martínez et al. 2018).

Fibrous mats are highly porous polymer nanofibers that are used for biological scaffolds. They allow a flux of waste products as well as nutrients and can provide topological stimuli to cells (e.g., periodontal ligament stem cells) in tissue culture (Kim, Kang et al. 2016). Therefore, releasable agents (e.g., fibroblast growth factor-II or bovine serum albumin (BSA)) or surface anchored moieties (peptide and protein sequences) are introduced to direct cell phenotype, proliferation, and migration (Jordan, Viswanath et al. 2016). Micron-sized polymersomes were functionalized with antibodies binding to vascular cell adhesion molecules for vascular targeting. The polymersomes were functionalized with an anti-ICAM-1 antibody, using modular biotin−avidin chemistry to bind the Intercellular Adhesion Molecule-1, which is a target for vascular delivery (Lin, Ghoroghchian et al. 2006).

The development of biosensors and diagnostic microarrays also relies on bioactive proteins attached to surfaces. A functional soybean peroxidase was covalently attached to a PS surface using plasma immersion ion implantation for microarray applications (MacDonald, Morrow et al. 2008). Biomolecules can be introduced to transducer element for instance by biotin-derivatized poly(l-lysine)-grafted oligo-ethylene glycol (PLL-g-OEGx-Biotin) copolymers. The synthesized copolymers are cationic at physiology pH, therefore surface biotinylation can be achieved by electrostatic adsorption on negatively charged sensor surfaces. Biotin-streptavidin interactions allow a subsequent attachment of biotinylated receptors (Han, Wang et al. 2017).

Hydrophobins are a small cysteine-rich proteins with a length of around 100 amino acids (aa) and eight conserved cysteine residues forming four disulfide bonds. They are highly amphipathic and self-assemble to form monolayers on surfaces and can thereby alter the wettability of a surface (Sunde, Kwan et al. 2008). Self-assembled hydrophobin

monolayers on hydrophobic materials lower the free surface energy by increasing the hydrophilicity facilitating the dispersion of particles in water and prevent particle aggregation (Valo, Laaksonen et al. 2010).

Adhesive peptides found in nature (e.g., fibrin, fibronectin, and mussel foot proteins) inspired the generation of biocompatible interfaces and functional coatings. Already in the early 90´s, tissue adhesives like fibrin were used in surgery promoting wound closure and healing (Atrah 1994, Coulthard, Esposito et al. 2010). The natural adhesives are biocompatible and biodegradable and are therefore often applied in medical treatments (e.g., for implants and construction of tissue replacement). Nano-fibrous poly(l-lactide) membranes were modified with thin fibrin nano-coating to promote cell attachment and proliferation (Bacakova, Musilkova et al. 2016). Many peptide coatings are designed for re-endothelialization of bare-metal stents. The WKYMVm peptide, a selective formyl peptide receptor agonist, and hyaluronic acid have been applied to bare-metal stents by dip-coating in a primary layer. Sirolimus was consecutively sprayed onto the primary layer showing anti-restenosis effects (Jang, Bae et al. 2015, Sim and Jeong 2017). Nitinol foil, a nickel titanium alloy, was aminosilanized with N-[3-trimethoxysilyl-propyl]ethylenediamine and coated with six-arm star-shaped polyethylene glycol (star-PEG). Following, a dip-coating bio-functionalization with recombinant peptides P-selectin, RGD, and LL-37 was applied. A combination of these peptides for coating increased the adhesion of angiogenic early outgrowth cells (EOCs) accelerating re-endothelialization of stents (Soehnlein, Wantha et al. 2011). A cell-recognizing peptide was covalently attached to hydrolyze and carboxylated PCL surfaces through site-controlled coupling chemistry using PDEA. The arginine-glycine-aspartic acid (RGD) peptide has been proved to be biologically important for enhancing cell attachment onto biomaterial surfaces (Sun and Önneby 2006).

1.2 Material binding peptides

An adsorption-based coating of surfaces with proteins or peptides is often challenging due to a non-oriented protein adsorption to the target surface. This might lead to non-functional or reduced functional enzymes falsifying the sensitivity of assay applications (Kumada, Tokunaga et al. 2006). Binding peptides or anchoring motives as fusion partners that enable a directed enzyme immobilization are therefore of great importance for the construction of functionally coated surfaces (Care, Bergquist et al. 2015).

Material binding peptides are short and highly diverse peptides (Seker and Demir 2011), that have a high binding affinity to a target material (e.g., gold (Seker, Wilson et al. 2014), steel (Zuo, Ornek et al. 2005) or PS (Kumada, Kuroki et al. 2010)). Material binding peptides were applied for instance for directed enzyme immobilization (Zernia, Ott et al. 2016), improved nanomaterial biocompatibility (Zhang, Zheng et al. 2012), vaccine development (Ha, Shin et al. 2016), controlled growth of ZnO crystal structures (Togashi, Yokoo et al. 2011) or the formation of hybrid biomaterials (Nguyen, Botyanszki et al. 2014).

Material binding peptides are very efficiently identified by phage display technologies (Seker and Demir 2011, Care, Bergquist et al. 2015). The Ph.D.-12 library is a frequently used commercial phage library presenting 12-mer peptides for binding studies. The library has been employed for instance to identify PS binding peptides (Qiang, Sun et al. 2017), particulate matter binding peptides (Liang Alvin, Tanaka et al. 2017), and peptides used for bio-mining of MoS_2 (Cetinel, Shen et al. 2018). The peptide library variants are N-terminally fused to the minor coat protein (pIII) of an M13 phage. In a biopanning experiment, the surface-presented peptide variants are bound to a target surface and weakly attached peptide variants are washed off in subsequent washing steps. Bound phages are eluted from the target surface (pH shift) and amplified in *Escherichia coli* (*E. coli)* cells for sequence analysis (see Figure 2) (Smith and Scott 1993).

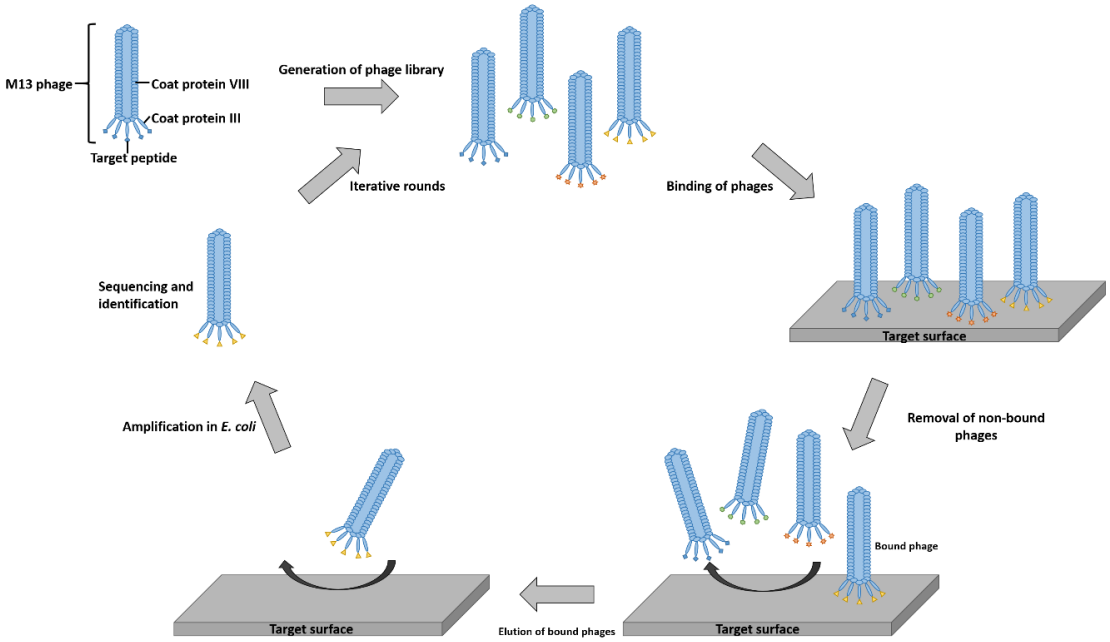

Figure 2: Scheme of a bio-panning experiment. The Ph.D.-12 Phage Display Peptide Library is a combinatorial library of random dodecapeptides (~10^9 variants). The peptides are N-terminally fused to the minor coat protein (pIII) of an M13 phage. The phages are bound to a target surface and non-binding phages are removed in a washing step. Bound phages are eluted from the target surface and amplified in *E. coli*. Beneficial binding peptide sequences are identified by sequencing. A biopanning experiment can be performed in iterative cycles to increase the binding affinity of peptides to the target surface. Scheme according to (Noren and Noren 2001).

1.2.1 Antimicrobial peptides

Antimicrobial peptides (AMPs) are small conserved amphipathic peptides that are produced throughout all kingdoms (Bulet, Stocklin et al. 2004). AMPs are components of the innate immune system and initiate adaptive immune host defenses against microbial pathogens (Oppenheim 2003). AMPs mainly act as antibiotics or fungicides but some AMPs also show for instance activity against viruses or cancer cells (see Figure 3). AMPs target the microbial cytoplasmic membrane and interact with the lipid membrane that is permeabilized subsequently. Besides a permeabilization of the membrane, some AMPs target intracellular mechanisms functioning as signaling molecules at sublethal concentrations (e.g., mitochondria, protein synthesis or DNA/RNA synthesis) (Malanovic and Lohner 2016, Sani and Separovic 2016).

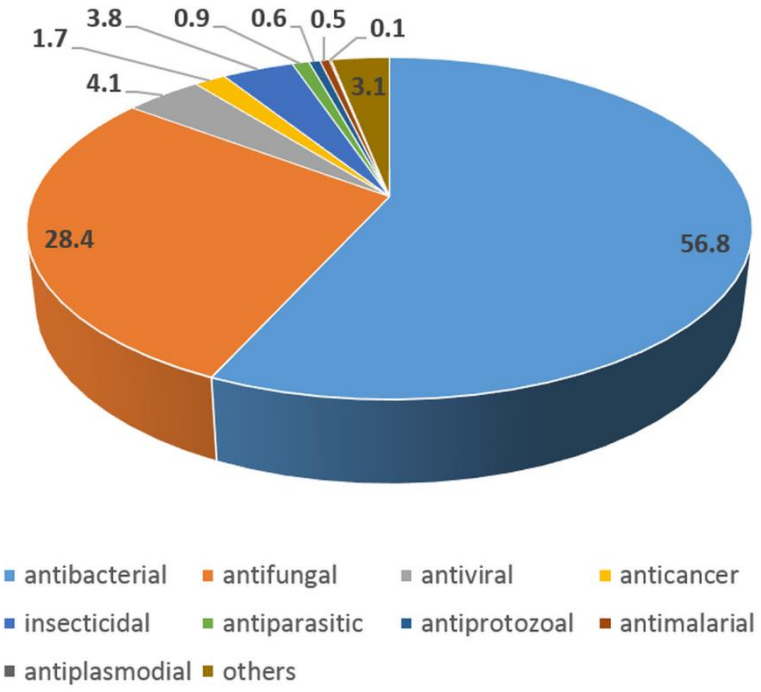

Figure 3: Distribution and abundance of antimicrobial peptides. AMPs are produced throughout all kingdoms with numerous activities. Scheme according to Fan et al. (Fan, Sun et al. 2016)

Antimicrobial activity of peptides is dependent on the amino acid composition of a peptide and on its physical-chemical properties, the so called interfacial activity that is described as the ability of a peptide to bind to a membrane, partition into the membrane-water interface and to alter the packing and organization of the lipids (Wimley 2010).

As of today, 3011 antimicrobial peptides are listed in the Antimicrobial Peptide Database.[1] The net charge of the peptides varies from -12 (Chrombacin; AP00612) to +30 (OaBac11; AP00684) and the size of the AMPs ranges from 2 (Gageotetrin A; AP02381) to 183 (ShLysG; AP02743) amino acids. The hydrophobic percentage, the ratio between the sum of the hydrophobic amino acids and the total number of amino acids, ranges from 0 % (SAAP; AP00528) to 100 % (Baceridin; AP02372) (Wang, Li et al. 2016). Basic amino acids like arginine and lysine are up to 50 % overrepresented in AMPs compared to common genomes, whereas the acidic amino acids, glutamate and aspartate are roughly underrepresented by 75 %. Additionally, hydrophobic amino acids are, in comparison to polar amino acids, overrepresented in AMPs (Wimley 2010).

[1] http://aps.unmc.edu/AP/main.php (2018/08/23)

AMPs can be classified into five different groups: (I) anionic peptides, (II) linear cationic α-helical peptides, (III) cationic peptides enriched for specific amino acids, (IV) anionic and cationic peptides that contain cysteine and form disulfide bonds and (V) anionic and cationic peptide fragments of larger proteins (Brogden 2005).

In order to attack microbial cells, AMPs have to be able get into close proximity of the membrane in a first step. Cell walls of gram-positive bacteria are composed of a porous 40-80 nm thick mesh and are generally easy to pass for AMPs. The outer cell membrane of gram-negative bacteria can be passed by cationic AMPs by a charge-exchange mechanism in which a cationic peptide is competing with Ca^{2+} and Mg^{2+} bound to lipopolysaccharides. Cationic AMPs are attracted by charged cell wall components like teichoic acid and lipoteichoic acid. Additionally, cationic AMPs are attracted by the inside-negative transmembrane potential of bacteria (Bechinger and Gorr 2017). AMPs may not be generally distributed on a cell surface than rather accumulate at the points where cell division, cell wall remodeling, or secretion take place (Choi, Rangarajan et al. 2016). AMPs attack selectively microbial cells due to the difference in eukaryotic and prokaryotic cell membranes. Eukaryotic membranes are, in contrast to bacterial membranes, composed of zwitterionic (overall neutral) lipid layers (Wakabayashi, Yano et al. 2017).

The insertion of AMPs into microbial membranes in mainly grouped into three different models (see Figure 4): the ‘barrel-stave model’, ‘carpet model’ and ‘toroidal-pore model’ (Brogden 2005). In the ‘barrel-stave model’ 3-11 parallel helical peptides form bundles in the membrane whereby the hydrophobic part of the helices is orientated to the lipid regions and the hydrophilic parts of the helices form a lumen in the bundle. The AMP alamethicin is associated with the ‘barrel-stave model’ (Yang, Harroun et al. 2001). The ‘carpet model’ describes the accumulation of AMPs to the membrane bilayer in a parallel way (Bechinger 2001). They disrupt the bilayer at higher concentration like detergents, which might lead to a formation of micelles. Transient toroidal wholes are formed and other peptides can access the membrane (Shai 1999). In the ‘toroidal-pore model’ helical AMPs insert into the membrane and the lipid monolayer is bent though the toroidal pore (Matsuzaki, Murase et al. 1996). The polar parts of the peptides associate to the head groups of the lipids and the lipids form a continuous bend to connect both leaflets of the membrane (Yamaguchi, Hong et al. 2002).

In principle, all proposed modes-of-actions lead to a disruption of the membrane integrity. The transmembrane potential and the pH gradient are destroyed as well as the regulation of the osmotic pressure. Further mechanisms of AMPs have been characterized, that target inner cellular processes like DNA and protein synthesis or cell wall synthesis. Additionally, some AMPs such as magainin and indolicidin are able to use multiple mechanisms to affect microbial cells to increase their efficiency (Peschel and Sahl 2006, Nguyen, Haney et al. 2011). Indolicidin for instance is directly binding DNA and interferes with the formation of the catalytic integrase-DNA complex (HIV-1) (Marchand, Krajewski et al. 2006). Indolicidin also induces an unselective permeabilization of liposomes containing negatively charged lipids (Rokitskaya, Kolodkin et al. 2011).

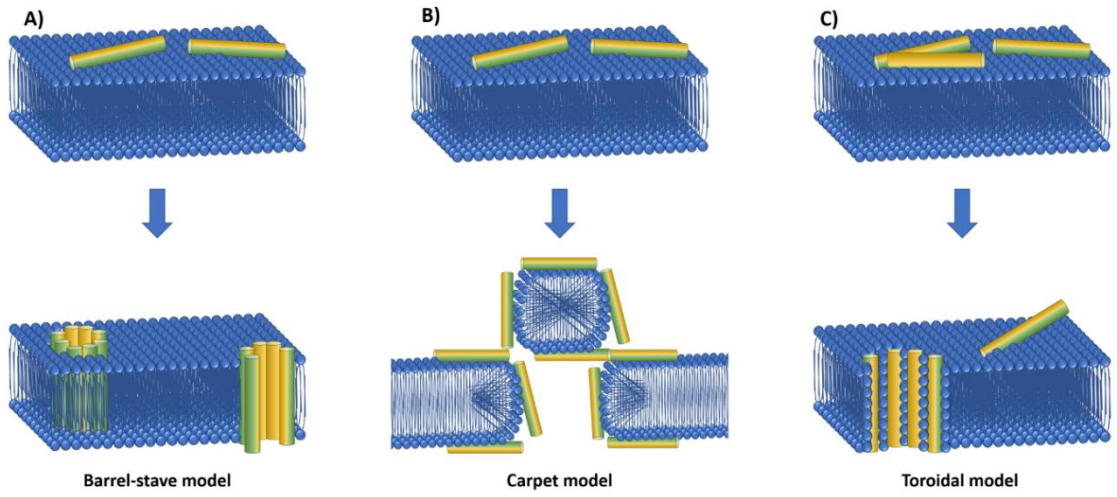

Figure 4: Disruption of bacterial membranes by AMPs. A) 'Barrel-stave model': the hydrophilic parts of the helices form a lumen in the bundle, B) 'Carpet model': AMPs disrupt the bilayer at higher concentration like detergents, which might lead to a formation of micelles. C) 'Toroidal-pore model': the lipid monolayer is bended though the toroidal pore (Brogden 2005, Sani and Separovic 2016).

1.2.2 Anchor peptides

Anchor peptides belong to the class of AMPs and in addition to their natural ability to bind to microbial membranes, they are also able to incorporate into synthetic polymers. The AMP Cecropin A (Steiner, Hultmark et al. 1981) was selected as a specific polymer membrane anchor to build functional nano-compartments with potential applications in synthetic biology, medicine (drug release) and industrial biotechnology (chiral nanoreactors, multistep syntheses, selective product recovery) (Noor, Dworeck et al.

2012). Therefore, Cecropin A was genetically fused to the fluorescent reporter protein eGFP and interactions with the tri-block copolymer polyisobutylene-polyethylene glycol-polyisobutylene (PIB-PEG-PIB) were investigated. The ability of the amphiphilic Cecropin A to anchor water soluble proteins like eGFP to a polymersome surface at ambient temperature, enabled the avoidance of chemical coupling steps to link polymers and proteins (Noor, Dworeck et al. 2012). Following, Cecropin A was used to functionalize poly(2-methyloxazoline)-poly(dimethylsiloxane)-poly(2-methyloxazoline) (PMOXA-PDMS-PMOXA) polymersomes (Klermund, Poschenrieder et al. 2016).

Up to date, a platform containing >65 different eGFP-anchor peptide fusion constructs as well as >20 biadhesive peptides was generated in our group (see Figure 5). The anchor peptides were fused to eGFP for an easy fluorescence-based detection (and quantification) on numerous surfaces. Therefore, the anchors were fused to the N- and C-terminal end of the reporter to investigate a potential influence on binding. Both fusion partners were functionally separated by a stiff spacer helix (17 amino acids: AEAAAKEAAAKEAAAKA) (Arai, Ueda et al. 2001) and a TEV cleavage site (7 amino acids: ENLYFQG) (Kapust and Waugh 2000). Binding of anchor was determined for instance for synthetic polymers (e.g., PP, PS, PE, and PET), metal surfaces like stainless steel as well as plant surfaces.

The polymer binding peptide LCI was able to immobilize the reporter protein eGFP in a 4.1 nm monolayer on a PP surface (Rübsam, Stomps et al. 2017). LCI was also used for semi-purification in a directed evolution campaign of a copper efflux oxidase (CueO laccase) in PP microtiter plates (MTP). The background noise of the assay system was minimized 20-fold due to the employed semi-purification process (Zou, Mate et al. 2018). A foliar fertilizer delivery system was established employing Plantaricin A as adhesion promoter to immobilize biohybrid microgels on plant surfaces. The pH-responsive microgels served as micro-containers to release Fe^{3+} ions preserving plant health and improving food production (Meurer, Kemper et al. 2017). Promising anchor peptides have to be further optimized by engineering tools to improve a functional and specific binding to selected surfaces in industrial applications (e.g., temperature stability, usage in laundry detergents, binding in presence of salts or stability in organic solvents).

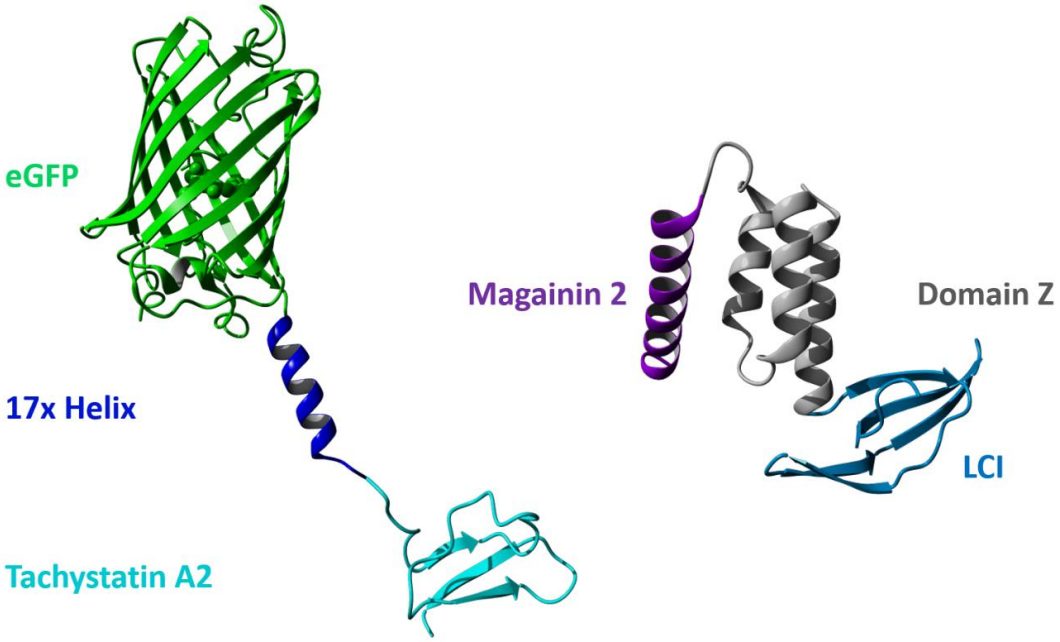

Figure 5: Schematic overview of eGFP-anchor peptide fusion constructs and biadhesive peptides. A) The N-terminal eGFP (PDB: 2Y0G) is separated from the C-terminal anchor peptide Tachystatin A2 (PDB: 1CIX) by a 17x Helix spacer unit with an incorporated TEV cleavage site. B) Biadhesive peptides consisted of two different anchor peptides (e.g., Magainin 2 (PDB: 2MAG) or LCI (PDB: 2B9K)) separated by the 17xHelix or the staphylococcal protein A domain Z (PDB: 2SPZ).

1.3 Protein engineering

In nature, evolutionary mechanisms ensure an adaptability to an ever-changing environment. Evolution is not directed towards any particular goal and occurs spontaneously over time due to reproduction failures (Arnold 1998). Mutational changes might be beneficial or adverse for the survival of organisms in a certain environment leading to a natural selection. As a result, proteins are highly optimized and specialized for a specific biological task. In protein engineering evolutionary strategies are applied to tailor proteins and enzymes for industrial process conditions, like an improved tolerance towards detergent or solvent concentrations or high process temperatures (Romero and Arnold 2009, Cheng, Zhu et al. 2015, Vojcic, Pitzler et al. 2015, Shivange, Roccatano et al. 2016, Qiang, Sun et al. 2017). Two commonly used approaches in protein engineering are rational protein design and directed evolution.

Rational protein design aims to improve enzymes with well-known structure-function relationships by applying computational approaches (Lutz 2010). Proteins (especially

short peptides) can be designed *de novo* (DFTamP1; specific activity against *Staphylococcus aureus* (Mishra and Wang 2012)) or engineered by a prediction of changes in a known protein structure. Therefore, information about the protein (e.g., from sequence molecular modeling, computational chemistry or X-ray crystallography) is needed. Localized and addressable enzyme properties, such as activity/selectivity, substrate profile or thermal resistance are often engineered by rational protein design (Shivange, Marienhagen et al. 2009). However, even though the sequence of a protein is well-known, the prediction of how changes in amino acids will affect the protein is often very difficult (Arnold 1998, Wong, Zhurina et al. 2006, Lutz 2010).

Directed evolution (DE) is an iterative algorithm to elucidate structure function relationships of target proteins based on random mutagenesis (Wong, Zhurina et al. 2006, Frauenkron-Machedjou, Fulton et al. 2018). DE techniques are often applied to engineer enzyme properties that are not fully understood, such as resistance towards organic solvents or ionic liquids and pH stability (Shivange, Marienhagen et al. 2009). One round of DE consists of three steps (see Figure 6): (I) diversity generation, (II) screening and (III) isolation of the improved variants (Guven, Prodanovic et al. 2010). In the first step, the gene of interest is mutated and introduced into a suitable host organism (e.g., *E. coli*, *Bacillus subtilis* or *Pichia pastoris*) In a second step, the resulting protein libraries are analyzed in a screening system that is reflecting the desired application conditions as close as possible. Identified beneficial variants are analyzed in the final step by identifying introduced mutational changes in the target gene. Improved variants can be used as a template for iterative rounds of directed evolution.

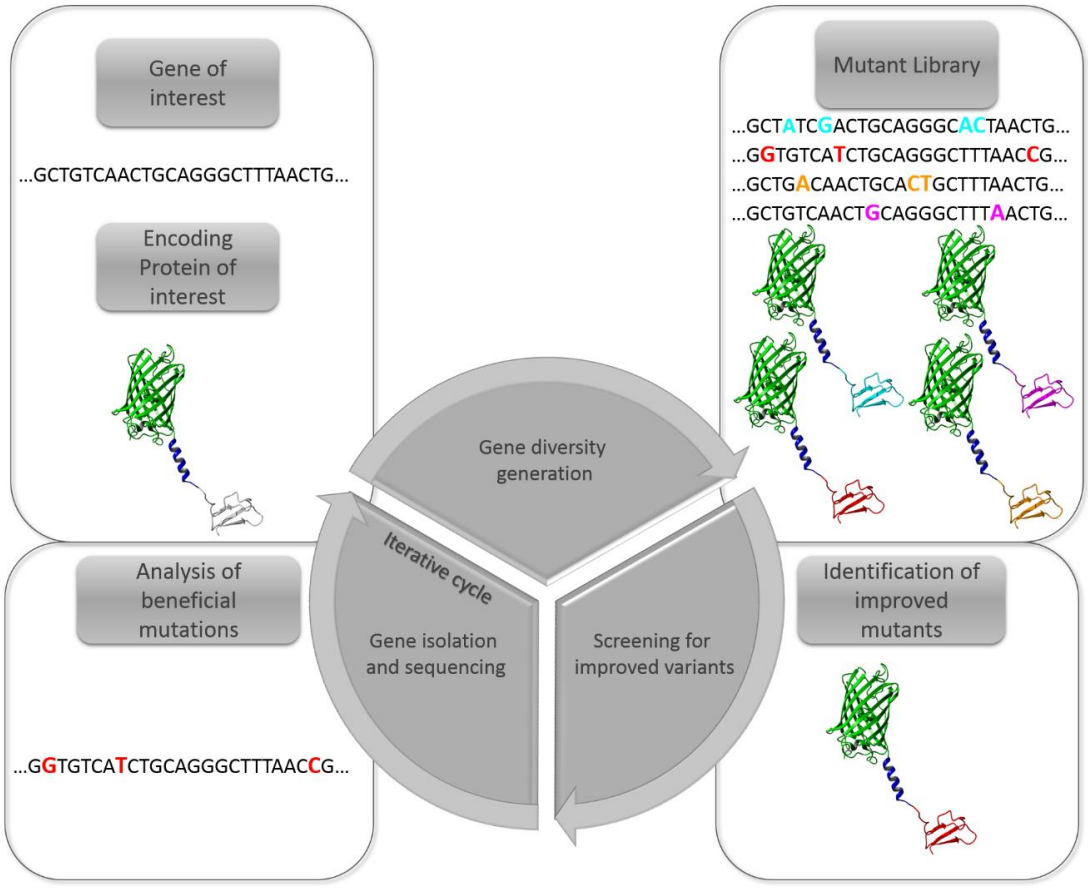

Figure 6: General overview of a directed evolution campaign. A directed evolution campaign is performed in three steps. I) gene diversity generation II) screening for improved variants and III) gene isolation and sequencing. Scheme according to Güven *et al. (Guven, Prodanovic et al. 2010)*

1.3.1 Diversity generation in directed evolution

A successful DE campaign is strongly dependent on the generated library size and quality of diversity generation (Wong, Zhurina et al. 2006, Ruff, Dennig et al. 2013). Diversity generation is referred to as the introduction of mutations into a specific DNA sequence or gene of interest. In traditional directed enzyme evolution campaigns, a mutational load of 1-3 mutations per 1000 base pairs (bp) is applied to be able to study single amino acid exchanges in the generated variants (Cheng, Zhu et al. 2015). A broad variety of diversity generation techniques exist and are listed in Table 1.

Table 1: Selected diversity generation methods for DE and rational protein design.

Technique	*Principle*	*Reference*
Generation of random mutant libraries		
Error-prone PCR (epPCR)	Incorrect incorporation of nucleotides using *Taq* DNA polymerase and $MnCl_2$	(Cadwell and Joyce 1992)
Sequence Saturation Mutagenesis (SeSaM)	Randomized target sequences at every single nucleotide position with universal bases; without polymerase bias	(Wong, Tee et al. 2004)
Recombination-based library generation		
DNA shuffling	Combination and accumulation of beneficial mutations from different gene variants, fragmentation of target genes with *DNase* I	(Stemmer 1994)
Staggered Extension Process (StEP)	Combination and accumulation of beneficial mutations from different gene variants; priming the template sequence with very short PCR cycles; growing fragments anneal to different templates	(Zhao, Giver et al. 1998)
Phosphorothioate-based DNA Recombination (PTRec)	Combination and accumulation of beneficial mutations from different gene variants; enzyme-free method that requires a short stretch of 12 bps for recombination; shuffling of five domains	(Marienhagen, Dennig et al. 2012)
Site-Directed Mutagenesis (SDM)	Focused introduction of point mutations by primer mismatches; QuikChange	(Kunkel 1985) (Wang and Malcolm 1999)
Site-Saturation Mutagenesis (SSM)	Focused saturation of codons by randomized primers (e.g., NNK)	(Miyazaki and Arnold 1999)
Iterative Saturation Mutagenesis (ISM)	Iterative cycles of saturation mutagenesis at rationally chosen sites (up to three amino acid positions)	(Reetz and Carballeira 2007)
OmniChange	Multi-site-saturation mutagenesis enables the discovery of cooperative effects of up to five amino acid substitutions. PLICing based	(Dennig, Shivange et al. 2011) (Blanusa, Schenk et al. 2010)
Casting epPCR (cepPCR)	Fragmentation of target gene and high-load epPCR. Mutated fragments were amplified using MEGAWHOP	(Yang, Ruff et al. 2017) (Miyazaki 2011)

DE campaigns are commonly designed utilizing error-prone polymerase chain reaction (epPCR) based protocols due to their robustness and simplicity (Rasila, Pajunen et al. 2009). epPCR protocols are based on *Taq* DNA polymerase (*Thermus aquaticus*) that lacks a 3'-5' proofreading exonuclease activity. A very high intrinsic error rate of *Taq* DNA polymerase ($8*10^{-6}$ mutations per bp and duplication) promotes an incorporation of non-

matching nucleotides. However, the natural error rate (1 substitution in 125,000 bp per PCR cycle) is insufficient for the randomization of commonly evolved genes (1,000-5,000 bp) (Cirino, Mayer et al. 2003). In order to generate high quality mutant libraries, the fidelity of the DNA polymerase can be adjusted by addition of $MnCl_2$, a supplementation of unbalanced deoxyribonucleotides (dNTP) concentrations or by increasing the number of amplification cycles (Cadwell and Joyce 1992, Cirino, Mayer et al. 2003). Apart from the robustness and simplicity, the major drawback of standard epPCR protocols is a fairly low mutational load that leads to an identification of only 30 % of beneficial positions (e.g., organic solvents or ionic liquids (Zhao, Kardashliev et al. 2014, Yang, Ruff et al. 2017). The redundancy of the genetic code and a biased DNA polymerase (high numbers of transitions) lead to a lack of subsequent mutations (Wong, Tee et al. 2004).

Random technologies can be combined with rational-design to overcome the limitations of DE (Lutz 2010). In semi-rational approaches, computationally selected protein positions are saturated by SSM. These small, functionally-rich libraries reduce the screening effort and often result in higher enzyme improvements. The alcohol dehydrogenase 5 (*Candida parapsilosis*) was mutated in a OmniChange library mutating four positions and screening of 3500 clones yielded in an improvement of 108-fold in initial activity towards methyl 3-hydroxyhexanoate (Ensari, Dhoke et al. 2018).

1.3.2 Screening systems

Apart from diversity generation, one bottleneck in DE is the ability to screen a sufficient diversity of the generated sequence space in a time and cost efficient manner. A protein of 100 amino acids can theoretically exist in 20^{100} (~1.27×10^{130}) different sequences (Tee and Schwaneberg 2007). A reliable high-throughput screening system plays a pivotal role for successful DE campaigns and has to reflect the final application conditions (“you get what you screen for”) (Arnold 1998, Schmidt-Dannert and Arnold 1999). Dependent on the library size and targeted properties, a screening format with low, medium or high throughput has to be selected in order to analyze a statistically meaningful fraction of the generated sequence space (Wong, Zhurina et al. 2006).

Even though microtiter plate (MTP) based formats enable only a medium throughput of 10^3-10^5 variants, they are the most common applied screening systems in DE (Tee and

Schwaneberg 2007). In fact, screening of small random libraries (1000-2000 variants per round) is often sufficient to identify improved variants (Zhao, Kardashliev et al. 2014). Recently, the full natural diversity of single amino acid exchanges in *Bacillus subtilis* lipase A (BSLA) was explored applying a colorimetric MTP-based screening system, revealing that 40-60 % of all BSLA positions improve organic solvent resistance (Frauenkron-Machedjou, Fulton et al. 2018).

The screening of large libraries is carried out by ultra-high-throughput screening systems (uHTS). uHTS is a key technology in pharmaceutical drug discovery and DE campaigns. uHTS screening systems commonly base on fluorescent or chemoluminescent detection methods (Winter, Ries et al. 2018). The fluorescent-activated cell sorting (FACS) is a powerful tool to analyze mutant proteins from large libraries. In an activity-based screening, cells, beads, or emulsion droplets can be sorted at extremely high event rates (up to 10^7 events/hour) (van Bloois, Winter et al. 2011, Korfer, Pitzler et al. 2016). The combination of FACS systems with whole cell screening approaches enables a phenotype/genotype-linkage which is prerequisite for DE campaigns (van Bloois, Winter et al. 2011).

Apart from classical FACS-based screening assays, strategies have been developed to link a fluorescent screening product to the cell surface. The Fur Shell principle is based on a phytase-catalyzed formation of a fluorescent hydrogel shell around *E. coli* cells. Each *E. coli* cell acts as a compartment in which a phytase and a glucose oxidase form H_2O_2 in a coupled reaction. A fluorescent monomer (Polyfluor 570) is co-polymerized in a PEG-acrylate-based polymerization forming a hydrogel shell around *E. coli* cells. The Fur-Shell technology has been expanded to cellulases, lipases, and esterases and enables the generation of polymer-hybrid cells for bio-based interactive materials (Pitzler, Wirtz et al. 2014, Lulsdorf, Pitzler et al. 2015).

Cells analyzed by FACS systems are in varied metabolic states and to identify best performing variants, a subsequent screening (e.g., in MTP) is usually required (Korfer, Pitzler et al. 2016). To overcome this drawback, the concept of *in vitro* compartmentalization within (w/o) single emulsion compartments was introduced (Tawfik and Griffiths 1998). Following, uHTS screening and in vitro enzyme library production were coupled within water-in-oil-in-water (w/o/w) emulsion compartments (InVitroFlow). Beneficially, *in vitro* compartmentalization in (w/o/w) emulsions enables

the production of toxic and membrane bound enzymes, since it is host-cell independent. The InVitroFlow was applied to develop an *in vitro* directed cellulase evolution protocol based on fluorescein-di-β-D-cellobioside as substrate within (w/o/w) emulsion compartments (Korfer, Pitzler et al. 2016).

2 Directed evolution of Tachystatin A2 towards improved polystyrene binding

2.1 Declaration

The PePevo protocol for directed evolution of anchor peptides was developed in cooperation with Dr. Kristin Rübsam. The work was equally distributed and accomplished (see XIV. Author contributions). Parts of this chapter were published by the author in the journal of Biotechnology and Bioengineering.

Rübsam K*, Weber L*, Jakob F, and Schwaneberg U (2018). "Directed evolution of polypropylene and polystyrene binding peptides." Biotechnol Bioeng 115(2): 321-330. *shared first co-authorship

2.2 Objective and main results

Material binding peptides enable surface functionalization of biological inert polymers (e.g., PS) with an efficient immobilization of enzymes, bioactive peptides or antigens (at ambient temperature in water). A tailoring of polymer binding anchor peptides (PBPs) for efficient binding under application conditions requires DE. A robust and generally applicable DE protocol was established by adapting common procedures to very short peptides like Tachystatin A2 (TA2, 44 aa). In order to sufficiently diversify TA2, an epPCR protocol with a very high mutation frequency (59 mutations/kb) was established. The reporter protein eGFP was used as a fusion partner of TA2 to directly quantify peptide binding on the PS-MTP surface by fluorescence analysis. The developed Peptide-Polymer *evo*lution protocol (PePevo protocol) was validated in a directed evolution campaign of TA2 towards improved PS binding. In this campaign, improved PS-binding TA2 variants were identified by the application of the anionic surfactant LAS (0.5 mM) as selection pressure. Applying the PePevo protocol in one round of DE, up to six fold stronger PS-binders (in the presence of 0.5 mM LAS) were identified (see Figure 7).

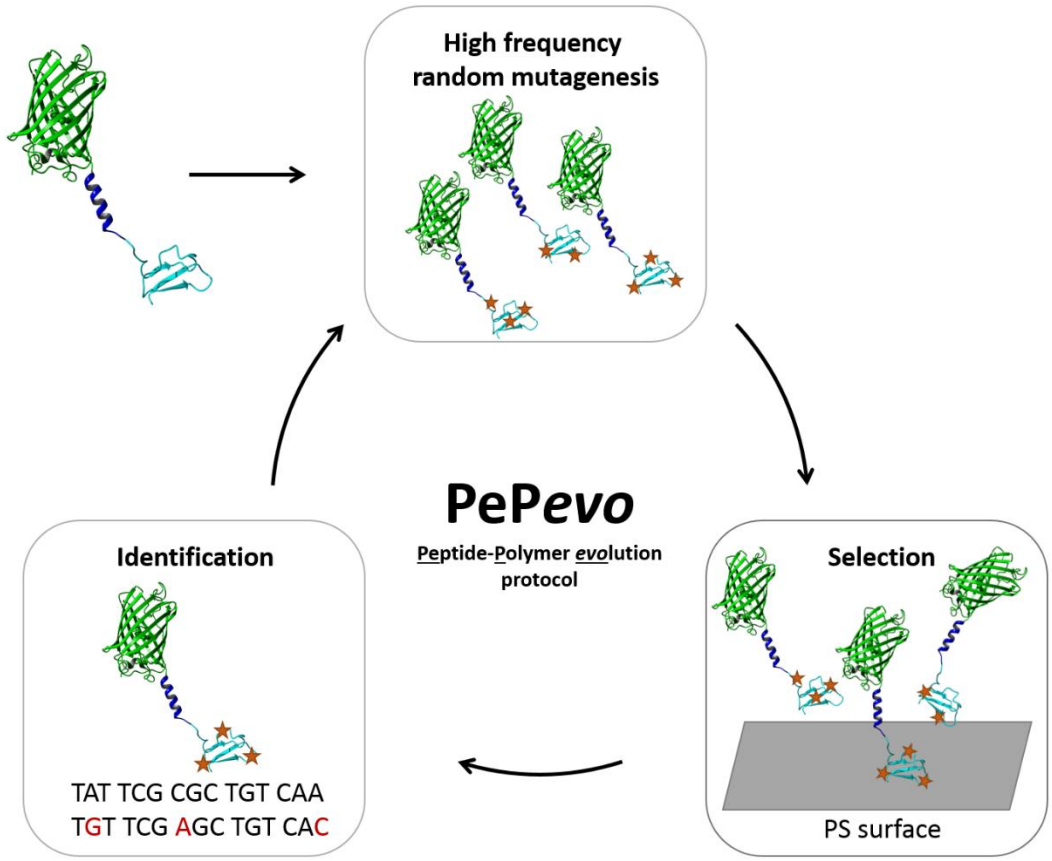

Figure 7: Peptide-Polymer *evo*lution protocol. The PeP*evo* protocol for polymer binding anchor peptides enables the engineering of binding peptides for application conditions. Tachystatin A2 was fused to eGFP and randomized in a high-mutation frequency epPCR. After immobilization on a PS-MTP-surface, non-specific proteins were removed in two washing steps whereas strong binding Tachystatin A2 variants were selected with the anionic surfactant LAS. The fluorescent fusion partner eGFP was used to quantify improved PS-binding Tachystatin A2 variants. Scheme according to (Rubsam, Weber et al. 2018).

2.3 State of the art

Material binding peptides are short selective adhesives, that are utilized to efficiently immobilize fusion partners (e.g., enzymes, bioactive peptides or antigens) on target supports (Care, Bergquist et al. 2015, Zernia, Ott et al. 2016). The high binding affinity of material binding peptides leads to an oriented immobilization in a monolayer on a surface and ensures an oriented and functional attachment of enzymes or reporter proteins (Kumada, Kuroki et al. 2010, Rübsam, Stomps et al. 2017). Since binding is performed from aqueous solutions, a change of bulk material properties and non-selective coupling reactions are prevented (Sanghvi, Miller et al. 2005, Liu, Ma et al. 2016). The broad applicability of material binding peptides for surface functionalization is a valuable tool

for applications in plastic industries including packaging, textiles or automotive industry as well as in biomedical applications like diagnostics and disposable laboratory ware (Yaman, Ozdogan et al. 2009, Moritomi, Watanabe et al. 2010, McKeen 2014).

The demand for functionalized plastics is ever increasing. Due to its good mechanical properties, the synthetic aromatic polymer PS ($(C8H8)_n$) belongs to the most widespread commodity polymers. PS is widely used for food containers, packaging foams, and plates (Kwon, Saido et al. 2014, Ho, Roberts et al. 2018). The hydrophobic PS is a durable thermoplastic that is resistant to hydrolysis and regarded as non-biodegradable (Ho, Roberts et al. 2018). Surface properties of PS are often adjusted to application demands by physical surface treatments (e.g., plasma or flame treatments) (Chan, Ko et al. 1996) or chemical modifications (e.g., wet chemical oxidations with e.g. nitric acid) (Penn and Wang 1994). Especially in biological applications, PS devices are functionalized to increase the bio-compatibility. Plasma treatment is used in tissue culture to activate the surface by increasing the amount of oxygen-containing moieties on the surface. Activated PS plates promote the adhesion and proliferation of cells in tissue culture. PS surfaces were treated with N_2-plasma to amino-functionalize and subsequently immobilize bovine serum albumin and trypsin for biological applications (Boulares-Pender, Prager-Duschke et al. 2009). However, proteins usually contain amino groups in their functional groups and therefore multiple anchoring points lead to non-productive orientations that can reduce flexibility and specific enzyme activity (Jonkheijm, Weinrich et al. 2008, Hernandez and Fernandez-Lafuente 2011).

The usage of polymer binding peptides promotes a directed immobilization of enzymes on solid supports (Rübsam, Stomps et al. 2017, Zou, Mate et al. 2018) and plenty of polymer binding peptides have been identified within the past years (e.g., for poly(methyl methacrylate) (PMMA) (Serizawa, Sawada et al. 2007), chlorine-doped polypyrrole (PPyCl) (Sanghvi, Miller et al. 2005), poly(L-lactide) (PLLA) (Matsuno, Sekine et al. 2008) and polystyrene (PS) (Serizawa, Techawanitchai et al. 2007)). PS-binding peptides are often identified in phage display based biopanning experiments (see Introduction 1.2; (Kumada, Tokunaga et al. 2006, Imanaka, Yamadzumi et al. 2016, Qiang, Sun et al. 2017). The PS-binding peptides PS19-1 and PS19-6, for instance, bind to hydrophilic PS surfaces with a maximum adsorption of 81 mg/m^2 and 86 mg/m^2 respectively. The binding peptides were applied for a functional immobilization of the enzyme glutathione S-transferase on a PS

support (Kumada, Kuroki et al. 2010). PS is composed of hydrophobic ethylene backbone, aromatic phenyl groups, and terminal sulfate groups and proteins adsorb to PS by electrostatic, hydrophobic, and aromatic stacking interactions (Shikiya, Tomita et al. 2013, Qiang, Sun et al. 2017).

Promising alternatives to short synthetic peptide libraries are naturally occurring adhesive peptides. The anchor peptides Cecropin A (37 aa) (Steiner, Andreu et al. 1988) and LCI (47 aa) (Gong, Wang et al. 2011) showed great potential for the functionalization of polymers (see Introduction 1.2.2). Synthetic polymers like PS are produced since the early 1950´s and in this evolutionary short period of time, a very limited evolutionary pressure existed for organisms to evolve efficient enzymes and peptides to target polymer degradation (Mor and Sivan 2008). However, the likelihood of identifying significantly improved PS-binders is very high due to the enormous variety and sequence space of peptides (e.g., TA2 with 44 aa can theoretically yield in 44^{20} variants) (Tee and Schwaneberg 2007). DE is a common strategy to adapt enzymes to industrial processes (see chapter 1.3.1). In classical epPCR-based DE campaigns, a mutational frequency of 1-3 mutations/kb is employed (Cheng, Zhu et al. 2015). Depending on average gene sizes (~1-5 kb), muteins contain 1-3 amino acid exchanges. In contrast, genes of anchor peptides range on average from 36 to 300 bp (12-100 aa) and are considerably shorter than enzyme genes. Consequently, a much higher mutational load (at least 20 mutations/kb) is needed to ensure a high gene diversity in a generated anchor peptide-mutant library. Applying directed evolution to tailor anchor peptides enables an adjustment of binding strength to application conditions which is pre-requisite for efficient bio-functionalization of polymers.

2.4 Methods

Chemicals used in this chapter were obtained from Sigma-Aldrich Corp. (St. Louis, USA), AppliChem GmbH (Darmstadt, Germany) or Carl Roth GmbH (Karlsruhe, Germany) in analytical-reagent grade or higher purity. Synthetic genes were ordered at GeneArt AG (Regensburg, Germany) and oligonucleotides were ordered from Eurofins Scientific SE (Ebersberg, Germany) in salt-free form. The enzymes used in this study were obtained from New England Biolabs GmbH (Frankfurt am Main, Germany). The PCR purification and plasmid extraction kits were obtained from Qiagen GmbH (Hilden, Germany) and

Macherey-Nagel GmbH & Co. KG (Düren, Germany). In this study, the plasmid pET28a(+) (Novagen, Darmstadt, Germany) was used as expression vector. The expression strain *E. coli* BL21-Gold (DE3) was ordered from Agilent Technologies (Santa Clara, USA). Black PS 96-well microtiter plates for binding studies were purchased from Greiner Bio-One GmbH (Frickenhausen, Germany).

2.4.1 Generation of eGFP-anchor peptide fusion constructs

The eGFP-TA2 fusion construct and the reference PS-binding peptide PS19 (RAFIASRRIKRP (Kumada, Tokunaga et al. 2006)) were generated as described in the Appendix chapter IV. eGFP-TA2 was generated by 'Phosphorothioate-based ligase-independent gene cloning' (PLICing) (Blanusa, Schenk et al. 2010) whereas the reference PS-binding peptide PS19 was generated in a two-step PCR (see Table 2) with overlapping primers (20 µM each; see Table 3).

Table 2: Two-step PCR conditions for generation of PS-binding peptide PS19.

Step	Temperature [°C]	Time [s]	Cycles [n]
Two step PCR –Step 1			
Initial denaturation	98	30	1
Denaturation	98	15	5
Annealing	60	30	5
Elongation	72	210	5
Halt	8	∞	
Two step PCR –Step 2			
Initial denaturation	98	30	1
Denaturation	98	15	20
Annealing	62	30	20
Elongation	72	210	20
Final elongation	72	300	1
Storage	8	∞	

2.4.2 Random mutagenesis of TA2

TA2 was mutated by random mutagenesis in an error prone polymerase chain reaction (epPCR) (Cadwell and Joyce 1992). The gene *ta2* (30 ng template pET28a(+)::eGFP_17xHelix_TEV-TA2) was amplified with Taq DNA polymerase (2.5 U), substituted with dNTPs (10 mM), Mn^{2+} (0.7 mM) and the primer pair FW-epTA2 and Rev-epTA2 (20 µM each; see Table 3).

Table 3: Primers used for epPCR and generation of reference peptide eGFP-PS19.

Primer name	Sequence 5' – 3'
FW-PS19	CAA GCC GTC GTA TTA AAC GTC CGT AAT AAC ACT GAG ATC CGG CTG CTA ACA AAG CCC GAA AG
Rev-PS19	GAC GGC TTG CAA TAA ATG CAC GAC CCT GAA AAT ACA GAT TTT CTG CTT TCG CTG C
FW-epTA2	GCG GAG AAC CTG TAC TTT CAG GGC
Rev-epTA2	CGG GCT TTG TTA GCA GCC GGA TCT CAG TGT TAT CA

The epPCR conditions are listed in Table 4. Parental DNA was digested (20 U *Dpn*I, 16 h, 37°C) and subsequently purified (PCR clean-up gel extraction kit, Macherey-Nagel, Düren, Germany). The vector backbone pET28a(+)::eGFP_17xHelix_TEV_TA2 was amplified by 'megaprimer PCR of whole plasmid' (MEGAWHOP) (Miyazaki 2011). The previously generated epPCR product (500 ng) was applied as megaprimer in the PCR reaction for the amplification of pET28a(+)::eGFP_17xHeli_TEV_TA2 template (60 ng) with PfuS DNA polymerase (2.5 U) and dNTPs (300 µM). The MEGAWHOP conditions are listed in Table 4. The parental DNA was digested (20 U *Dpn*I, 16 h, 37°C), purified (PCR clean-up gel extraction kit, Macherey-Nagel, Düren, Germany), and subsequently transformed into *E. coli* BL21-Gold (DE3).

Table 4: PCR conditions for TA2 epPCR library generation.

Step	Temperature [°C]	Time [s]	Cycles [n]
epPCR TA2			
Initial denaturation	94	120	1
Denaturation	94	30	25
Annealing	60	30	25
Elongation	68	120	25
Final elongation	68	600	1
Storage	8	∞	
MEGAWHOP			
Elongation	72	300	1
Initial denaturation	98	90	1
Denaturation	98	45	25
Annealing	55	45	25
Elongation	72	240	25
Final elongation	72	600	1
Storage	8	∞	

2.4.3 Cultivation of eGFP-TA2 epPCR library in 96-well microtiter plates

The cultivation of the eGFP-TA2 epPCR library in 96-well microtiter plates was performed according to (Rübsam, Stomps et al. 2017). Colonies were transferred into 96-well microtiter plates (MTP; PS, flat bottom) containing LB medium (150 µL/well; 10 g/L tryptone, 10 g/L NaCl, 5 g/L yeast extract) supplemented with kanamycin (50 µg/mL) and cultivated overnight (37°C, 900 rpm, 70 % humidity; Multitron Pro, Infors AG). After cultivation, glycerol (80 µL/well, 50 % (v/v)) was added and the master plates were stored at -80°C. Pre-cultures (150 µL/well LB medium + 1 % Glc; 50 µg/mL kanamycin) were inoculated from master plates using a replicator and cultivated for 24 h (37°C, 900 rpm, 70 % humidity; Multitron Pro, Infors AG). Main-cultures (115 µL/well TB medium (12 g/L tryptone, 24 g/L yeast extract, 5 g/L glycerol, 17 mM KH_2PO_4 and 72 mM K_2HPO_4), supplemented with kanamycin (50 µg/mL)) were inoculated with 20 µL of pre-culture, cultivated for 2 h (37°C, 900 rpm, 70 % humidity; Multitron Pro, Infors AG) and induced at an OD_{600}=0.6-0.8 with IPTG (15 µL/well; 0.1 mM). The eGFP-TA2 epPCR library was cultivated for 48 h (20°C, 900 rpm, 70 % humidity; Multitron Pro, Infors AG). Reference eGFP-TA2 WT, as well as the eGFP control were transferred in three replicates per plate each.

2.3.4 Determination of critical micelle concentration

The critical micelle concentration (CMC) of the anionic detergent LAS was determined using a bubble pressure tensiometer (Bubble Pressure Tensiometer-BP100, KRÜSS GmbH, Hamburg, Germany). LAS (M (LAS): 326.49 g/mol, ϱ (LAS): 922 kg/m³, CAS Number 27176-87-0, Sigma Aldrich, Darmstadt, Germany) was diluted in Tris/HCl buffer (50 mM, pH 8.0) in serial dilutions from 0-5 mM and incubated at room temperature overnight. The settings of the device were: 25°C, diameter of capillary 0.346 mm, velocity of surface detection 20 mm/min, dipping depth of capillary 10 mm, and rinsing of capillary 30 s. The surface age of bubbles was measured over a time of 50,000 ms.

2.4.5 Screening of eGFP-TA2 epPCR library for improved binding to PS in presence of LAS

The binding strength of TA2 and the generated eGFP-TA2 epPCR library towards PS in presence of the surfactant LAS was analyzed using the Assay for Better polymer Binding Anchor peptides (ABBA). In the immobilization step, eGFP-TA2 variants were bound to the

wells of black PS MTPs (flat bottom). Therefore, cell free extracts (CFE) (10 µL/well) was supplemented to 90 µL/well Tris/HCl buffer (50 mM, pH 8.0) and incubated for binding (10 min, room temperature, 600 rpm; MTP shaker, TiMix5, Edmund Bühler GmbH, Hechingen, Germany). Subsequently, the MTP wells were washed with Tris/HCl buffer (100 µL/well; 50 mM, pH 8.0, 5 min, room temperature, 600 rpm) in two washing steps to remove unspecific CFE proteins. In a final selection step, the anionic surfactant LAS (100 µL/well, 0.5 mM) was supplemented and incubated with the bound peptide variants (5 min, room temperature, 600 rpm). After removal of all liquids and desorbed peptides, the fluorescence of the bound eGFP-TA2 variants was measured directly on the PS surface with the 96-well MTP reader FLUOstar Omega (BMG LABTECH GmbH, Ortenberg, Germany; excitation (Ex) 485 nm, emission (Em) 520 nm, gain 1000, 35 reads/well).

2.5 Results

The results section was divided into four parts. In the first part an epPCR library of the anchor peptide TA2 (132 bp) was generated. The development of a high-throughput screening system for short anchor peptides was described in the second part by determining key performance parameters. Therefore, the applied CFE volume, influence of the applied surfactant concentration for selection, and standard deviation of the screening system in 96-well MTP format were established. The PeP*evo* protocol was validated in the third part by one round of DE to improve the binding of TA2 to PS in presence of the anionic surfactant LAS. The binding strength of identified eGFP-TA2 variants was characterized in the fourth part with respect to the eGFP-TA2 WT and binding was compared to reported PS-binding peptide PS19.

2.5.1 Generation of the TA2 epPCR library

In DE campaigns, usually 10^3 clones are screened with a mutational frequency of approximately 1-3 mutations/kb leading to one to three aa substitutions per enzyme (Cheng, Zhu et al. 2015). Thereby, a fraction of 40-60 % of active variants is targeted to ensure an identification of beneficial variants in small libraries (Tee and Schwaneberg 2007, Zhao, Kardashliev et al. 2014). In order to sufficiently mutate short genes of anchor peptides (*ta2*: 132 bp), a mutation frequency of ~20 mutations/kb is required. The

mutation frequency has to be adjusted by varying, for instance, the applied $MnCl_2$ concentration (here 0.5-1.5 mM) in the epPCR.

The generation of *ta2* epPCR library was carried out with 0.7 mM $MnCl_2$. The library contained 418 (46.4 %) inactive variants (fluorescence signal of <0.8-fold or less relative to the eGFP-TA2 WT). Sequencing of 50 clones revealed a mutation frequency of 59.4 mutations/kb in the *ta2* gene with a ratio (Ts/Tv) of 57.3/38.8 %. Consecutive mutations (2 variants had two times consecutive mutations) were detected in 25 % of all sequenced variants. This mutation frequency resulted in an average number of 4.4 amino acid substitutions per TA2 variant (see Figure 8).

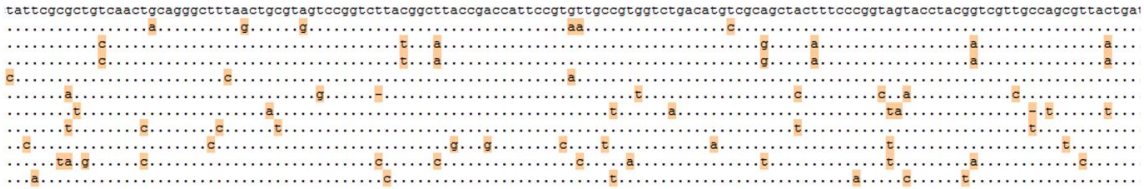

Figure 8: Mutation frequency of *ta2* variants. The *ta2* gene was mutated by epPCR. Mutations were analyzed by sequencing and mutations of 10 clones are highlighted in orange.

2.5.2 Performance criteria of the ABBA screening system

The developed ABBA screening system is based on the detection of the immobilized fluorescent fusion partner eGFP on the surface of 96-well MTP plates (see Figure 9). eGFP-TA2 variants are immobilized from CFE by incubation in black PS-MTPs (Greiner Bio-One, 96-well, F-Bottom, fluorotrac). During the two successive washing steps, background proteins with weak hydrophobic interactions to PS-MTPs are removed. Only target peptides with a high PS-binding affinity remain immobilized on the PS-surface. The surfactant LAS (0.5 mM) is used as selection pressure and is supplemented in a competition buffer. Weak binding eGFP-TA2 variants are detached from the PS-surface and strong binding eGFP-TA2 variants remain attached. The binding of each eGFP-TA2 variants is quantified by the detection of eGFP fluorescence employing a FLUOstar Omega MTP reader (Ex: 485 nm, Em: 520 nm, gain 1000, 35 reads per well).

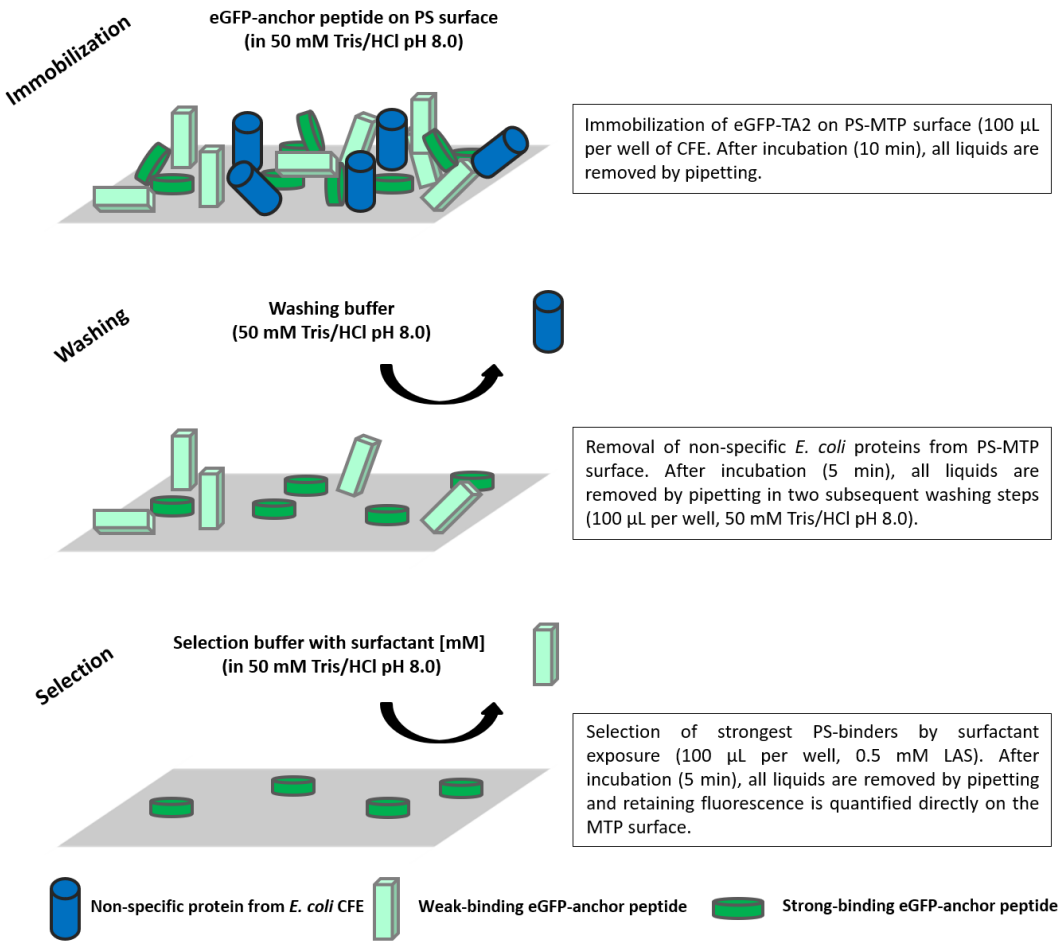

Figure 9: Selection of strong-binding TA2 variants with ABBA. eGFP-TA2 WT and eGFP-TA2 epPCR library variants are transferred into black 96-well PS-MTPs. The peptides are immobilized on the PS-surface. Non-specific CFE proteins are removed in two washing steps. For selection, the anionic surfactant LAS is applied to the PS-surface and weak binding peptides are removed. Strong binding target peptides are directly quantified on the PS-surface by detecting the fluorescent fusion partner eGFP. Scheme according to (Rubsam, Weber et al. 2018).

The reliability of a MTP-based screening system is pre-requisite for a successful DE campaign. The standard deviation of an assay is the key performance parameter for a reliable screening system. Screening systems that have a standard deviation below 18 % are regarded as reliable and are employed in DE campaigns (Tee and Schwaneberg 2007). The ABBA screening system was optimized in 96-well MTPs by adapting peptide expression conditions. The applied eGFP-TA2 concentration was optimized to reach a complete surface coverage in 96-well PS plates for a robust and reliable ABBA screening system. Therefore, the CFE volume was varied. An effective selection pressure was established by a variation of surfactant concentrations (0.001-5 mM LAS) in the selection step, as well as the determination of the CMC of LAS.

2.5.3 Determination of applied CFE volume for an optimized standard deviation in ABBA

In the immobilization step, the surface of the PS plates is covered with eGFP-TA2. A full coverage of the surface area was targeted to exclude false negative results by poor expression variants. Therefore, the CFE volumes (0.5-50 µL) were varied in the coating step. The assay volume of 100 µL/well was kept constant by the addition of Tris/HCl buffer (50 mM, pH 8.0). An efficient coating of the MTP surface with eGFP-TA2 was ensured by applying a minimum of 10 µL CFE/well. After a selection with 0.5 mM LAS a remaining fluorescence of 99.3 ± 8.8 RFU was detected on the PS surface (see Figure 10). The MTP surface was saturated with CFE volumes of 10-50 µL and led to an elimination of good expression variants. When lower CFE concentrations (< 10 µL) of eGFP-TA2 were used in the immobilization step, a dependency between applied concentration and detected RFU on the surface were observed. The eGFP control was used as negative control. eGFP could be removed completely from the PS-MTP surface after a selection with 0.5 mM LAS at any tested concentration.

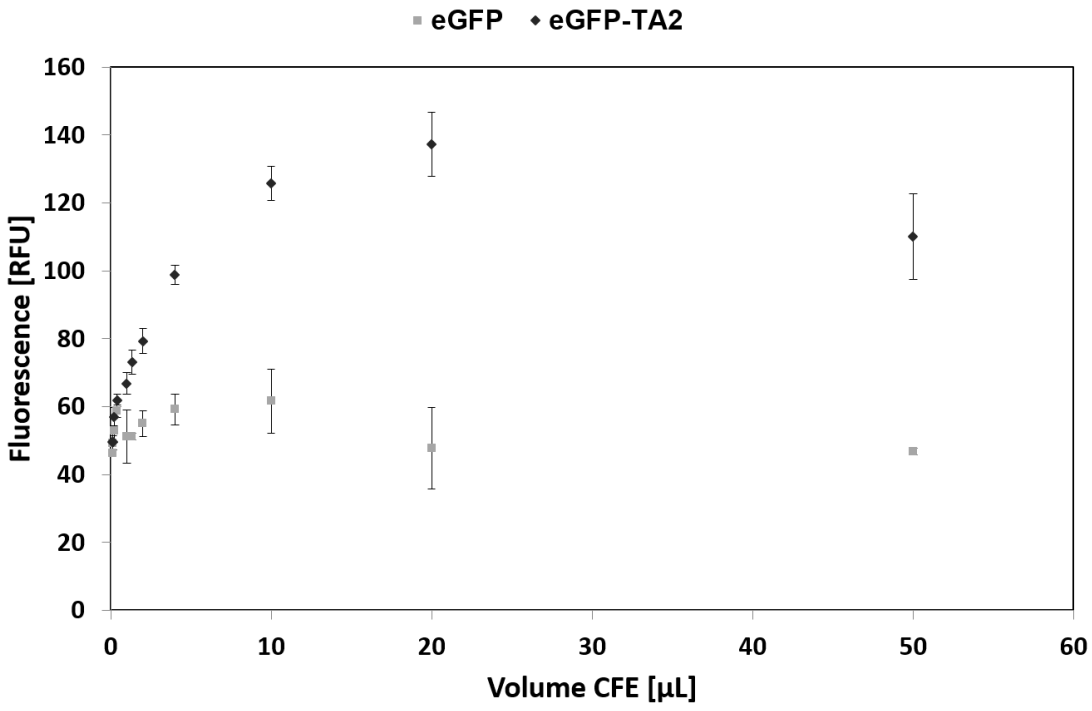

Figure 10: Surface saturation of PS-MTPs with eGFP-TA2. PS-MTP surface was saturated with eGFP (black diamonds) and eGFP-TA2 (grey triangle) CFEs. The CFE amount in immobilization step was varied between 0.5-50 µL in 100 µL working volume and remaining fluorescence was detected after selection with 0.5 mM LAS. Scheme according to (Rubsam, Weber et al. 2018).

Additionally, a calibration curve of eGFP-TA2 fluorescence was determined to detect the linearity of the ABBA screening system. Therefore, eGFP-TA2 was purified by metal affinity chromatography. eGFP-TA2 was coated on the PS surface in serial dilutions (0.1-7 µM) (see Figure 11). After two successive washing steps with Tris/HCl buffer (50 mM, pH 8.0), the remaining fluorescence was measured on the PS surface. A linear range of eGFP-TA2 fluorescence was determined from 0.1-7 µM of applied protein concentration that corresponded to 70.8-105839 RFU.

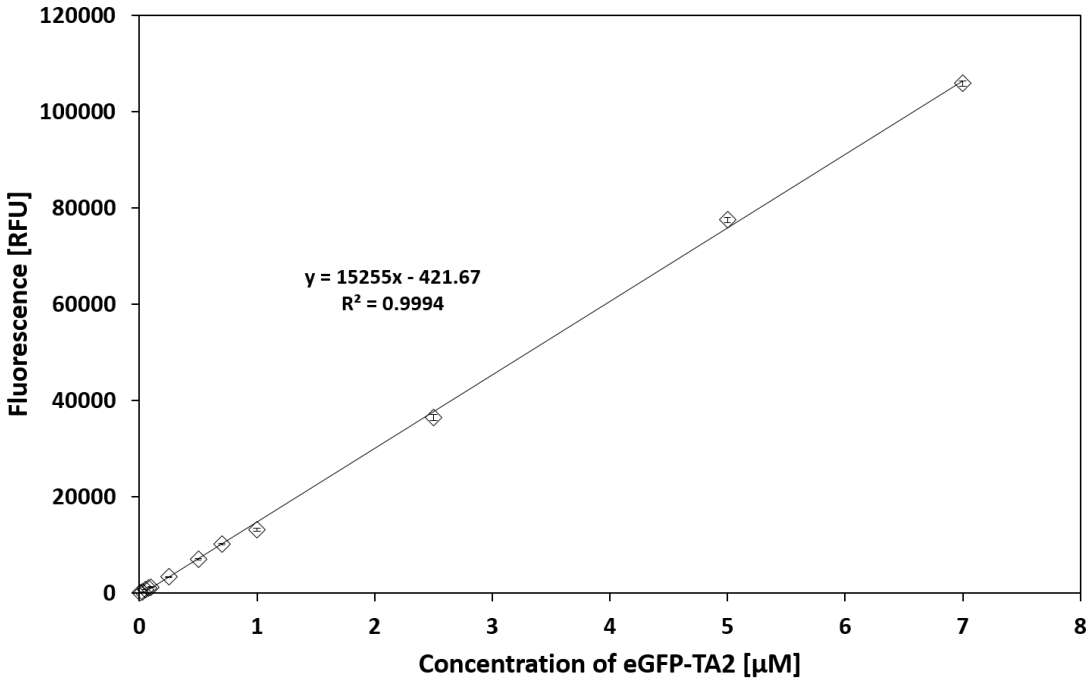

Figure 11: Linearity of ABBA screening system. The linearity of detected eGFP-TA2 was determined by serial dilutions of purified protein. After two successive washing steps with Tris/HCl buffer (50 mM, pH 8.0), the remaining fluorescence was measured on the PS surface. Scheme according to (Rubsam, Weber et al. 2018).

In summary, the performance of the ABBA screening using 10 µL CFE/well ensures an efficient PS-surface coverage eliminating expression muteins. Therefore, 10 µL CFE/well were selected for the screening of the eGFP-TA2 epPCR library.

2.5.4 Adjustment of the selection pressure in ABBA

The screening of eGFP-TA2 epPCR library was performed in black PS MTP plates that enabled a fluorescence detection. These plates are composed of hydrophobic surfaces.

Many *E. coli* proteins have hydrophobic patches on their surface and adsorb to PS plates (Rosano and Ceccarelli 2014). In order to remove unspecifically attached *E. coli* protein background from the PS surface and to remove weak-binding eGFP-TA2 variants, the anionic surfactant LAS was applied as selection pressure in the ABBA screening. Anionic detergents promote protein unfolding by electrostatic or hydrophobic interactions with surface-attached proteins (Otzen 2011).

The behavior of surfactants is strongly dependent on the critical micelle concentration (CMC). The CMC of a surfactant is the value at which surface active ions or molecules in solution associate into micelles. Each surfactant has a characteristic CMC value at a given temperature and electrolyte concentration. Above the CMC, monomers and micelles exist in dynamic equilibrium (Tadros 2013). In dilutions below the CMC, the surface tension is proportionally dependent on the logarithmic concentration of detergent. Higher concentrations above the CMC do not influence the surface tension, a plateau is reached. At the point of CMC, the surfactant exhibits a sharp concentration dependent discontinuity (Chakraborty, Chakraborty et al. 2011).

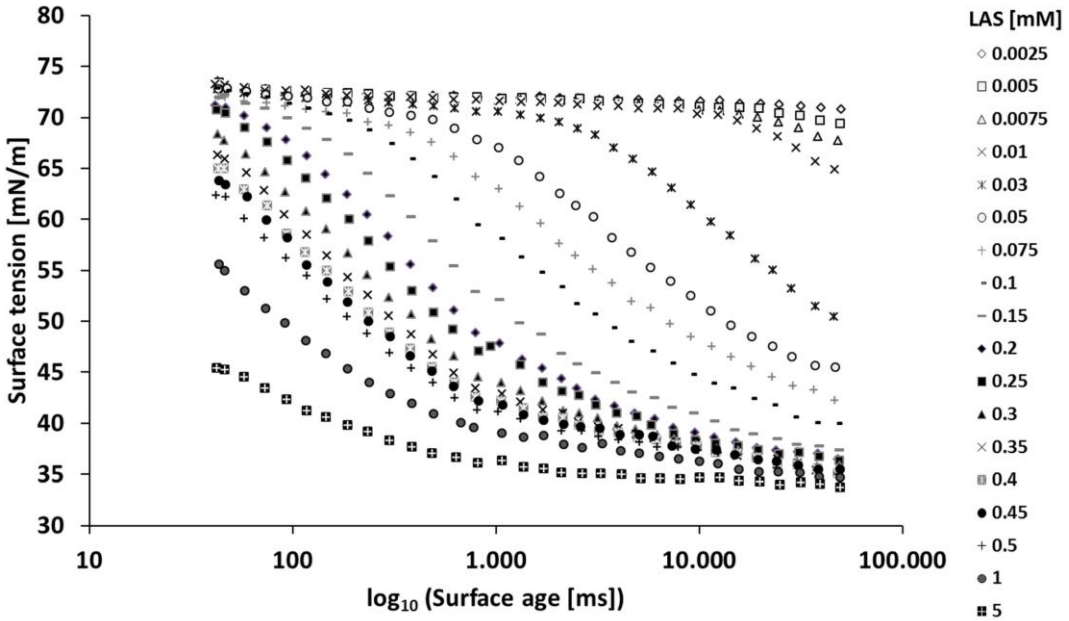

Figure 12: Surface tension of LAS in dependence of surface age. The surface tension (mN/m) of LAS was analyzed in serial dilutions (0.0025-5 mM in 50 mM Tris/HCl pH 8.0) over a time of 50,000 ms (log10 (surface age[ms])). Surface tension is decreasing with increasing LAS concentration.

Serial dilutions of LAS in Tris/HCl buffer (50 mM, pH 8.0) were analyzed at a surface age of 50,000 ms to determine the CMC of LAS under assay conditions (see Figure 12). The surface tension (mN/m) of LAS was plotted over the logarithmic (log10) concentration of LAS [mM]. The logarithmic concentration was in a linear range between 0.0075 and 0.1 mM LAS. Increasing LAS concentrations (0.2-1 mM) did not result in a significant change of surface tension and were used to determine the plateau. The CMC of LAS war calculated to 0.105 mM LAS (see Figure 13).

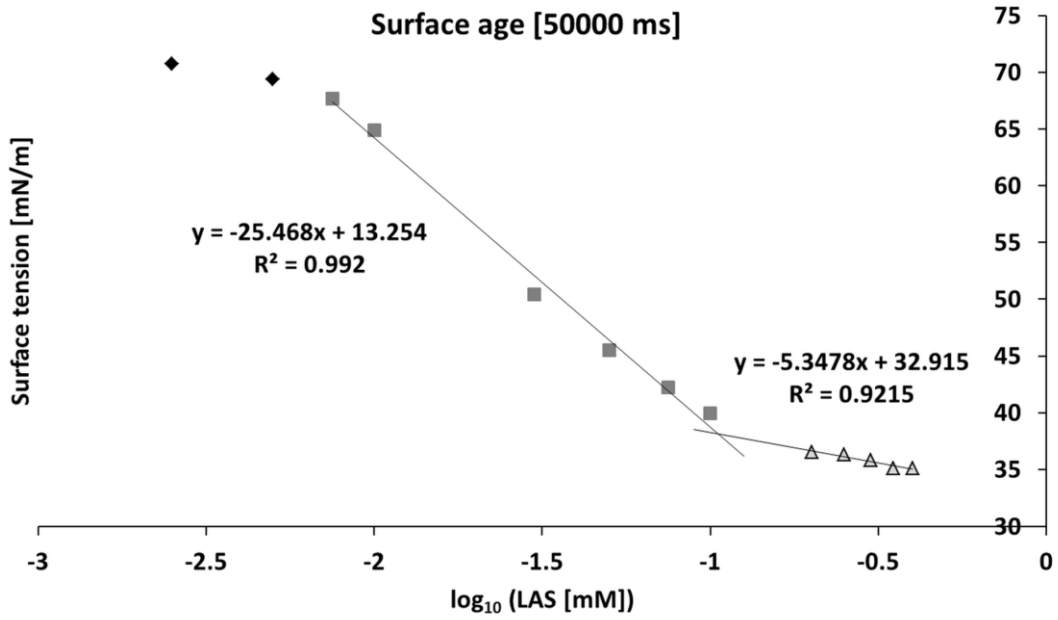

Figure 13: Critical micelle concentration of LAS. Surface tension (mN/m) was plotted against logarithmic concentration of LAS [mM] at a surface age of 50,000 ms. The calculated lines of linear decrease in surface tension (grey squares) and plateau (grey triangles) were extrapolated to the point of intersection.

A concentration-dependent release of eGFP and eGFP-TA2 from the PS-MTP surface was investigated in presence of increasing LAS concentrations (see Figure 14). Lower LAS concentrations (0-0.1 mM) below the CMC of LAS (0.105 mM) did not strongly effect the binding of eGFP-TA2 to the PS surface. LAS concentrations above the CMC (from 0.1-5 mM) had a strong desorptive effect on eGFP-TA2, whereby an increase from 0.5-5 did not lead to a proportional detachment of eGFP-TA2 from the surface. Finally, a LAS concentration of 0.5 mM was applied as selection pressure for the screening of the epTA2

library and an average fluorescence value of 99.3 ± 4.2 RFU was detected. LAS desorbed 53 % of initially immobilized eGFP-TA2 from the surface (0 mM LAS, 208.2 ± 16.6 RFU). Improved PS-binding eGFP TA2 variants could be identified within the linear range of the developed ABBA screening (lower detection limit 70 RFU). No significant difference in fluorescence was detected when the PS wells were incubated with either the negative control eGFP or selection buffer (0.5 mM LAS in 50 mM Tris/HCl, pH 8.0; 48-66 RFU; Figure 14).

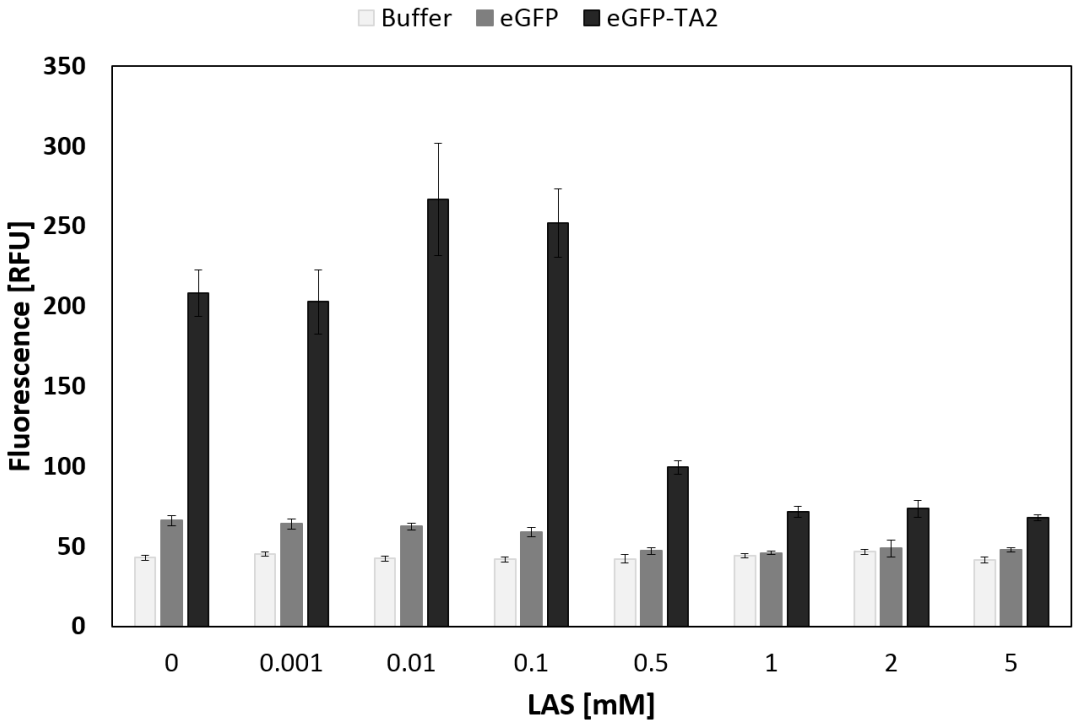

Figure 14: Concentration adjustment of the selection pressure LAS. Immobilized eGFP-TA2 was washed with Tris/HCl buffer (50 mM, pH 8.0) containing different LAS concentrations (0.001-5 mM). Fluorescence signal of remaining eGFP was detected for buffer-treated PS-wells (white), PS-wells incubated with eGFP (light grey), and PS-wells incubated with eGFP-TA2 (black). Scheme according to (Rubsam, Weber et al. 2018).

2.5.5 Standard deviation of eGFP-TA2 in ABBA

A final standard deviation of 10.6 % was obtained with optimized parameters in the ABBA screening system (see Figure 15; lysis (1 mg/mL lysozyme, 150 µL/well), 10 µL/well eGFP-TA2 CFE, two subsequent washing steps (Tris/HCl (50 mM, pH 8.0, 100 µL/well)), and selection with LAS (0.5 mM, 100 µL/well). The standard deviation was determined by performing the ABBA screening with eGFP-TA2 in a complete 96-well MTP.

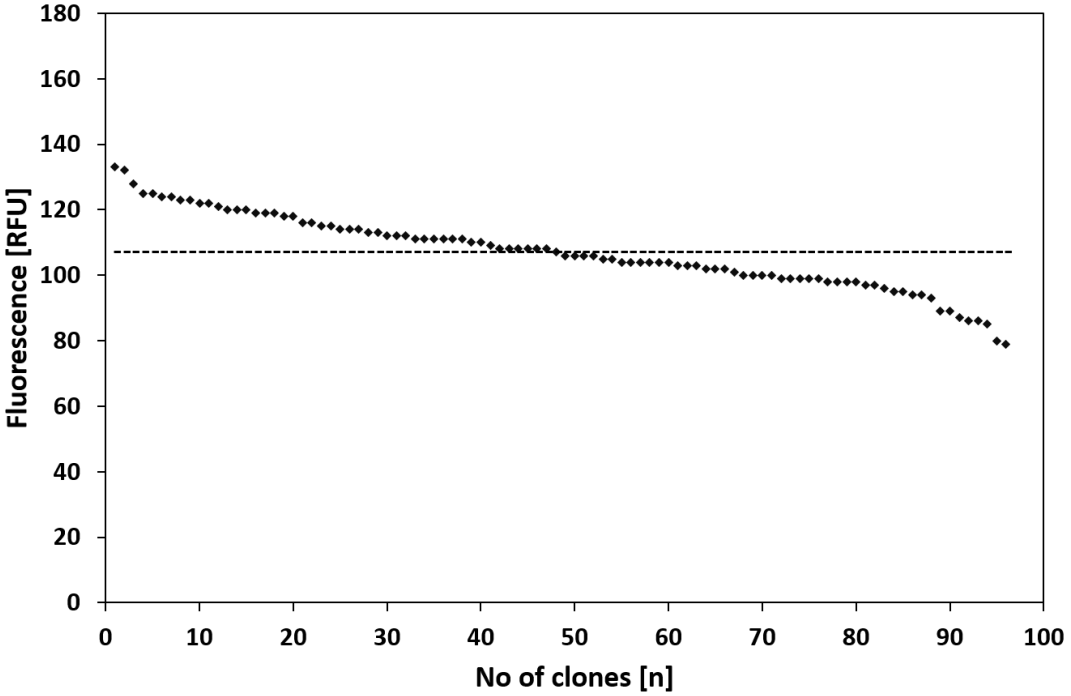

Figure 15: Standard deviation of eGFP-TA2 in ABBA. eGFP-TA2 was incubated in 96 replicates on a PS-MTP and eluted with LAS (0.5 mM). Detected fluorescence in the PS-MTP wells was plotted in descending order. All RFU values were used to determine the standard deviation of the ABBA screening (10.6 %). The population mean (107 RFU) is indicated by a dashed line. Scheme according to (Rubsam, Weber et al. 2018).

2.5.6 Validation of the directed PePevo protocol for polymer binding anchor peptides

The anchor peptide TA2 was evolved for stronger PS-binding in presence of the anionic surfactant LAS (0.5 mM) to validate the applicability of the PePevo protocol. The ABBA screening system was applied to analyze 1000 variants from the generated eGFP-TA2 epPCR library. The detected relative fluorescence units [RFU] represented a direct quantification of the amount of immobilized eGFP-TA2. The background fluorescence of the negative control eGFP was subtracted from each fluorescence value of eGFP-TA2 variants and eGFP-TA2 wild type. A relative improvement of eGFP-TA2 variants was determined by dividing the fluorescence values of eGFP-TA2 variants by fluorescence values of the eGFP-TA2 wild type (see Equation 1).

Equation 1: $$Relative\ improvement = \frac{RFU\ (eGFP{-}TA2\ variant)}{RFU\ (eGFP{-}TA2\ WT)}$$

eGFP-TA2 variants were defined as improved PS-binders if the ratio was >1.5. Screening of the eGFP-TA2 library towards improved PS-binding in presence of 0.5 mM LAS identified variant TA2-M1-PS with a 6.3 fold higher fluorescence signal in comparison to the eGFP-TA2 WT. The mutations, fluorescence values, and relative improvements of the best two variants are listed in Table 5.

Table 5: eGFP-TA2 variants identified by DE with improved PS-binding in presence of 0.5 mM LAS.

Variants	Amino acid substitutions	Fluorescence [RFU]	Fold of improvement
eGFP	-	50.8 ± 7.8	
eGFP-TA2 WT	-	82.0 ± 8.2	1.0
TA2-M1-PS	R3S, L6P, V12K, S15P, C29R, R30L, F33S, Y44H	250.8 ± 13.9	6.3
TA2-M2-PS	F9C, C24S, G26D, S31G, C41S, Y44Q	241.8 ± 40.8	6.0

2.5.7 Characterization of identified eGFP-TA2 variants TA2-M1-PS and TA2-M2-PS

Both identified improved variants were characterized with regards to their binding strength and specificity by an analysis of binding to PS as well as PP in presence of the anionic surfactant LAS (0.5 mM) and the non-ionic surfactant Triton X-100 (1 mM). Binding of eGFP-TA2 was compared to the binding of the reported PS-binding peptide PS19 (Kumada, Tokunaga et al. 2006). Therefore, TA2-M1-PS, TA2-M2-PS, eGFP-TA2 WT, the eGFP control, and the reference peptide eGFP-PS19 were produced in a MTP plate with 6 replicates each.

The binding strength of eGFP-TA2 WT to PS and PP in presence of LAS and Triton X-100 was comparable to the reference peptide eGFP-PS19. The analysis of PP- and PS-binding in presence of Triton X-100 (1 mM) showed, that both, the eGFP-TA2 WT as well as eGFP-PS19 bound stronger to PP than PS. The generated variant TA2-M2-PS showed an up to 3.4-fold improved PP-binding in presence of Triton X-100 and an up to 2.3-fold improved PS-binding in presence of Triton X-100 (1 mM). The detected binding of both variants TA2-M1-PS and TA2-M2-PS to PS in presence of Triton X-100 was surprisingly significantly lower than the comparable binding to PP. The analysis of PP- and PS-binding in presence of LAS showed, that both variants TA2-M1-PS and TA2-M2-PS and showed an up to 6.5-

fold improved binding to PS and also an up to 9.9-fold improved binding to PP in presence of 0.5 mM LAS (see Figure 16).

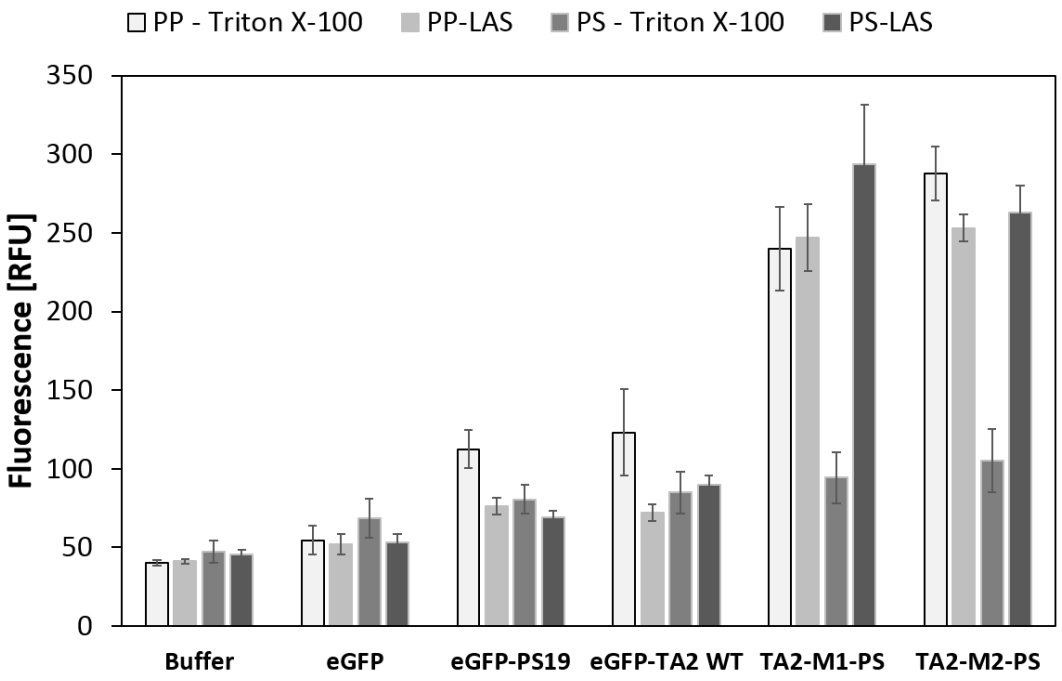

Figure 16: Characterization of identified improved eGFP-TA2-PS variants. PP-and PS MTP plates were incubated with buffer, eGFP control, eGFP-PS19, eGFP-TA2 WT, TA2-M1-PS, and TA2-M2-PS. Remaining fluorescence was detected after elution with 1 mM Triton X-100 and 0.5 mM LAS. Scheme according to (Rubsam, Weber et al. 2018).

2.6 Discussion

Bio-functionalization of polymers is often necessary for bio-sensor/chip technologies or for the production of medical devices. DE offers novel and exciting opportunities to tailor short peptides for a targeted surface binding. Anchor peptides have a great potential to become commonly applied for surface functionalization and offer unique advantages as they enable an immobilization of proteins on a given surface in monolayers. The coating can be performed in aqueous solution at ambient temperature (Rübsam, Stomps et al. 2017). Additionally, several chemical functionalities (e.g., carboxyl, hydroxyl, thiol or amines) can be introduced onto surfaces, which expands conventionally used chemical and physical surface modification techniques. Surface binding peptides were identified with binding affinities for numerous materials (e.g., (noble-) metals, silicon nitride, and polymers) as reviewed comprehensively by Care *et al*. and Seker *et al*. (Seker and Demir 2011, Care, Bergquist et al. 2015). Advantageously, simple and industrially used

techniques (e.g., dip coating, spraying or foulard processing) can be used to immobilize proteins for surface functionalization including sophisticated 3D structures (e.g., medical devices).

Industrial application of enzymes often include a high performance under non-natural conditions (e.g., the presence of surfactants). Therefore, enzymes for laundry, bakery, or production of chemicals have been reengineered extensively (Korfer, Pitzler et al. 2016, Molina-Espeja, Vina-Gonzalez et al. 2016, Sheldon and Pereira 2017). Since 2010, more than 500 successful DE campaigns have been reported yearly, that enabled an adaptation of target enzymes application conditions (Cheng, Zhu et al. 2015). The evolution of anchor peptides required a protocol that enabled the introduction of sufficient diversity in anchor peptide mutant libraries. The PeP*evo* protocol represented a first DE protocol capable of generating a high diversity in very short anchor peptide genes. PeP*evo* was validated by DE of TA2 towards an improved binding strength to PS in presence of the anionic surfactants LAS. A very high mutational frequency was used to diversify the *ta2* gene. A frequency of 59 mutations/kb was determined that led to an average of 4.4 aa substitutions per generated TA2 variant. Previously performed DE campaigns reported mutagenesis frequencies with a mutational load of 33 mutations/kb (casting epPCR) (Yang, Ruff et al. 2017) and 11.7 mutations/kb (epPCR-high) (Zhao, Kardashliev et al. 2014), respectively. The obtained mutational frequency obtained by the developed PeP*evo* protocol was almost twice as high.

The developed ABBA screening system was optimized to a standard deviation of 10.6 % and proved to be a robust and reliable tool for the analysis of the eGFP-TA2 epPCR library. In classical DE campaigns, screening systems with a standard deviation of up to 18 % are routinely employed (Tee and Schwaneberg 2007). The ABBA screening system was employed to identify PS-binding eGFP-TA2 variants that showed improved binding in presence of the applied anionic surfactant LAS (0.5 mM LAS). The fluorescent fusion partner eGFP was used as a reporter protein. eGFP was immobilized by the TA2 variants on the PS MTP surface and quantification of fluorescence was proportional to the anchor peptide binding. The developed ABBA screening system had to exclude expression variants reliably (Jakob, Lehmann et al. 2013). Therefore the applied concentration of eGFP-TA2 in the immobilization step proved to be crucial to obtain surface saturation in

the PS-MTP plates. Finally, a CFE volume of 10 µL/well which corresponded to an eGFP-TA2 concentration of 5.9 ± 0.6 µM was required for surface saturation.

In the performed PeP*evo* campaign, eGFP-TA2 variants were identified that bound 6.5-fold (TA2-M1-PS) stronger to PS in presence of the anionic surfactant LAS compared to the eGFP-TA2 WT. Both variants, TA2-M1-PS and TA2-M2-PS, which were evolved for improved PS-binding (in presence of LAS) revealed additionally a stronger binding to PP. An improved binding to PP was observed in presence of Triton X-100 (up to 4.4 fold) as well as LAS (up to 9.9 fold). Surprisingly, neither TA2-M1-PS nor TA2-M2-PS showed improved binding to PS in presence of Triton X-100. These binding studies reveal that the selectivity of an evolved peptide variant significantly depends on the selected polymer as well as selection pressure. It demonstrated as well, that anchor peptides can be evolved towards a high binding specificity when DE is performed in iterative rounds.

The reported PS-binding peptide eGFP-PS19 (Kumada, Tokunaga et al. 2006) showed a comparable binding strength to PS as well as to PP to eGFP-TA2 in presence of Triton X-100 (1 mM) and LAS (0.5 mM) (see Figure 15). The evolved eGFP-TA2 variants showed, in comparison to eGFP-PS19, a considerably increased binding to the investigated hydrophobic PS (TA2-M1-PS (14.9-fold) and TA2-M2-PS (13.0-fold) in presence of LAS. These results confirmed that DE is a powerful algorithm to engineer anchor peptides for application conditions.

3 Ultra-high-throughput screening system for directed polymer binding peptide evolution

3.1 Declaration

Parts of this chapter were submitted by the author to the journal Biotechnology and Bioengineering.

Apitius L, Rübsam K, Jakesch C, Jakob F, Schwaneberg U (2019). Ultra-high-throughput screening system for directed polymer binding peptide evolution.

3.2 Objective and main results

A great challenge of the *Anthropocene era* will be the reduction and prevention of accumulated plastics in the environment. One possibility to reduce plastic waste in the environment is an enzymatic degradation. In order to bring microorganisms that release polymer-degrading enzymes into close distance to the polymer particles, an adhesion promoter is needed. Anchor peptides fulfill these requirements and enable a targeted immobilization of whole cells on polymer surfaces. An esterase A-based *E. coli* cell surface display (CSD) screening system was developed, that enabled DE of anchor peptides for improved binding strength to polymers. The ultra-high-throughput screening system allowed an enrichment of improved binding LCI variants from a culture broth by an immobilization of whole cells on PP-beads. The PP-binding peptide LCI was diversified by a simultaneous saturation of five positions (Y29, D31, G35, E42, and D45) whereby theoretically 3.2 million variants could be generated. Applying the CSD system, the generated LCI diversity was analyzed by screening in total 10 million clones. LCI was screened for an improved binding to PP beads in presence the surfactant LAS (0.25 mM). Identified LCI variants revealed an up to 12-fold improved PP-binding strength in presence of LAS (0.125 mM). The CSD system is a first whole-cell ultra-high-throughput screening system to improve anchor peptides (see Figure 17).

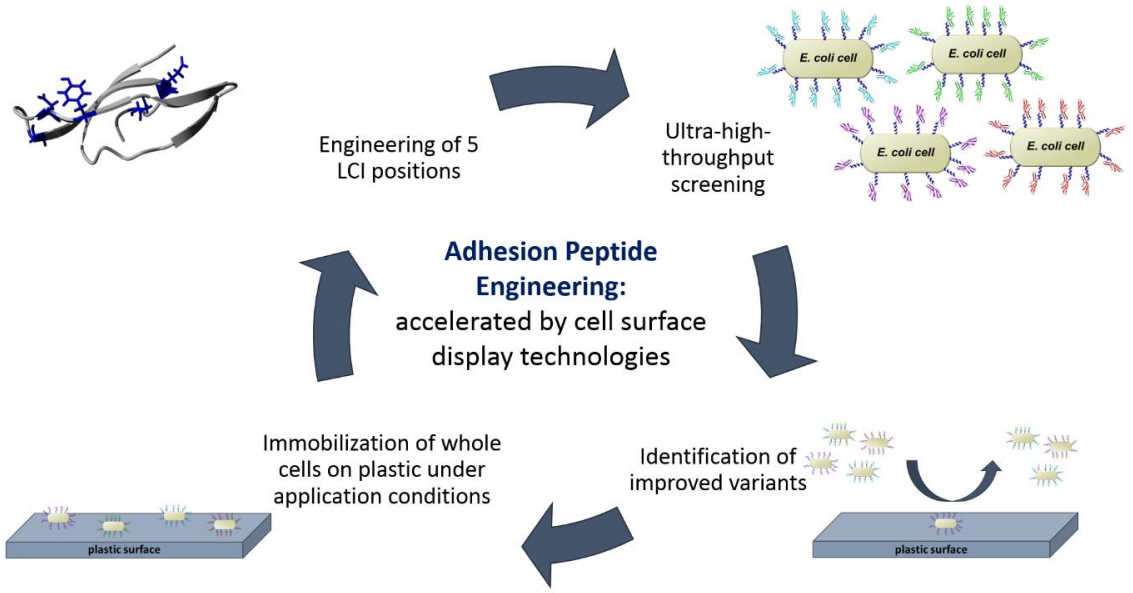

Figure 17: Schematic overview of the ultra-high-throughput CSD screening system. The anchor peptide LCI was saturated at five positions. An esterase A-based display system was used to present mutated LCI variants on the surface of *E. coli* cells. Whole cells were immobilized on PP-beads and improved binding variants were identified after cell recovery.

3.3 State of the art

In 2017, the global production of plastics was estimated to be 8,300 million metric tons (Mt). Plastic waste is accumulating in the environment and a drastic increase of plastic waste in landfills is predicted in 2050 (12,000 Mt) (Geyer, Jambeck et al. 2017). Main causes for a global environmental pollution are inadequate handlings of waste management, disposal and recycling of plastics (Geyer, Jambeck et al. 2017). In nature, plastics degrade slowly and degradation can take several hundreds of years (Barnes, Galgani et al. 2009). Therefore, it is of uttermost importance to develop degradation strategies for plastics, including an enhanced bio-degradation. The production of plastics started in the 1950´s which is, from an evolutionary point of view, a relatively short time span. Consequently, the evolutionary pressure for organisms to evolve enzymes for efficient plastic degradation was rather low (Hopewell, Dvorak et al. 2009, Tokiwa, Calabia et al. 2009). However, some plastic degrading organisms exist, that are able to degrade polymers like PET, PP, and PS (Cacciari, Quatrini et al. 1993, Shah, Hasan et al. 2008, Auta, Emenike et al. 2017, Pathak and Navneet 2017). A first step, to ensure an efficient

degradation of plastics is to bring organisms into close proximity or to attach organisms to the targeted polymer surfaces.

Material binding peptides can be employed as adhesion promoters to immobilize bacteria on plastics surfaces. Material binding peptides offer versatile advantages for a directed enzyme immobilization (Qiang, Sun et al. 2017, Zernia, Frank et al. 2018), a formation of hybrid biomaterials (Nguyen, Botyanszki et al. 2014) or improved nanomaterial biocompatibility (Zhang, Zheng et al. 2012). Particulate matter binding peptides that bind components like Cu and Zn were employed as probes for the detection of air pollution (Liang Alvin, Tanaka et al. 2017). In biomining, a molybdenite (MoS_2) binding peptide was coated on magnetic nanoparticles to harvest the trace element as a by-product in copper and tungsten mines (Cetinel, Shen et al. 2018).

Target-specific binding peptides are often identified by phage, mRNA or cell surface display technologies (Smith 1985, Mattheakis, Bhatt et al. 1994, Boder and Wittrup 1997). The use of display systems allows the generation and screening of large libraries in an ultra-high throughput (uHTS) set-up. Randomized peptide libraries in phage displays commonly consist of short peptides with a length of 6 to 43 amino acids. These libraries can contain up to 10^{12} phage particles (Galan, Comor et al. 2016). Synthetic phage peptide libraries are commonly generated for medical applications, such as binding studies of bioactive peptides, epitope mapping (B-cells and T-cells) or the development of peptide-mediated drug delivery systems (Wu, Liu et al. 2016). mRNA display systems are *in vitro*-based technologies that contain up to 10^{14} peptide sequences and offer the highest screening throughput (Cotten, Zou et al. 2012). mRNA display systems were for instance employed for DE campaigns of scaffold proteins like the DNA binding domain of the retinoid-X-receptor, which was engineered towards functional ATP recognition (Cho and Szostak 2006).

Microbial cell surface displays are possible systems often used in DE campaigns to display binding peptides (van Bloois, Winter et al. 2011) due to a general applicability and simplicity in handling. Especially antibodies and scaffold proteins were engineered applying yeast display technologies as reviewed comprehensively by Boder *et al.* and Könning *et al.* (Boder, Raeeszadeh-Sarmazdeh et al. 2012, Konning and Kolmar 2018). In yeast display technologies, library sizes of up to 10^9 mutants are generated. However, yeast display systems are, in comparison to bacterial display systems, comparably time-

consuming due to a slower growth rate of yeast cells (Benatuil, Perez et al. 2010, Salema and Fernandez 2017). Enzymes, antibodies, nanobodies, and peptides have been improved by the application of bacterial display systems (Jose, Betscheider et al. 2005, Bidlingmaier, Su et al. 2015, Salema and Fernandez 2017). A commonly applied bacterial cell surface systems is based on an esterase (*EstA*) of *Pseudomonas aeruginosa. EstA* has been applied for a functional surface presentation of enzymes (e.g., LipA (*B. subtilis*) or cutinase (*F. solani pisi*)) (Becker, Theile et al. 2005) or hybrid catalysts (Grimm, Sauer et al. 2018) on the *E. coli* cell surface. The autotransporter *EstA* belongs to the GDSL-family of lipolytic enzymes and is part of the type V_a secretion pathway (Upton and Buckley 1995, Wilhelm, Tommassen et al. 1999, Henderson, Navarro-Garcia et al. 2004). An N-terminal passenger domain is fused to the C-terminal anchor domain of *EstA*. The autotransporter is secreted into the periplasm whereby the C-terminal anchor domain forms a β-barrel structure that inserts into the outer cell membrane. The extracellular domain (catalytically inactivated) and the passenger domain are finally translocated to the cell surface (Becker, Theile et al. 2005, Wilhelm, Rosenau et al. 2011). A surface presentation of approximately 36,000 *EstA* copies has been reported for *E. coli* cells (Becker, Michalczyk et al. 2007).

The natural occurring material binding anchor peptide LCI (Gong, Wang et al. 2011) binds to PP by forming a dense monolayer of 4.1 nm on the surface (Rübsam, Stomps et al. 2017). The usage of LCI as fusion partner of a CueO laccase enabled semi-purification of the enzyme in 96-well microtiter plates in a DE campaign (Zou, Mate et al. 2018). The binding of LCI was additionally optimized in a peptide evolution campaign (PeP*evo*, epPCR based) (Rubsam, Weber et al. 2018) and in a knowledge gaining directed evolution (KnowVolution) campaign for improved PP-binding strength in presence of Triton X-100. KnowVolution of LCI yielded a 5.4 fold improved PP-binder (Y29R, G35R) in presence of Triton X-100 (Rübsam, Davari et al. 2018). Both engineering strategies based on screening of around 1000 clones in MTP format requiring lysis of *E. coli* cells to determine improved binding strength.

3.4 Material & Methods

Chemicals used in this chapter were obtained from Sigma-Aldrich Corp. (St. Louis, USA), AppliChem GmbH (Darmstadt, Germany) or Carl Roth GmbH (Karlsruhe, Germany) in analytical-reagent grade or higher purity. Synthetic genes were ordered at GeneArt AG (Regensburg, Germany) and oligonucleotides were ordered from Eurofins Scientific SE (Ebersberg, Germany) in salt-free form. The enzymes used in this study were obtained from New England Biolabs GmbH (Frankfurt am Main, Germany). The PCR purification and plasmid extraction kits were obtained from Qiagen GmbH (Hilden, Germany) and Macherey-Nagel GmbH & Co. KG (Düren, Germany). The plasmids pET22b(+) and pET28a(+) (Novagen, Darmstadt, Germany) were utilized as expression vectors. The expression strain *E. coli* BL21-Gold (DE3) was ordered from Agilent Technologies (Santa Clara, USA). PP-beads (Moplen HF501N) were purchased from LyondellBasell Industries (Cologne, Germany). Black PP 96-well microtiter plates were obtained from Greiner Bio-One GmbH (Frickenhausen, Germany). The FITC-tagged anti-E-epitope antibody (NB600-525) was obtained from Novus Biologicals, (Littleton, USA).

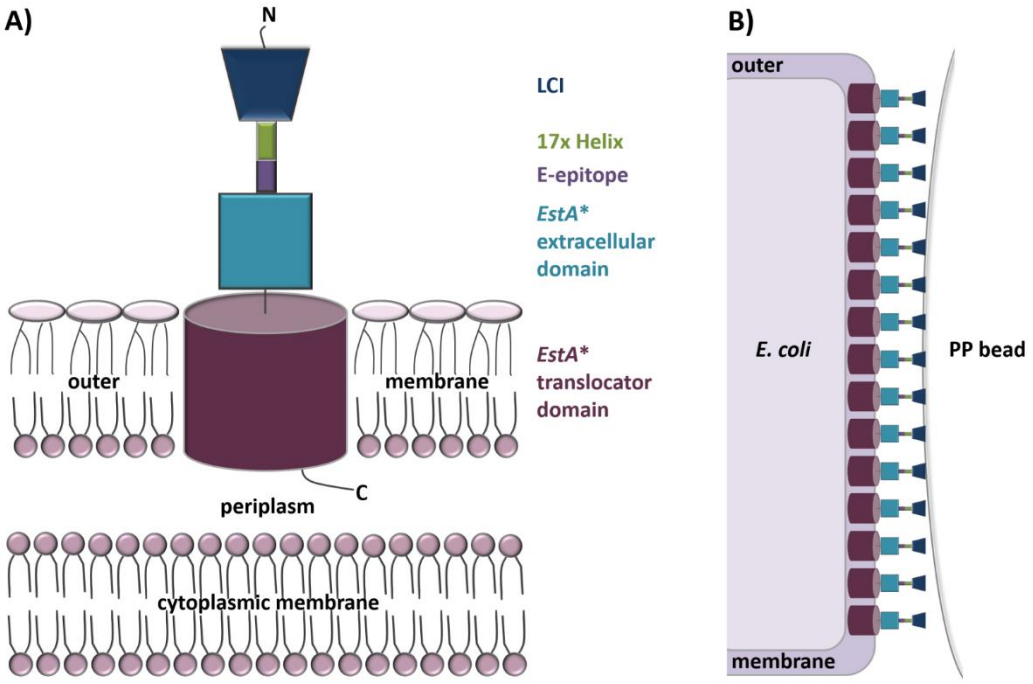

Figure 18: Surface-displayed LCI immobilizes whole cells on PP beads. A) The PP-binding peptide LCI (PDB: 2B9K) is translocated as a passenger of the *EstA* autotransporter (PDB: 3KVN) to the cell surface of *E. coli.* **B)** LCI immobilizes *E. coli* cells on PP-beads.

3.4.1 Generation of LCI-CSD construct, CSD control and LCI-CSD-SSM library

LCI-CSD (see Figure 18) and CSD control were cloned by PLICing (Blanusa, Schenk et al. 2010) in a pET22b(+) backbone according to the protocols described in the Appendix chapter IV. The autotransporter *EstA* was catalytically inactivated by an introduction of the mutation S38A (indicated by *) (Becker, Theile et al. 2005). The target sequence *ompA-lci-17xhelix-e-eptitope-estA** was amplified using the primers pair FW CSD-LCI and REV-CSD-LCI. The vector backbone was amplified using the primers pair FW-CSD-pET22b and REV-CSD-pET22b. All primers carried complementary phosphorothioated nucleotides (PTOs) at the 5'-end (see Table 6). The CSD-control was cloned as a negative control by deleting *lci* from the pET22b::LCI-17xHelix-CSD backbone in a two-step-PCR with the overlapping primer pair FW-CSD-control and Rev-CSD-control (see Table 6).

Table 6: Primers used for the generation of CSD constructs.

Name	Sequence 5' → 3'
FW-CSD-pET22b*	gca gaa gca gca GCA AAA GAA G
REV-CSD-pET22b*	atg tat atc tcC TTC TTA AAG TTA AAC
FW-CSD-LCI*	gag ata tac atA TGA AAA AAA CCG CGA TTG
REV-CSD-LCI*	tgc tgc ttc tgc TTT GCG ATC
FW-CSD-control	GCA GAA GCA GCA GCA AAA GAA GCC GCT G
REV-CSD-control	CTG CTG CTT CTG CCG CGT TCG CCA CGG TC
FW-LCI-CSD-5SSMs**	TAT TGG GTG GGT ATT TAT **NNK** GTG TGG **NNK** CGC AAA G
REV-LCI-CSD-5SSMs**	CAC CCA ATA **MNN** TTT GCT GCT **MNN** ATA **MNN** TTT GCT TTT G
FW-LCI-CSD-LW1	TAT TGG GTG GGT ATT TAT **CAG** GTG TGG **TCT** CGC AAA TAA TAA CAC TG
REV-LCI-CSD-LW1	CAC CCA ATA **ATC** TTT GCT GCT **AGT** ATA **ACA** TTT GCT TTT G
FW-LCI-CSD-LW2	GGT TAT TGG GTG GGT ATT TAT **GGG** GTG TGG **GGG** CGC A
REV-LCI-CSD-LW2	CAC CCA ATA ACC TTT GCT GCT **CGC** ATA **AAC** TTT GCT TTT G
FW-LCI-CSD-LW3	GGT TAT TGG GTG GGT ATT TAT **GTG** GTG TGG **CAT** CGC A
REV-LCI-CSD-LW3	CAC CCA ATA ACC TTT GCT GCT GTC ATA GTA TTT GCT TTT G

*** Lower case letters indicate phosphorothioated nucleotides (PTOs)**
**** NNK and MNN indicate positions for site saturation mutagenesis**

The LCI positions Y29, D31, G35, E42, and D45 (see Figure 19) were simultaneously diversified by site-saturation mutagenesis (SSM) to generate the LCI-CSD library. The template pET22b::LCI-17xHelix-CSD was amplified (see Table 7) using the degenerated NNK primers FW-LCI-CSD-5SSMs and REV-LCI-CSD-5SSMs (see Table 6).

Table 7: PCR conditions for LCI-CSD library generation (SSM).

Step	Temperature [°C]	Time [s]	Cycles [n]
Initial denaturation	98	120	1
Denaturation	98	30	25
Annealing	60	45	25
Elongation	72	600	25
Final elongation	72	600	1
Storage	8	∞	

NNK primers enable the introduction of 32 codons, whereby N codes for A, C, G or T and K codes G and T. One stop codon and all 20 proteinogenic amino acids can be introduced at each SSM position (Reetz and Carballeira 2007). The amplified plasmid DNA (7589 bps) was purified by gel extraction (NucleoSpin® Gel and PCR Clean-up Macherey-Nagel GmbH & Co. KG (Düren, Germany)) and subsequently transformed into electro-competent *E. coli* BL21-Gold (DE3).

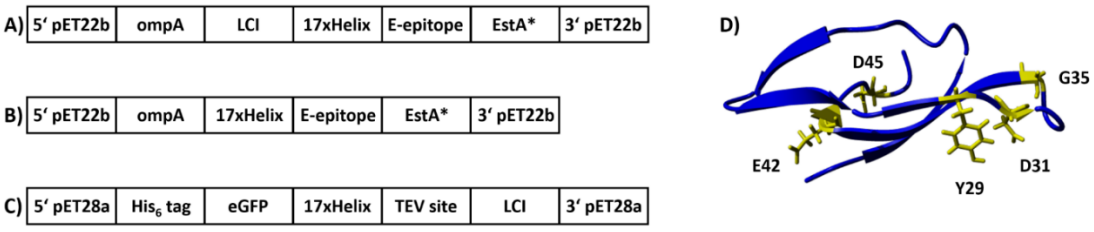

Figure 19: Schematic overview of generated CSD-constructs. CSD-constructs were cloned into a pET22b backbone. **A)** The LCI-CSD construct consisted of (5`-3`) *ompA signal sequence*, *lci*, *17x spacer helix*, *e-epitope*, and *estA** **B)** The CSD control construct consisted of (5`-3`) *ompA signal sequence*, *17x spacer helix*, *e-epitope*, and *estA** **C)** Characterization of improved variants was performed using the eGFP reporter protein. Therefore beneficial mutations were transferred into the pET28a::eGFP-17xHelix-TEV-LCI construct. **D)** Amino acid sequence of LCI indicating the five targeted positions for simultaneous saturation (Y29, D31, G35, E42, and D45).

Beneficial mutations were transferred into the eGFP-LCI system according to the protocols described in the Appendix chapter IV using the pET28a::eGFP-17xHelix-TEV-LCI template and the primer pairs FW-LCI-CSD-1/REV-LCI-CSD-1, FW-LCI-CSD-2/REV-LCI-CSD-2 or FW-LCI-CSD-3/REV-LCI-CSD-3 (see Table 6) and the PCR program shown in Table 7. All generated constructs (see Figure 19) were transformed into electro-competent *E. coli* BL21-Gold (DE3) cells and successful cloning was confirmed by sequencing (Eurofins Genomics GmbH, Ebersberg, Germany).

3.4.2 Production of LCI-CSD library

The production of CSD-control, LCI-CSD-WT and LCI-CSD library was performed in 1 L shaking flasks. Previously, electro-competent *E. coli* BL21-Gold (DE3) cells (3x 50 µL competent cells) were transformed with plasmids (57 ng each) of CSD-control, LCI-CSD-WT and LCI-CSD library by electroporation (1700 V, Eporator®, Eppendorf, Hamburg, Germany). After transformation, SOC media (45 min, 500 µL; 20 g/L tryptone, 2 g/L NaCl, 5 g/L yeast extract, 2.5 g/L KCl, 10 mM $MgCl_2$, 10 mM $MgSO_4$, and 20 mM glucose) was used for cell recovery. The recovered cells were transferred into 200 mL LB media (10 g/L tryptone, 10 g/L NaCl, and 5 g/L yeast extract) supplemented with ampicillin (100 µg/mL). The cells were grown to an OD_{600} of 0.8 (20 h, 30°C, 200 rpm, 70 % humidity; Multitron Pro, Infors AG). The cells were cultivated for 2 h (37°C, 200 rpm, 70 % humidity; Multitron Pro, Infors AG) after induction with ITPG (0.1 mM).

3.4.3 Production of eGFP-LCI and eGFP-LCI variants

eGFP, eGFP-LCI WT and eGFP-LCI variants were produced in 96-well MTP plates according to the protocol described in chapter 2.4.3 (twelve replicates each).

3.4.4 E-epitope staining

The autotransporter *EstA* is translocated through the outer membrane of *E. coli* cells. The translocation of *EstA* and the passenger peptide LCI was visualized by staining the surface presented E-epitope with a FITC-tagged anti-E-epitope antibody (NB600-525, Novus Biologicals, Littleton, USA). Therefore, the OD_{600} of pET22b-EV, CSD-control, and LCI-CSD-WT producing *E. coli* cells was normalized to 0.5. PBS buffer (500 µL; pH 7.4; 140 mM NaCl, 10 mM KCl, 6.4 mM Na_2HPO_4, 2 mM KH_2PO_4) supplemented with 0.2 % (w/v) BSA) was used to wash 300 µL of cells. The anti-E-epitope antibody (10 µL; 1 % (v/v) in PBS buffer pH 7.4) was supplemented to the cell pellet and incubated on ice protected from light (10 min). Superfluous antibody was removed by washing of cells with PBS buffer pH 7.4 (500 µL). The labeled cells were resuspended in PBS buffer pH 7.4 (20 µL) for fluorescence microscopy (Leica TCS SP8 microscope, Ex: 485 nm, Em: 520 nm, argon laser 1 % intensity, gain 1000, Leica Microsystems GmbH (Wetzlar, Germany).

3.4.5 Immobilizing of whole cells on PP beads

Surface-presented LCI variants enabled an enrichment of whole cells on PP beads (Moplen HF501N, LyondellBasell Industries (Cologne, Germany)) from a culture broth. Therefore, CSD-control, CSD-LCI and LCI-CSD library (50 mL each) were produced as described in Chapter 3.4.2 and the cells were incubated subsequently with PP beads (2.5 g, 10 min, and room temperature). Beads and attached cells were transferred to PP disposable columns (Pierce™ Disposable Columns, 10 mL, Cat No: 29924, Thermo Fisher Scientific (Darmstadt, Germany)). In ten subsequent washing steps (10x 5 mL PBS buffer pH 7.4) weakly attached cells were washed out. In three selection steps (2x 5 mL LAS (0.05 mM in PBS buffer pH 7.4) and 1x 5 mL LAS (0.25 mM in PBS buffer pH 7.4) weakly immobilized cells were detached from the PP beads. In each selection step, the cells were incubated with the surfactant for 5 min. Following, LAS and detached cells were washed out by five washing steps (5x 5 mL PBS buffer pH 7.4). Immobilized cells on PP beads were transferred to LB agar plates for cell recovery overnight (37°C, 70 % humidity; Multitron Pro, Infors AG). Three single colonies were transferred into 5 mL LB media (supplemented with ampicillin (100 µg/mL)). After cultivation overnight (37°C, 200 rpm, 70 % humidity; Multitron Pro, Infors AG) the plasmids were isolated (NucleoSpin® Plasmid, Macherey-Nagel GmbH & Co. KG (Düren, Germany)) for sequencing analysis (Eurofins Genomics GmbH, Ebersberg, Germany).

3.4.6 Characterization of improved LCI-CSD variants

Quantification of binding towards PP in presence of the anionic surfactant LAS was performed by a detection of the reporter protein eGFP. Therefore, mutations of identified improved PP-binding LCI variants were transferred to the pET28::eGFP-LCI system (see chapter 3.4.1). For quantification of binding the ABBA screening system was used and performed according to chapter 2.4.5. The fluorescence of the immobilized eGFP-LCI variants was measured directly on the PP surface with the 96-well MTP reader FLUOstar Omega (BMG LABTECH GmbH, Ortenberg, Germany; Ex: 485 nm, Em: 520 nm, gain 1000, 35 reads/well).

3.4.7 Immobilization of LCI-CSD-3 on a PP film

The LCI-mediated binding of whole cells to a PP surface was visualized by Environmental Scanning Electron Microscopy (ESEM). For analysis, the PP foil was cut into pieces (1 cm^2) and cleaned by sonication in NaOH (0.5 M, 10 mL, 30 min, Bandelin Sonorex Digitec (Berlin, Germany)) followed by sonication in ddH_2O (100 mL, 30 min, Bandelin Sonorex Digitec (Berlin, Germany)). After the cleaning process, the PP foil was sterilized by incubation in absolute EtOH (70 %, 50 mL, 30 min). The sterilized PP-foil was air-dried subsequently.

LCI-CSD WT, LCI-CSD-3, and the negative control pET22-EV were produced in *E. coli* BL21-Gold (DE3) cells in 100 mL shaking flasks. Pre-cultures (10 mL LB media supplemented with ampicillin (100 µg/mL)) were inoculated from glycerol stocks and grown overnight (37°C, 200 rpm, 70 % humidity; Multitron Pro, Infors AG). A final OD_{600} of 0.025 from each pre-culture was used to inoculate the main-cultures. The main-cultures were grown (37°C, 200 rpm, 70 % humidity; Multitron Pro, Infors AG) to an OD_{600} of 0.8 and were induced with ITPG (0.1 mM). The cells were cultivated for 4 h (37°C, 200 rpm, 70 % humidity; Multitron Pro, Infors AG).

The cell density of LCI-CSD, LCI-CSD-3, and pET22-EV was normalized to an OD_{600} of 0.5. Normalized cells were incubated on the PP foil (100 µL, 10 min). Superfluous and weakly attached cells were washed off with PBS buffer pH 7.4. Immobilized cells were fixed with glutaraldehyde (3 % in PBS buffer pH 7.4, 16 h, 4°C; Agar scientific (Wetzlar, Germany)) on the PP-film for ESEM analysis. The fixing solution was removed with Soerensen's phosphate buffer (0.1 M, 15 min; Merck KGaA (Darmstadt, Germany)) followed by dehydrating steps in ascending alcohol series (see Table 8).

Table 8: Ascending alcohol series for dehydration of *E. coli* CSD cells.

EtOH [%]	Time [min]
30	10
50	10
70	10
90	10
100	10
100	10
100	10

Following, the cells were dried by critical point drying in liquid CO_2 (E3100 Critical Point Dryer, Quorum Technologies (Lewes, Great Britain)) and the samples were sputtered with a 10 nm layer of Au-Pd (Bal-tec™ (Pfäffikon, Switzerland)) to avoid charging effects of the PP foil (Sputter Coater EM SCD500, Leica (Wetzlar, Germany)). Microscopy was performed in a high vacuum environment by ESEM (ESEM XL30 FEG, FEI, Philips (Eindhoven, Netherlands). Settings of the instrument were: accelerating voltage: 10 kV, working distance: 10.1 mm, magnification: 1000/5000x.

3.5 Results

The results were divided into three sections. The generation and production of the LCI-CSD library was described in the first section. The second section focused on the establishment of screening conditions, in which the selection pressure and washing procedure were optimized. Identified improved PP-binding LCI variants were characterized by the ABBA screening system in the third section. In this section, the immobilization of cells on a PP-foil was additionally visualized by ESEM.

3.5.1 Generation and production of LCI-CSD library

Five LCI positions (Y29, D31, G35, E42, and D45) were saturated simultaneously to generate the LCI-CSD library. All five positions were identified to be key contact positions for PP-binding in presence of the non-ionic surfactant Triton X-100 (Rübsam, Davari et al. 2018). The usage of degenerative primers with five NNK positions theoretically led to the generation of 3.2 million LCI variants in the LCI-CSD library. Ten randomly selected clones were analyzed by sequencing to evaluate the quality of the library. The sequence analysis showed that all five positions were targeted in the diversification and that in each of the clones at least two codons were mutated. On average, 5.5 nucleotides were exchanged per *lci* gene (see Table 9).

The introduction of a stop codon at any of the five SSM positions resulted in truncated LCI variants. Beneficially, these variants were excluded in the developed screening system since a functional autotransporter was not produced.

Table 9: Sequence analysis of mutated LCI SSM positions.

Position	29	31	35	42	45
AA LCI WT	**Y**	**D**	**G**	**E**	**D**
Codon LCI WT	**tac**	**gac**	**ggt**	**gaa**	**gat**
#1	atc		ggc	gag	
#2				ggg	ctt
#3	tag	gcg	gcg	ggt	gtt
#4				ggt	ggg
#5				gcg	tgt
#6				tgg	ttt
#7				ttg	gtg
#8	tgt	act	gat	cag	tct
#9	gtt	gcg		ggg	ggg
#10				gtg	cat

The LCI-CSD library was produced in *E. coli* cells. In order to analyze the generated diversity of LCI variants, the complete transformation mixture (amount of DNA: 0.17 µg) was used for cell cultivation. The number of analyzed clones was estimated by calculating the transformation efficiency. The transformation efficiency of $2.1*10^7$ CFU/µg DNA ($6.3*10^7$ CFU/µg DNA for used three aliquots) accounted for ~10.7 million LCI-CSD variants.

The growth of the LCI-CSD library was optimized to 30°C and 20 h, followed by 2 h cultivation after induction with 0.1 mM ITPG at an OD_{600} of 0.8. For the establishment of the ultra-high-throughput screening system, the negative control pET22-EV (empty vector, represents *E. coli* protein background), CSD-control (72.3 kDa), LCI-CSD WT (77.8 kDa), and LCI-CSD library (77.8 kDa) were produced. A successful production was confirmed by sodium dodecyl sulfate polyacrylamide gel electrophoresis (SDS-PAGE) using a 5 % stacking gel and a 12 % separating gel (Figure 20 A) (Laemmli 1970).

The translocation of the complete CSD-complex to the cell surface is of great importance for an efficient immobilization of the *E. coli* cells by the anchor peptide LCI (and its variants). Therefore, the translocation of CSD-control and LCI-CSD WT was proven by E-epitope staining using a fluorescent FITC-labeled anti E-epitope antibody. For both, CSD-control and LCI-CSD WT, a homogeneous green fluorescence was detected on the *E. coli* cell surface (Figure 20 C and D), whereas for the negative control pET22b-EV no fluorescence was detectable (Figure 20 B).

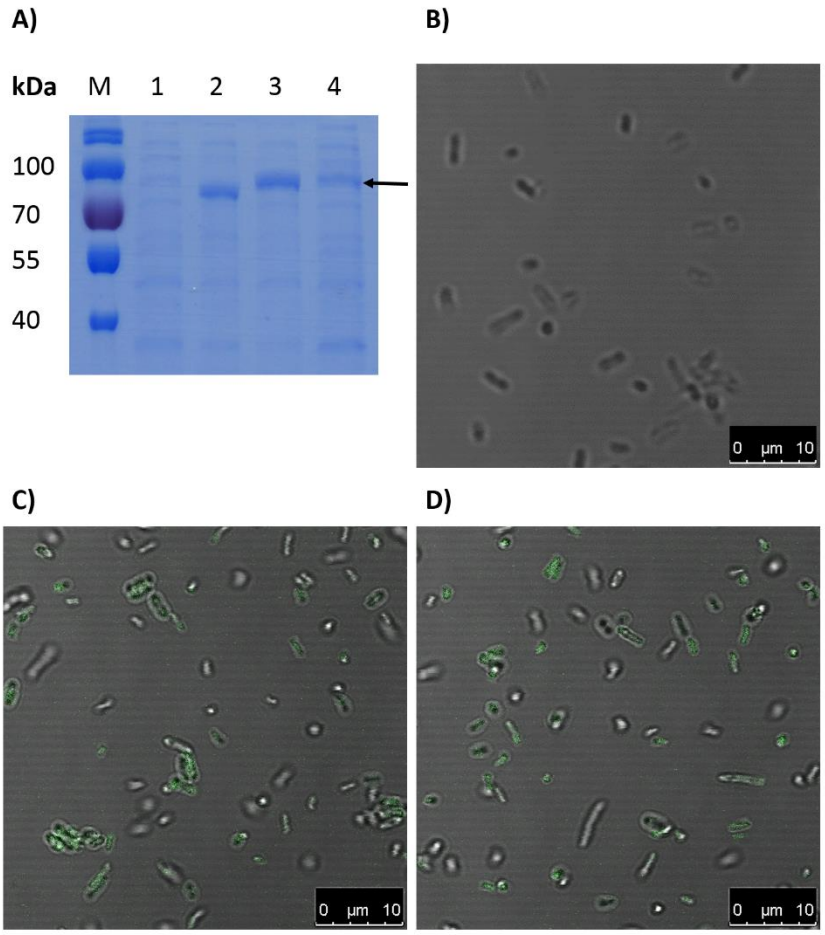

Figure 20: Surface-presented CSD-constructs were detected with an anti-E-epitope antibody. A) Production of CSD constructs. 1: pET22-EV, 2: CSD control (72.3 kDa), 3: LCI-CSD WT (77.8 kDa), 4: LCI-CSD library (77.8 kDa). M: PageRuler™ Prestained Protein Ladder, 10 to 180 kDa. Translocated CSD-constructs were visualized on the *E. coli* surface by a FITC-labeled anti-E-epitope antibody. **B)** negative control pET22b-EV **C)** CSD-control, and **D)** LCI-CSD-WT (Leica TCS SP8 microscope, Ex: 485 nm, Em: 520 nm, argon laser 1 % intensity, gain 1000, Leica Microsystems GmbH (Wetzlar, Germany).

3.5.2 Establishment of the ultra-high-throughput screening system (uHTS)

The ultra-high-throughput screening system was established using *E. coli* BL21-Gold (DE3) cells presenting the LCI-CSD library, the reference LCI-CSD WT or the CSD-control on the cell-surface. The cells were incubated with PP beads for immobilization. PP beads and attached *E. coli* cells were transferred into disposable columns. Superfluous and weakly attached cells were washed out with PBS buffer. *E. coli* cells presenting weak-binding LCI variants were eluted with 0.25 mM LAS in a selection step. LAS was removed to avoid further toxicity to *E. coli* cells by a subsequent washing step with PBS buffer. PP-beads with immobilized *E. coli* cells were transferred onto agar plates for cell recovery. Recovered *E. coli* cells with strong binding LCI variants were sequenced (see Figure 21).

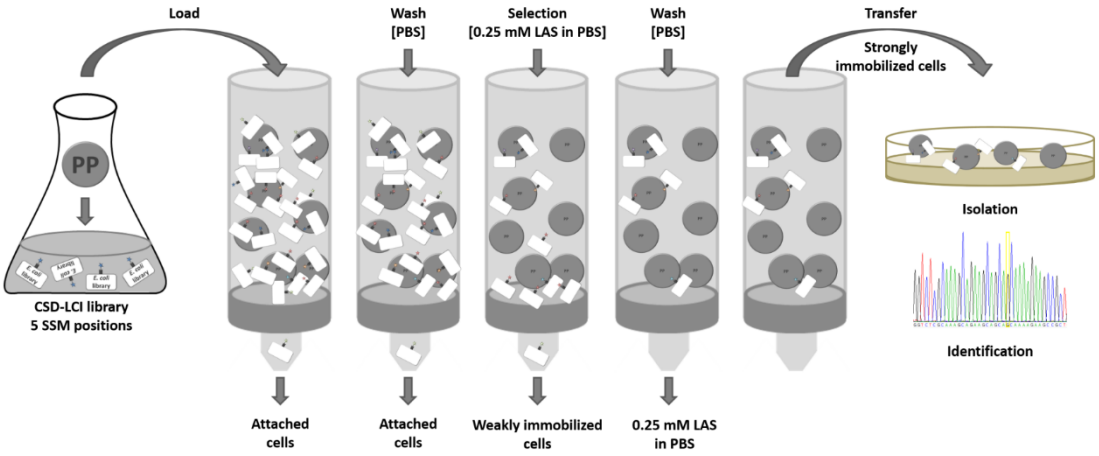

Figure 21: Schematic overview of CSD-based screening system for anchor peptides. PP-beads were incubated with the culture broth of the LCI-CSD library (10 min). After transfer into disposable PP-columns attached cells were washed out (10x 5 mL PBS buffer pH 7.4). Weakly immobilized cells were removed in the selection step (2x 5 mL LAS (0.05 mM in PBS buffer pH 7.4), 1x 5 mL LAS (0.25 mM in PBS buffer pH 7.4)). Detached cells and remaining LAS were removed with PBS (5x 5 mL PBS buffer pH 7.4). Immobilized cells were recovered from PP beads on LB agar plates overnight (37°C, 70 % humidity; Multitron Pro, Infors AG).

3.5.2.1 Viability of *E. coli* cells during screening

The viability of LCI-CSD WT presenting *E. coli* cells during screening was monitored by incubation with LAS (0.25-0.5 mM). The cells were normalized to an OD_{600} of 0.1 and incubated for 10 min in PBS buffer (see Figure 22A), 0.25 (22B) and 0.5 mM LAS (in PBS buffer, pH 7.4) (22C). After incubation, the cells (50 µL) were plated on LB agar plates (supplemented with ampicillin (100 µg/mL) and incubated overnight (37°C, 200 rpm, 70 % humidity; Multitron Pro, Infors AG). A comparable cell growth on all plates confirmed, that LAS was not toxic to the *E. coli* cells under investigated conditions.

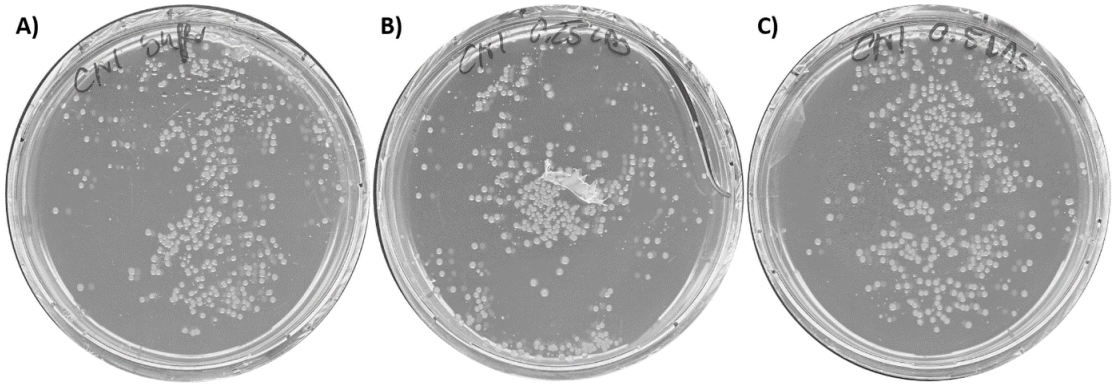

Figure 22: Viability of *E. coli* cells in different LAS concentrations. LCI-CSD WT presenting *E. coli* cells incubated for 10 min in **A)** 0, **B)** 0.25 and **C)** 0.5 mM LAS (in PBS buffer, pH 7.4).

3.5.2.2 Optimization of screening parameters

The screening parameters of the ultra-high-throughput screening system were optimized by a variation of the washing steps. Sufficient washing enabled a discrimination between improved LCI-CSD variants and both reference constructs (CSD-LCI WT and CSD-control). For a final screening, the following conditions were used: 10x 5 mL PBS, 2x 5 mL LAS (0.05 mM), 1x 5 mL LAS (0.25 mM), 5x 5 mL PBS. A significant difference in numbers of attached cells to PP beads were obtained. CSD-control (see Figure 23A): 50 colonies, LCI-CSD WT (see Figure 23B): 64 colonies and LCI-CSD library (see Figure 23C): ~1300 colonies. Three variants were selected for a validation of the screening system. Therefore, the variants were sequenced and obtained mutations were introduced into the eGFP-LCI fusion construct for quantification of binding strength using the ABBA screening system.

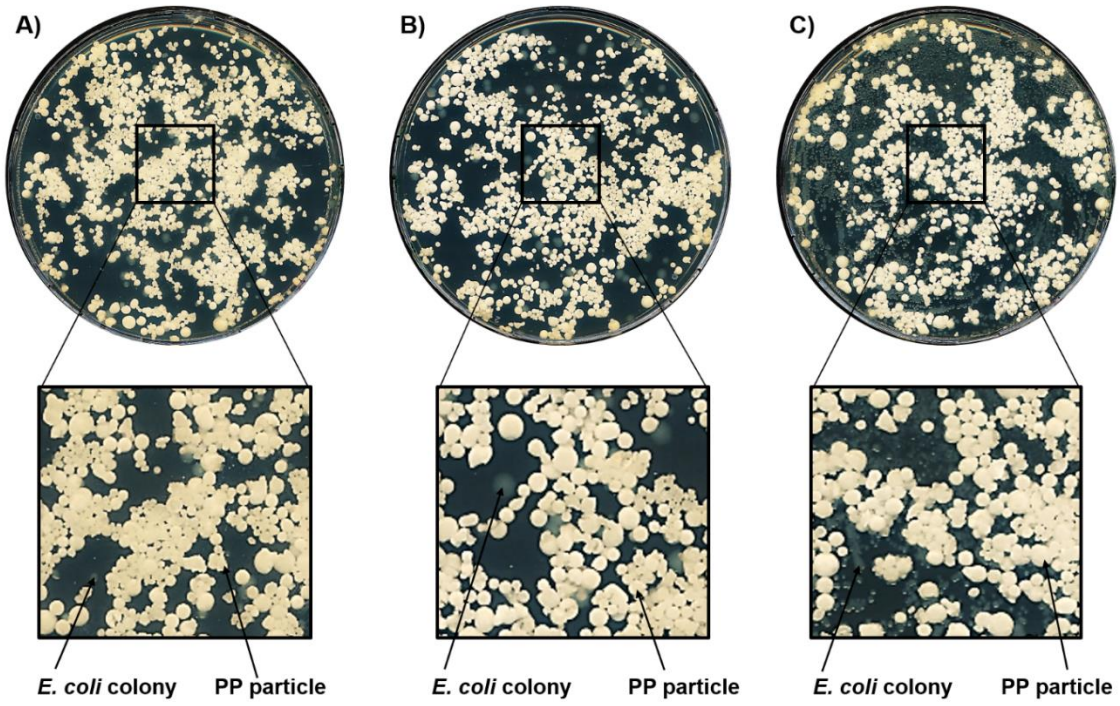

Figure 23: Selection of improved binding variants with 0.25 mM LAS. *E. coli* cells immobilized on PP were transferred to LB agar plates for cell recovery. **A)** CSD control, **B)** LCI-CSD-WT and **C)** LCI-CSD-library.

3.5.3 Characterization of identified LCI-CSD variants

Three different LCI-CSD variants were identified by sequencing, LCI-CSD-1 (Y29C/D31T/G35D/E42Q/D45S), LCI-CSD-2 (Y29V/D31A/E42G/D45G), and LCI-CSD-3 (E42V/D45H). The mutations were transferred to *egfp-lci* by site-directed mutagenesis (see chapter 3.4.1) for the quantification of PP-binding strength. The obtained variants were named eGFP-LCI-CSD-1, eGFP-LCI-CSD-2, and eGFP-LCI-CSD-3. PP-binding strength of all three variants was quantified using the ABBA screening system in 12 replicates each (see chapter 2.5.2). Improvement of eGFP-LCI variants was calculated relative to eGFP-LCI WT after subtraction of eGFP background fluorescence (see Table 10). Variant LCI-CSD-1 was not expressible as eGFP-fusion construct and binding was not determined.

Table 10: Relative improvement of LCI-CSD variants towards PP-binding in presence of LAS.

Name	Mutations	RFU 0.05 mM LAS	RFU 0.125 mM LAS	RFU 0.25 mM LAS	RFU 1 mM Triton X-100
eGFP-LCI WT	-	159.5±32.9	14.3±6.6	14.0±8.3	94.0±8.1
eGFP-LCI-CSD-2	Y29V/D31A/E42G/D45G	257.0±35.1	62.9±10.0	13.8±3.2	112.4±18.4
eGFP-LCI-CSD-3	E42V/D45H	669.7±106.6	173.6±29.1	36.9±7.5	238.0±46.7

As selection pressure, the anionic surfactant LAS and the non-ionic surfactant Triton X-100 (Rübsam, Davari et al. 2018) were chosen. Each surfactant has a characteristic CMC, the value at which surface-active ions associate in solution and form micelles. Above this value, monomers and micelles exist in dynamic equilibrium (Tadros 2013). The CMC of LAS at room temperature in Tris/HCl buffer (50 mM, pH 8.0) was determined to be 0.105 mM (see Figure 13), whereas the CMC of Triton X-100 was reported to be 0.27 mM at the same conditions (Rübsam, Davari et al. 2018). Three different LAS concentrations (0.05, 0.125 and 0.25 mM LAS) and one Triton X-100 concentration (1 mM) were selected for an efficient screening of the generated LCI-CSD variants. The variant eGFP-LCI-CSD-3 showed the highest improvement compared to the eGFP-LCI WT (0.05 mM LAS: 4.2±0.6-fold; 0.125 mM LAS: 12.1±1.5-fold; 0.25 mM LAS: 2.6±0.2-fold; and Triton X-100: 2.5±0.4-fold) (see Figure 24).

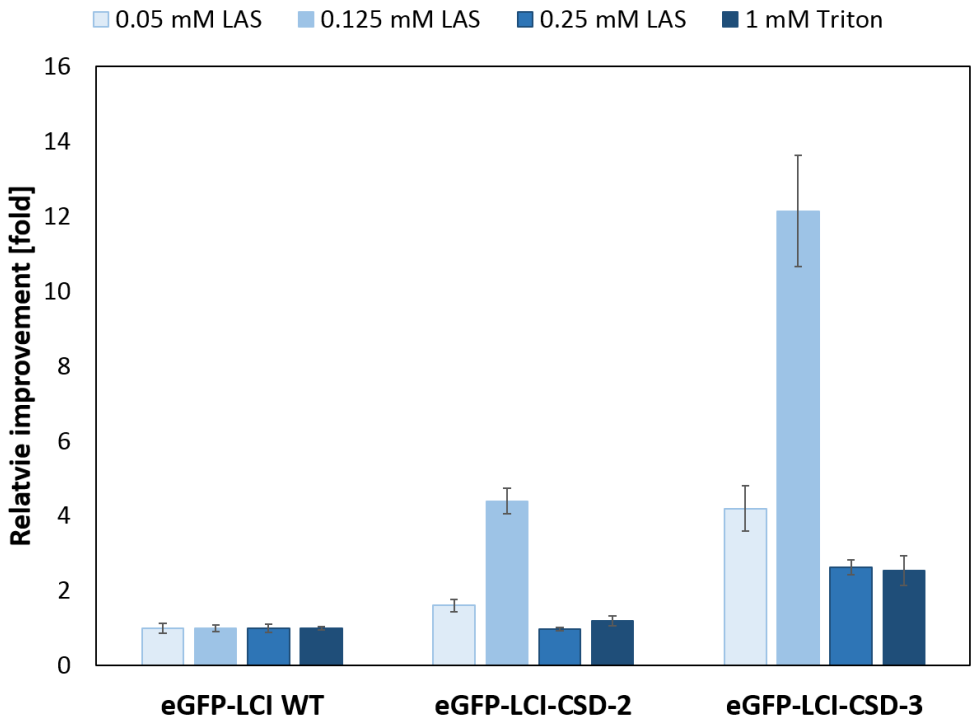

Figure 24: Binding of LCI-CSD variants in presence of varied LAS (0.05, 0.125, and 0.25 mM) and Triton X-100 (1 mm) concentrations. Binding of eGFP, eGFP-LCI WT, eGFP-LCI-CSD-2, and eGFP-LCI-CSD-3 was quantified by measuring the fluorescence of eGFP on the PP-surface in 96-well-MTPs. The relative improvement of eGFP-LCI-CSD variants was calculated with respect to eGFP-LCI WT.

3.5.4 Visualization of immobilized *E. coli* cells on a PP foil

Anchor peptides can act as adhesion promoter for enzymes and reporter proteins. The ability of surface-presented LCI (variants) to function as adhesion promoting peptides for *E. coli* cells was analyzed by ESEM measurements. ESEM analysis showed, that *E. coli* cells presenting LCI-CSD and LCI-CSD-3 were immobilized on a PP film, whereas *E. coli* cells without LCI bound very poorly (negative control pET22-EV). LCI-CSD immobilized many cells on the PP-foil (clusters of cells and single cells) in comparison to the variant LCI-CSD-3 that immobilized less cells on the surface and no formation of clusters was observed (see Figure 25).

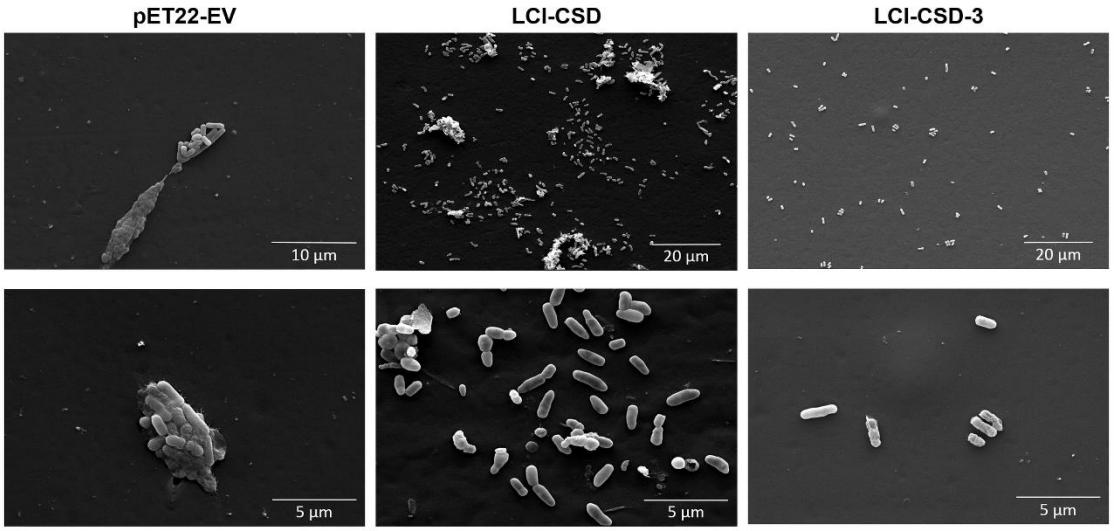

Figure 25: ESEM analysis of immobilized *E. coli* cells on a PP foil. LCI-CSD and LCI-CSD-3 were presented on the surface of *E. coli.* The cells were immobilized on a PP foil. pET22-EV was used as negative control. Settings of the instrument were: accelerating voltage: 10 kV, working distance: 10.1 mm, magnification: 1000/5000x (ESEM XL30 FEG, FEI, Philips (Eindhoven, Netherlands)).

3.6 Discussion

The widespread commodity polymer PP is extensively used as packaging material or in the automotive industry and is the second most produced non-fiber plastic (21 %) after PE (36 %) (Geyer, Jambeck et al. 2017). Huge amounts of PP waste are generated that accumulate in the environment. Accumulated plastics in the environment are slowly degraded by e.g. photo-, bio-, thermooxidative degradation, and/or friction (Barnes, Galgani et al. 2009, Browne, Crump et al. 2011). As a promising strategy to convert plastic waste into carbon dioxide, water, and new biomass, microbial degradation of plastic particles is investigated (Grima, Bellon-Maurel et al. 2000).

However, most polymer particles cannot diffuse through cellular membranes of microbial cells. Fungi overcome this problem by secreting enzyme cocktails for an efficient biomass degradation (Mäkelä, Donofrio et al. 2014). An effective depolymerization of polymers requires a close proximity of microorganisms to polymers and a release of polymer-degrading enzymes (e.g., esterases or cutinases). In the best case, the polymer is broken down and the monomers are mineralized thereafter or used as carbon/nitrogen source for microorganisms (Shah, Hasan et al. 2008). The empowerment of microorganisms to attach to polymer surfaces is pre-requisite to ensure efficient degradation. Therefore, adhesion-promoting peptides can be displayed on an organism's

surfaces. Binding peptides, like anchor peptides, can be improved in binding strength and specificity to enable rapid degradation and metabolization of target polymers. In the last two decades, DE emerged as standard algorithm to tune enzymes/peptides to application demands (Rubsam, Weber et al. 2018). Screening throughput and selected engineering strategy are key factors for a successful DE campaign since even short peptides such as LCI can theoretically yield in 20^{47} variants (Tee and Schwaneberg 2007). SSMs of target peptides allow a focused library generation and a discovery of cooperative effects of amino acid substitutions (Reetz, Carballeira et al. 2006, Dennig, Shivange et al. 2011, Ensari, Dhoke et al. 2018). Five previously reported LCI positions were selected for simultaneous site saturation mutagenesis (Rübsam, Davari et al. 2018). A saturation of these five selected positions Y29, D31, G35, E42, and D45 can theoretically yield in $3.2*10^6$ variants (Reetz, Carballeira et al. 2006). Taken into consideration the transformation efficiency of the used *E. coli* BL21-Gold (DE3) cells, 10.7 million generated LCI variants were analyzed in the developed CSD screening system. This number of clones accounts for a three times coverage of the theoretically generated diversity of LCI. The identified variant eGFP-LCI-CSD-3 (E42V/D45H) showed a 12.1-fold improved binding strength to PP in presence of the anionic surfactant LAS (0.125 mM, see Figure 24). This increase in binding strength in one round of DE is remarkable since usually improvement factors of around two are reported for a single round of evolution (Tee and Schwaneberg 2007, Pitzler, Wirtz et al. 2014). In the previously reported MTP-based PeP*evo* (Rubsam, Weber et al. 2018) and KnowVolution campaigns (Rübsam, Davari et al. 2018) 1000 clones were screened, yielding in an 6.3 fold improved PS-binder (Tachystatin A2) and a 5.4 fold improved PP-binder (LCI) in presence of surfactants (0.5 mM LAS and 1 mM Triton X-100, respectively).

DE of anchor peptides requires screening systems that facilitate a high throughput to cover a meaningful amount of generated diversity. Phage display systems, yeast display systems or bacterial display systems offer appropriate set-ups. Phage display libraries contain up to 10^{12} phage particles and offer the highest screening throughput. However, phage display libraries are limited in the size of displayed peptides (Lee, Choi et al. 2003) and the transduction efficiency of *E. coli* cells (Galan, Comor et al. 2016). Yeast display libraries contain up to 10^7-10^9 displayed peptide variants (Benatuil, Perez et al. 2010) and enable post-translational modifications (Bowley, Labrijn et al. 2007). Post-translational

modifications of peptides, like extensive glycosylation might interfere with the binding performance of target peptides. Additionally, the growth rate of yeast display systems is slower in comparison to bacterial display systems. In DE campaigns, *E. coli* is the most commonly used host. *E. coli* was selected for DE of anchor peptides due to its robustness and easy handling, for instance high transformation efficiency (10^9), stable heterologous protein expression and fast cultivation. Beneficially, a high copy number of target peptides is displayed on the cell surface of *E. coli* (>10^4 peptides per cell) (Becker, Michalczyk et al. 2007) ensuring a strong adhesion to the target materials. The developed *E. coli* display screening system is therefore an efficient ultra-high throughput screening system suitable for the display of adhesive anchor peptides. It offers a simple handling and selection of improved peptide binders employing only polymer beads, disposable columns and agar plates.

4 Biadhesive peptides for assembling of bare-metal implants and compound loaded micro-containers

4.1 Declaration

Parts of this chapter were submitted by the author to the journal of Macromolecular Bioscience

Apitius L, Buschmann S, Schönauer D, Bergs C, Jakob F, Pich A, and Schwaneberg U (2019). Biadhesive peptides for assembling of bare-metal implants and compound loaded micro-containers.

Parts of this chapter were filed for patent application:

Schwaneberg U, Sözer S, Mertens M, Davari MD, Jakob F, Islam S, **Weber L**. 2018. Fusion Peptides or Proteins, their Use, and Systems and Kits based thereupon, for the Separation and/or Detection of Plastics, particularly of Microplastics. EP18178726.8.

4.2 Objective and main results

In medical applications, devices such as implants are bio-functionalized to increase biocompatibility. In this chapter, the design and application of biocompatible biadhesive peptides (peptesives) is described. Peptesives are composed of two anchor peptide domains with different material-binding properties. The anchor peptides were used as adhesion promoters as they are to bind to chemically different materials. Stainless steel is commonly used as backbone for medical stents and the biodegradable polymer PCL is applied for the fabrication of tissue growth scaffolds and drug delivering micro-containers. For the construction of peptesives, five potential anchor peptides were fused to the fluorescent reporter protein eGFP and the binding to stainless steel and PCL was investigated by confocal microscopy. A selective stainless steel binding peptide (Dermaseptin S1) and PCL-binding peptides (LCI, TA2 and Thanatin) were genetically fused as peptesives using the separator Domain Z for functional separation. The

Dermaseptin S1-DZ-LCI-mediated assembly of kanamycin-loaded PCL micro-containers on stainless steel was visualized by FE-SEM analysis and fluorescent microscopy. The antimicrobial effect of kanamycin-loaded micro-containers was shown by growth inhibition of *E. coli* DSM 498 cells (see Figure 26).

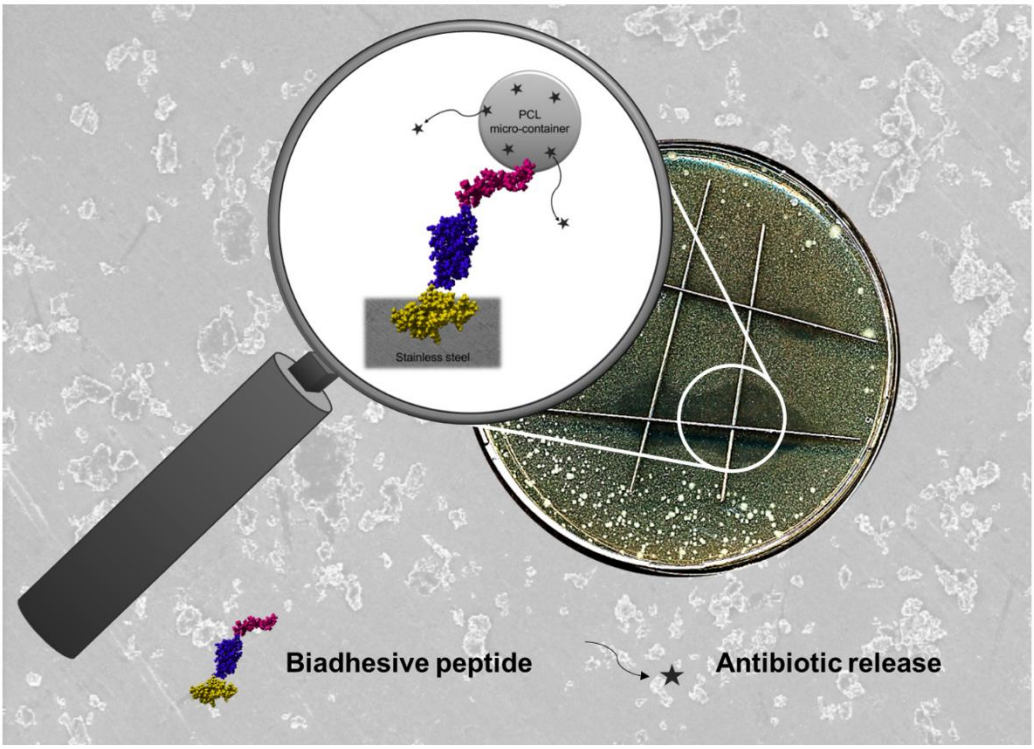

Figure 26: Biadhesive peptides assemble bare-metal implants and kanamycin-loaded PCL micro-containers.

4.3 State of the art

For 2017, the global market of biomaterials was estimated to 88.4 billion US$ with a compound annual growth rate of 15 % (Jaganathan, Balaji et al. 2015). Biomaterials find numerous applications in medical devices such as drug delivery systems, hybrid organs, synthetic blood vessels or bone treatments. Biomaterials are of high medical interest due to their biocompatibility and biodegradability. Thereby, the construction of many biomaterials is inspired by nature. Especially, natural occurring adhesive peptides such as fibrin, fibronectin or mussel foot proteins led to the development of advanced bio-interfaces and functional coatings. Already in the 1990´s, fibrin was used as sealant in tissue adhesives and surgery promoting wound closure and healing (Atrah 1994, Coulthard, Esposito et al. 2010).

Many functional coatings are peptide based. Implants were coated with peptides to stimulate re-endothelialization, to minimize implant-associated bacterial infections or to reduce biofilm formation (Yang, Whiteside et al. 2015). A peptide used for the coating of bare-metal stents is the WKYMVm peptide. WKYMVm functions as a selective formyl peptide receptor agonist. The peptide was used in combination with hyaluronic acid to form a primary layer on bare-metal stents by dip-coating. Following, the immunosuppressive and antiproliferative sirolimus was applied in a secondary layer by spraying. The bifunctional bare-metal stent coating improved the adherence of endothelial cells (WKYMVm) and inhibited restenosis (sirolimus) (Jang, Bae et al. 2015, Sim and Jeong 2017). For the development of a pro-healing stent, re-endothelialization of polystyrene has been investigated. A bifunctional peptide has been applied that consisted of a PS-binding motif as well as a binding motif for human endothelial cells. The cell-binding motif was able to specifically bind to endothelial cells and directed them to the PS surface thereby reducing inflammatory responses (Meyers, Kenan et al. 2011).

The generation of bio-adhesive materials was often inspired by the strong adhesion of mussel foot proteins to surfaces. Especially, the catecholic amino acid 3,4-dihydroxyphenylalanine (Dopa) was used to anchor conjugated hydrophilic PEG chains onto carrier materials (Ko, Cadieux et al. 2008). Many antifouling and antimicrobial coatings are based on PEG, since the hydrophilic PEG has a repelling effect on hydrophobic bacteria (Morra 2000, John, Rajpurkar et al. 2007, Minardi, Ghiselli et al. 2007). Dopa forms reversible non-covalent or irreversible covalent interactions and is therefore capable to bind to both organic and inorganic surfaces. Dopa has frequently been used in adhesive hydrogels, nano- and micro-composites, and self-healing hydrogels as reviewed comprehensively by Forooshani and Lee (Kord Forooshani and Lee 2017).

Bare-metal stents commonly consist of stainless steel (316L), cobalt-chromium or nickel-titanium alloys. Functionalization of bare-metal stents has been performed by coating of porous drug eluting layers and magnetic silicon or carbon nanoparticles. They were also coated with SAMs (Chen, Habraken et al. 2015). SAMs are composed of head groups (hydrocarbon chains with alkylthiols, alkylamines, or alkanoic acids) that can adhere to metal surfaces (Ruan, Bayer et al. 2002). The assembling of SAMs is performed in two steps, a solution immersion and dip-evaporation cycle. Thereby, dodecylphosphonic acid or phosphoundecanoic acid (in dry THF) are used to immerse the

stent followed by a heating step (120°C for 18 h) to evaporate the solvent (Ruan, Bayer et al. 2002).

This chapter focused on the design and application of biocompatible biadhesive peptides that immobilize compound-loaded PCL micro-containers on a stainless steel surface (see Figure 27).

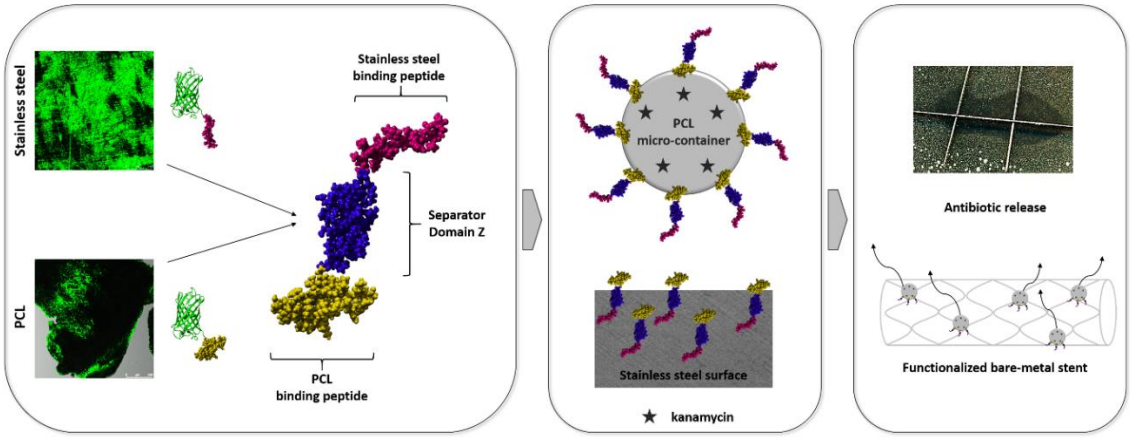

Figure 27: Schematic immobilization of kanamycin-loaded PCL particles on stainless steel. A stainless steel-binding anchor peptide (Dermaseptin S1) and a PCL-binding anchor peptide (LCI) were fused to form a biadhesive peptide. As a functional separator Domain Z was used. DS1-DZ-LCI assembled PCL micro-container and stainless steel. The release of kanamycin from the PCL micro-containers was confirmed by bacterial growth inhibition (*E. coli* DSM 498).

4.4 Methods

Chemicals used in this chapter were obtained from Sigma-Aldrich Corp. (St. Louis, USA), AppliChem GmbH (Darmstadt, Germany) or Carl Roth GmbH (Karlsruhe, Germany) in analytical-reagent grade or higher purity. Synthetic genes were ordered at GeneArt AG (Regensburg, Germany) and oligonucleotides were ordered from Eurofins Scientific SE (Ebersberg, Germany) in salt-free form. The enzymes used in this study were obtained from New England Biolabs GmbH (Frankfurt am Main, Germany). The PCR purification and plasmid extraction kits were obtained from Qiagen GmbH (Hilden, Germany) and Macherey-Nagel GmbH & Co. KG (Düren, Germany). The plasmid pET28a(+) (Novagen, Darmstadt, Germany) was used as expression vector and the used expression strain *E. coli* BL21-Gold (DE3) was ordered from Agilent Technologies (Santa Clara, USA). The micro-containers were synthesized from polycaprolactone (PCL) flakes (Mn: 10,000 g/mol)

(Sigma-Aldrich Corp., St. Louis, USA)) and as stainless steel surface, Implantat-Spezialstahl was used (Ergste 1.4441 LA Cat no. 5500238) (Zapp AG, Ratingen, Germany).

4.4.1 Generation of eGFP-anchor peptides for binding analysis

The cloning of anchor peptides (eGFP-LCI, eGFP-TA2, eGFP-DS1, eGFP-THA, and DS1-eGFP) was performed by PLICing (Blanusa, Schenk et al. 2010) as described in the appendix chapter IV.

4.4.2 Generation of biadhesive peptides

The synthetic genes of biadhesive peptides *ds1-dz-lci*, *dsi-dz-ta2*, and *dsi-dz-tha* were codon-optimized for *E. coli* (see Figure 35B) and cloned as described in the appendix chapter IV.

4.4.3 Production of anchor peptides

The eGFP-anchor peptide fusion proteins eGFP-DS1, eGFP-LCI, eGFP-TA2, eGFP-THA, and DS1-eGFP were produced as described in the appendix chapter IV.I.II according to Rübsam *et al.* (Rübsam, Stomps et al. 2017). For binding analysis to stainless steel and PCL, purified anchor peptides were used. Purification was performed by affinity chromatography using a His_6 tag (50 mM Tris/HCl buffer pH 8.0; column: 5 mL HiTrap™ HP; ÄKTAprime plus, GE-Healthcare, Buckinghamshire, UK). The peptides were eluted from the HiTrap™ HP column using a gradual elution with imidazole (0-0.5 M in 50 mM Tris/HCl buffer pH 8.0). The purity of anchor peptides was confirmed by sodium dodecyl sulfate polyacrylamide gel electrophoresis (SDS-PAGE) using a 5 % stacking gel and a 12 % separating gel (Laemmli 1970).

4.4.4 Production of peptesives

Single colonies of DS1-DZ-LCI, DS1-DZ-TA2, and DS1-DZ-THA were transferred into LB medium supplemented with kanamycin (50 µg/mL) for an overnight cultivation (37°C, 200 rpm, 70 % humidity; Multitron Pro, Infors AG). Glycerol (0.5 mL, 50 % (v/v)) was added to 1 mL of each culture for storage at -80°C. The three peptesives as well as the negative control pET28-EV were produced in 250 mL shaking flasks. Therefore, pre-cultures were inoculated from glycerol stocks and cultivated in 5 mL LB medium (supplemented with

kanamycin (50 µg/m)) overnight (37°C, 200 rpm, 70 % humidity; Multitron Pro, Infors AG). Main cultures were cultivated in 50 mL LB medium (supplemented with kanamycin (50 µg/mL)) and inoculated from the pre-culture to a final OD_{600} of 0.025. Peptesive production was induced with ITPG (0.1 mM) at an OD_{600} of 1. For an optimization of culture conditions, different temperatures (20°C/30°C/37°C) were selected and cultivation was performed for 16 h (200 rpm, 70 % humidity; Multitron Pro, Infors AG). After cultivation, the cells were harvested (15,000 rpm, Sorvall RC 6+, Thermo Fisher Scientific (Darmstadt, Germany)) and subsequently discarded. The cultivation supernatant was stored at 4°C and concentrated 3-fold to a final volume of 1 mL (EMD Millipore Amicon™ Ultra-0.5 Centrifugal Filter Units, MWCO 10 kDa, Thermo Fisher Scientific (Darmstadt, Germany)). The expression of peptesives was analyzed by tricine SDS-PAGE (16 %) (Schagger 2006).

4.4.5 Synthesis of kanamycin-loaded PCL micro-containers

For the synthesis of kanamycin-loaded PCL micro-containers, kanamycin sulfate (20 % (w/w); AppliChem GmbH (Darmstadt, Germany)) and polycaprolactone (PCL) flakes (Mn: 10,000 g/mol, transition temperature Tg: 60°C, density: 1.146 g/mL at 25°C; Sigma-Aldrich Corp. (St. Louis, USA)) were heated up to 60°C in a water bath (WNE 10 Memmert GmbH+Co. KG (Schwabach, Germany)). Both components were pre-homogenized via continuous stirring and cooled to room temperature. The polymer batch was grinded manually and transferred into a twin screw extruder (59°C, 60 rpm, retention time 2 min, Micro 15cc Twin Screw Compounder, Xplore Instruments BV, Netherlands). Following, the extruded and homogenized kanamycin-loaded PCL micro-containers were milled under intensive stirring in absolute EtOH (800 rpm, 3 days, 20°C, c = 0.21 g/mL) and finally stored at 4°C until further usage. Morphology and size distribution of kanamycin-loaded PCL micro-containers were analyzed by dynamic light scattering (DLS) (triplicates, Mastersizer 2000, Malvern Panalytical GmbH, Kassel, Germany) as well as by confocal microscopy (transmission and Ex: 335 nm, Em: 454 nm, 405 nm diode laser, Leica Microsystems GmbH (Wetzlar, Germany)).

4.4.6 Binding analysis of anchor peptides to stainless steel and PCL

A stainless steel plate (Implantat-Spezialstahl, Ergste 1.4441 LA Cat no. 5500238, Zapp AG (Ratingen, Germany)) was cut into pieces of 1 cm^2 size and cleaned by sonication in NaOH (1 M, 50 mL, 30 min, Bandelin Sonorex Digitec (Berlin, Germany)) followed by sonication in ddH_2O (500 mL, 30 min, Bandelin Sonorex Digitec (Berlin, Germany)). Finally, the stainless steel was incubated in absolute EtOH (50 mL) for sterilization.

The binding of eGFP-DS1, eGFP-LCI, eGFP-TA2, eGFP-THA, and DS1-eGFP to stainless steel and PCL particles was investigated by confocal microscopy. Therefore, purified anchors were used (see 4.4.3). For coating of stainless steel and PCL, eGFP-anchor peptides (5 µM in 50 mM Tris/HCl buffer pH 8.0, 10 min) were incubated for 10 min at room temperature. Subsequently, non-bound peptides were removed in three subsequent washing steps (1 mL 50 mM Tris/HCl buffer pH 8.0 each). An unspecific binding of eGFP was prevented by a washing step with LAS (100 µL, 0.5 mM in 50 mM Tris/HCl buffer pH 8.0) followed by one washing step with Tris/HCl buffer (1 mL 50 mM pH 8.0) (Rubsam, Weber et al. 2018). A binding of anchor peptides to stainless steel and PCL was confirmed by a detection of eGFP fluorescence on the respective surface (Leica TCS SP8 microscope, Ex: 485 nm, Em: 520 nm, gain 1000).

4.4.7 Visualization of immobilized PCL micro-containers on stainless steel

DS1-DZ-LCI and the negative control pET28-EV (100 µL, 3x concentrated supernatant) were incubated with PCL micro-containers (50 µL) and stainless steel slides. After incubation (10 min), non-bound peptides and PCL micro-containers were washed off with absolute EtOH (3x1 mL) and ddH_2O (3x1 mL). To increase the surface coverage, the immobilization procedure was repeated once. Following, the coated samples were air-dried. Immobilized PCL micro-containers on the stainless steel surface were detected by confocal microscopy (Ex: 485 nm, Em: 520 nm, 405 nm diode laser, Leica Microsystems GmbH (Wetzlar, Germany) and FE-SEM. As a pre-requisite for FE-SEM analysis, the coated samples were sputtered with a 4 nm layer of Au-Pd to avoid charging effects of PCL. The following settings were used for FE-SEM measurements: accelerating voltage: 3 kV, working distance: 8.0/8.4 mm, magnification: 700x (S-4800 FE-SEM (Hitachi, (Schaumburg, USA)).

4.4.8 Antimicrobial assay of kanamycin-loaded PCL micro-containers immobilized on stainless steel

Cultivation supernatants of DS1-DZ-LCI and pET28-EV (1 mL, 5x concentrated) were incubated with sterilized stainless steel wires (10 min). After incubation, kanamycin-loaded PCL micro-containers were added (0.5 mL, 10 min). All samples and control experiments were performed as described in Table 11. Coated stainless steel wires were washed with absolute EtOH (2x 5 mL) to remove non-bound peptides and PCL micro-containers. In a control experiment, kanamycin (12.5 µg per agar plate) was added to a DS1-DZ-LCI coated sample after washing. All air-dried coated stainless steel wires were transferred in empty petri-dishes.

Table 11: Antimicrobial effect of immobilized kanamycin-loaded PCL micro-containers on stainless steel – sample preparation.

Sample	peptesive	peptesive	pET28-EV control	peptesive control	PCL control	kanamycin control
DS1-DZ-LCI (1 mL)	+	+	-	+	-	+
pET28-EV (1 mL)	-	-	+	-	-	-
kanamycin-loaded PCL (0.5 mL)	+	+	+	-	+	+
ddH_2O (0.5/1 mL)	-	-	-	+ (0.5 mL)	+ (1 mL)	-
kanamycin (12.5 µg)	-	-	-	-	-	+
E. coli DSM 498 (cfu)	200,000	20,000	200,000	200,000	200,000	200,000

E. coli DSM 498 cells were incubated in LB-medium (5 mL) and grown overnight (37°C, 200 rpm, 70 % humidity; Multitron Pro, Infors AG). Main cultures (10 mL LB medium) were inoculated with pre-culture to a final OD_{600} of 0.025. Cells were cultivated until mid-logarithmic phase (37°C, 200 rpm, 70 % humidity; Multitron Pro, Infors AG). The cell density of *E. coli* DSM 498 was normalized to an $OD_{600}=1*10^{-5/-6}$ accounting for 200,000 or 20,000 cfu, respectively. The cells were transferred into tempered LB-agar (0.8 %, 25 mL, 37°C). Subsequently, the liquid agar containing the cells was poured onto the previously prepared stainless steel wires. The cells were cultivated in the agar overnight (37°C, 70 % humidity; Multitron Pro, Infors AG). A formation of halos around the stainless steel wires indicated a growth inhibition of *E. coli* DSM 498 cells by the released kanamycin from coated stainless steel wires.

4.5 Results and discussion

The ability of biadhesive peptides to specifically bind two different materials enables an application as assembling promoter. In this study, stainless steel and PCL were selected as target materials due to their medical application in stent technology. Especially stent implants in the urinary tract often cause biofilm formation and encrustation (Keane, Bonner et al. 1994). In order to use biocompatible peptides as adhesion promotors for the immobilization of drug releasing polymers on stainless steel, a platform of peptesive peptides has been established.

4.5.1 Identification and selection of anchor peptides for the generation of peptesives

Material binding peptides offer efficient and easy-handling possibilities for surface functionalization (Seker and Demir 2011, Care, Bergquist et al. 2015). Naturally occurring anchor peptides such as TA2 (Osaki, Omotezako et al. 1999) and LCI (Gong, Wang et al. 2011) are reported to have strong binding affinities to biologically inert polymers (e.g., PS and PP). The anchor peptide LCI forms a dense monolayer of 4.1 nm PP surface when coated from aqueous solutions at ambient temperature (Rübsam, Stomps et al. 2017). The Pe*Pevo* protocol was developed to tune binding strength and specificity of anchor peptides application conditions (Rubsam, Weber et al. 2018).

The fluorescent reporter protein eGFP was utilized to quantify immobilized anchor peptides on stainless steel or PCL surfaces. For a functional separation of eGFP and the selected anchor peptides, a stiff spacer helix (17 amino acids: AEAAAKEAAAKEAAAKA) (Arai, Ueda et al. 2001) with an incorporated TEV cleavage site (7 amino acids: ENLYFQG) (Kapust and Waugh 2000) was introduced. The anchor peptides LCI (47 aa), TA2 (44 aa), and THA (Thanatin, 21 aa) (Fehlbaum, Bulet et al. 1996) already proved to have high binding strength as polymer- (PS and PP) and plant leaf surface-binders (Meurer, Kemper et al. 2017, Rübsam, Stomps et al. 2017, Rubsam, Weber et al. 2018). In all reported binding studies, these anchors were fused C-terminally to eGFP (referred to as C-anchors). The surface binding properties of DS1 (Dermaseptin S1, 29 aa) (Brand, Leite et al. 2002) have not been investigated yet. Hence, binding of N-terminal anchor (DS1-eGFP) as well as a C-terminal anchor (eGFP-DS1) fusion peptides were investigated.

Confocal microscopy was used to analyze the binding strength of DS1-eGFP, eGFP-DS1, eGFP-LCI, eGFP-TA2, and eGFP-THA to stainless steel as well as PCL (see Figure 28).

Interestingly, the strongest binding to stainless steel was detected for DS1-eGFP whereas the eGFP-DS1 was removed almost completely from the stainless steel surface after washing with LAS (0.5 mM in 50 mM Tris/HCl pH 8.0). LAS reduces unspecific binding of eGFP and was used in the washing process to minimize background fluorescence (Rubsam, Weber et al. 2018). The fluorescence of eGFP-LCI was significantly decreased in comparison to DS1-eGFP. eGFP-TA2 and eGFP-THA did not show any strong binding to the stainless steel surface. As PCL-binders, eGFP-LCI and eGFP-TA2 showed strongest binding after washing. In contrast, binding of DS1-eGFP and eGFP-DS1 was not detectable on the PCL surface after washing. Dependent on the binding analysis, the N-anchor DS1 was selected as a stainless steel binding peptides and LCI, TA2, and THA were selected as suitable C-terminal PCL binders for the generation of peptesives.

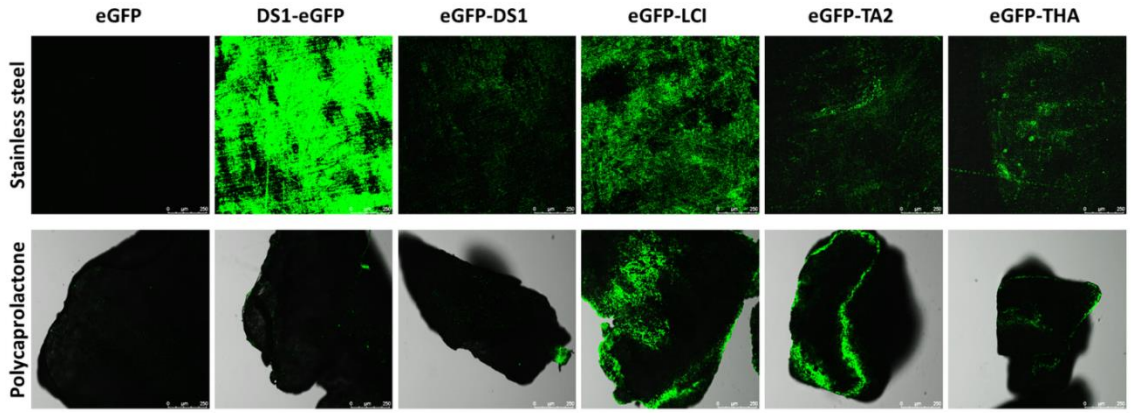

Figure 28: Analysis of eGFP-anchor peptide binding to stainless steel and PCL. Binding of eGFP-anchor peptides (DS1, LCI, TA2, and THA) as well as the negative control eGFP was investigated. Anchor peptides were incubated (10 min, ambient temperature) on stainless steel or PCL particles. In three successive washing steps (3x 1 mL ddH_20) and one washing step with LAS (0.5 mM, 0.5 mL) superfluous peptides were removed. Binding strength of eGFP-anchor peptides was analyzed by confocal microscopy (Leica TCS SP8 microscope, Ex: 485 nm, Em: 520 nm, argon laser 1 % intensity, gain 1000, Leica Microsystems GmbH (Wetzlar, Germany).

4.5.2 Production of peptesives in *E. coli* BL21

The generated peptesives were composed of two anchor peptides that were separated by the spacer staphylococcal protein A Domain Z (DZ, 58 aa, see Figure 5). DZ forms three antiparallel α-helices so that the N- and C-terminus of the protein are located on opposite sides (Tashiro, Tejero et al. 1997). For the generation of peptesives, the N-terminal anchor peptide DS1 and a C-terminal anchor peptide (LCI, TA2, or THA) were used.

Anchor peptides belong to the class of antimicrobial peptides and possess a potential toxicity to their production host (Chen, Li et al. 2017, Khosa, Scholz et al. 2018). Therefore, the production of the selected peptesives (<15 kDa) can be challenging. Additionally, AMPs tend to attach to bacterial membranes (Brogden 2005) and are often associated to the crude extracts after cell lysis. The spacer protein DZ is reported to increase peptide solubility and was selected as separator of both anchor peptides (Samuelsson, Moks et al. 1994). Accordingly, the expression of DS1-DZ-LCI, DS1-DZ-TA2, and DS1-DZ-THA in *E. coli* BL21-Gold (DE3) was optimized. The finally used expression conditions (30°C, 16 h, 200 rpm, 70 % humidity, 50 mL LB medium) were selected as suitable balance between soluble peptesive expression and cell viability. A production of the peptesive DS1-DZ-TA2 was not detectable at any temperature (see Figure 29). As a negative control pET28-EV was selected which represents the natural protein background of *E. coli* cells. Due to their toxicity to the host organisms, the peptesives DS1-DZ-LCI and DS1-DZ-THA caused cell lysis and were enriched from culture broth. After dialysis against water they were applied without further purification steps in binding studies (EMD Millipore Amicon™ Ultra-0.5 Centrifugal Filter Units, MWCO 10 kDa, Thermo Fisher Scientific (Darmstadt, Germany)). Protein production and concentration was visualized by a separation in Tricine-SDS gels (see Figure 29).

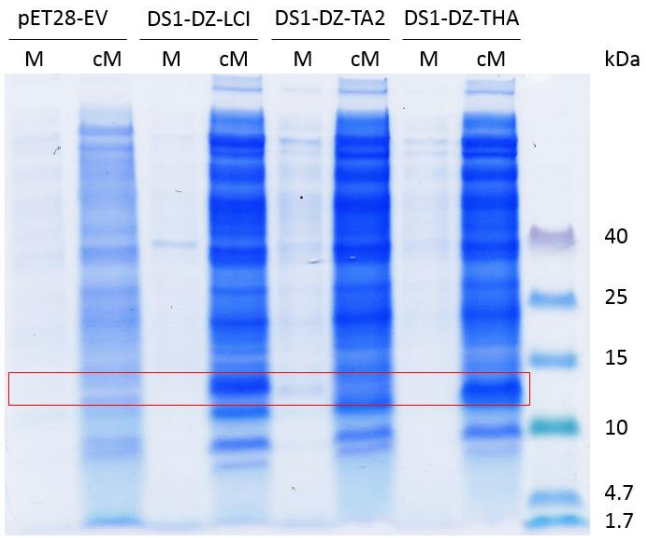

Figure 29: Expression analysis of peptesives. The peptesives DS1-DZ-LCI, DS1-DZ-TA2, and DS1-DZ-THA were produced at 30°C for 16 h. The peptides were enriched from the culture media (M) and were concentrated three fold (cM). As negative control pET28-EV was used. Expected sizes: DS1-DZ-LCI (14.9 kDa), DS1-DZ-TA2 (14.6 kDa), and DS1-DZ-THA (11.9 kDa) (Tricine-SDS, 16 %).

4.5.3 Synthesis of cl-PCL particles

A reduction of bacterial infections after surgery is often facilitated by the application of antibiotic-eluting stents. As a model antibiotic kanamycin sulfate was selected for the loading of PCL micro-containers. Kanamycin sulfate is active against gram positive and negative cocci and bacteria (Database).

The inexpensive, biodegradable, and biocompatible polymer PCL (Labet and Thielemans 2009) is approved by the FDA and is therefore often used for implants or stents. PCL is especially suited for long term drug delivery in cancer therapies (Zhang, Liu et al. 2015). Kanamycin-loaded PCL micro-containers (20 % (w/w) kanamycin sulfate) were synthesized via extrusion. Subsequently, the micro-containers were dispersed in absolute EtOH. A leaching of kanamycin from PCL loaded micro-containers is prevented since it is not soluble in absolute EtOH (Database). The low melting temperature of PCL at 60°C (Ulery, Nair et al. 2011) enables an extrusion process and is beneficially not limited by the thermal resistance of kanamycin (decomposition temperature >250°C).

The size distribution and morphology of PCL micro-containers was determined DLS analysis and confocal microscopy (see Figure 30). In confocal analysis, a size distribution

of <5-25 µm was determined (63-fold magnification). The analysis of PCL micro-containers with DLS measurements showed an average particle size of 39.9±48.7 µm. The size distribution indicated a highly polydisperse product (Mastersizer 2000, Malvern Panalytical GmbH, Kassel, Germany). A further purification by size exclusion was relinquished since the development of platform for bifunctional adhesion promoters was aimed.

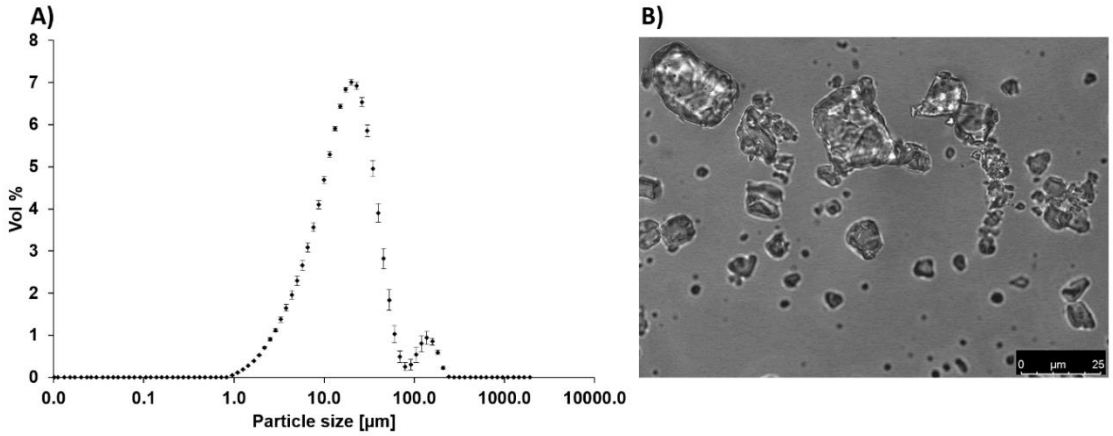

Figure 30: Morphology and size distribution of cl-PCL particles in EtOH. Morphology and size distribution of PCL micro-containers in EtOH was determined by **A)** DLS analysis (Mastersizer 2000; Size range 0.020-2000 µm, Malvern Panalytical GmbH (Kassel, Germany)) and **B)** confocal analysis (Leica TCS SP8 microscope; 63-fold magnification, zoom 2, PMT Trans detector, gain 300, Leica Microsystems GmbH (Wetzlar, Germany)).

4.5.4 Peptesive mediated immobilization of PCL micro-containers on stainless steel

The ability of peptesives (DS1-DZ-LCI and DS1-DZ-THA) to function as assembling promoter was investigated by confocal microscopy (see Figure 31) and confirmed by FE-SEM analysis (see Figure 32). In both experiments, pET28-EV was used as negative control. The use of DS1-DZ-LCI as adhesion promoter resulted in the highest amount of immobilized PCL micro-containers on stainless steel (see Figure 31B). DS1-DZ-THA (see Figure 31C) immobilized less PCL micro-containers on the stainless steel surface in comparison to DS1-DZ-LCI. As expected, the negative control (see Figure 31A) did not function as adhesion promoter for the immobilization of PCL micro-container on the stainless steel surface.

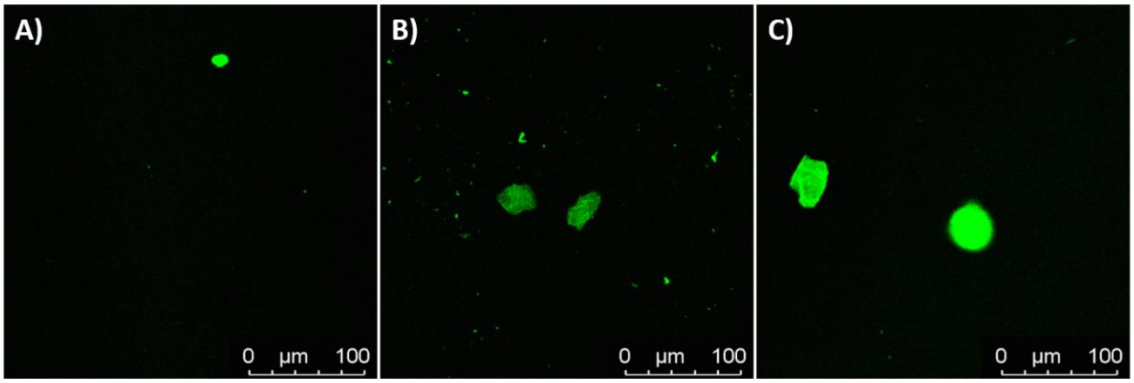

Figure 31: Confocal study of peptesive mediated immobilization of PCL micro-container on stainless steel. A) Negative control (kanamycin-loaded PCL micro-container immobilized on stainless steel with pET28-EV supernatant) **B)** kanamycin-loaded PCL micro-container immobilized on stainless steel with DS1-DZ-LCI. **C)** kanamycin-loaded PCL micro-container immobilized on stainless steel with DS1-DZ-THA.

In a detailed FE-SEM analysis the assembly PCL micro-containers and stainless steel was investigated applying the negative control pET28-EV (see Figure 32A) and DS1-DZ-LCI (see Figure 32B) as adhesion promoter. The FE-SEM analysis confirmed the results of confocal microscopy and verified, that only by the application of the adhesion promoter DS1-DZ-LCI PCL micro-containers were immobilize efficiently on stainless steel. The detected micro-containers ranged in size from <5-15 µm on the stainless steel surface. Larger particles were removed during the washing process. When the negative control pET28-EV was used for immobilization, only few PCL micro-containers (<10 µm) were detected on the stainless steel surface.

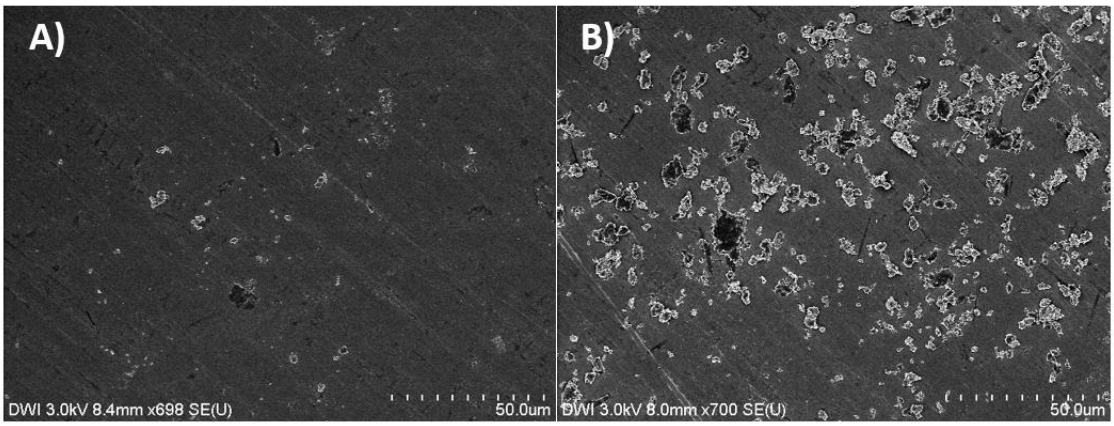

Figure 32: FE-SEM analysis of peptesive mediated immobilization of PCL micro-containers on stainless steel. A) PCL micro-containers immobilized on stainless steel with negative control pET28-EV. **B)** PCL micro-containers immobilized on stainless steel with DS1-DZ-LCI. FE-SEM settings: S-4800 FE-SEM, accelerating voltage: 3 kV, working distance: 8.0/8.4 mm, magnification: 700x (Hitachi, (Schaumburg, USA)).

4.5.5 Antimicrobial effect stainless steel coated with PCL micro-containers

PCL micro-containers were immobilized on stainless steel wires and the antimicrobial properties were investigated by a growth inhibition assay of *E. coli* DSM 498 cells (see Figure 33). The peptesive DS1-DZ-LCI (5x concentrated supernatant) was used as adhesion promoter to immobilize kanamycin-loaded PCL micro-containers on stainless steel wires. Following controls were used: stainless steel wires incubated with pET28-EV (5x concentrated peptesive free supernatant), the peptesive DS1-DZ-LCI only (potential antimicrobial effect of the applied peptesive), kanamycin-loaded PCL micro-containers (PCL control; potential adherent effect of kanamycin to stainless steel), and kanamycin positive control (additionally added kanamycin after washing). A tempered liquid agar (37°C) that contained a cell density of 200,000 or 20,000 colony forming units (cfu) was poured onto the coated stainless steel wires. The cells were cultivated in the agar overnight (37°C, 200 rpm, 70 % humidity; Multitron Pro, Infors AG).

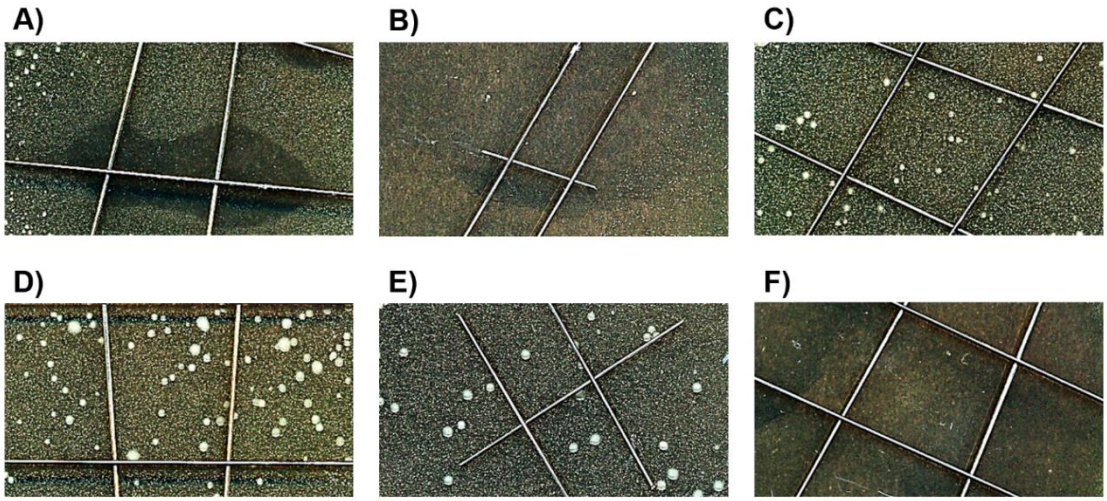

Figure 33: Antibiotic effect of PCL-coated stainless steel on *E. coli* DSM 498. Kanamycin-loaded PCL micro-containers were immobilized on stainless steel wires with **A)** peptesive (DS1-DZ-LCI; 200,000 cfu), **B)** peptesive (DS1-DZ-LCI; 20,000 cfu), **C)** pET28-EV control, **D)** PCL control, **E)** peptesive control, and **F)** kanamycin positive control. A halo formation indicated growth inhibition of incubated *E. coli* DSM 498 cells by the released kanamycin.

An inhibited growth of *E. coli* DSM 498 cells (200,000 cfu) was observed by a clear halo formation around the coated wires when PCL micro-containers were immobilized by DS1-DZ-LCI on stainless steel wires (see Figure 33A). The growth of *E. coli* DSM 498 cells was inhibited almost completely at an incubated cell number of 20,000 cfu (see Figure 33B). In all performed control experiments (see Figure 33C-E) no antimicrobial effect on *E. coli* DSM 498 cells was detected. As expected, the growth of *E. coli* DSM 498 cells was inhibited by the kanamycin positive control (see Figure 33F).

5 Targeting microplastics in the void of diluted suspensions

5.1 Declaration

The technology of enzymes (cutinases) fused to anchor peptides for enhanced microplastic degradation was developed in cooperation with Shohana Islam (see XIV. Author contributions). Parts this chapter were published by the author in Environment International:

Islam S & **Apitius L**, Jakob F and Schwaneberg U (2019). "Targeting microplastic particles in the void of diluted suspensions." Environment International 123: 428-435.
*shared first co-authorship

Parts of this chapter were filed for patent application:

Mussmann N, Wieland S, Degering C, Zimmermann W, Wei R, Jakob F, Islam S, Schwaneberg U, **Weber L**, Rübsam K, Eidener J, Haarmann T, Lorenz P, Schwerdtfeger R. 2018. Mittel erhaltend PolyesteraseI. DE 2018P35186

5.2 Summary and main results

The worldwide production of plastics and hence the production of plastic waste (8,300 million metric tons (Mt) in 2017) is of severe global concern for the environment and human health. An accumulation of plastic waste in landfills and in the natural environment predicted to be 12,000 Mt by 2050. Plastic waste management has to be improved, since only 9 % of all plastics have been recycled in 2015 (Geyer, Jambeck et al. 2017). The ubiquitous accumulation of plastic waste in the environment will make it a geological indicator of the *Anthropocene era* (Zalasiewicz, Waters et al. 2016). Plastics like PE, polyvinyl chloride (PVC), PP, PS, PET, or polyurethane (PUR) are building blocks for numerous applications (e.g., packaging, automotive industry, health sector, textiles or pipes) (Shah, Hasan et al. 2008). In the environment plastic waste is broken down by e.g. photo-, bio-, thermo-oxidative degradation, and friction (Barnes, Galgani et al. 2009, Browne, Crump et al. 2011). During degradation of plastic, microplastic particles are

formed (<5 mm) (Zheng, Yanful et al. 2005, Ivar do Sul and Costa 2014). Microplastics attract and store toxic compounds such as polychlorinated biphenyls (PCBs), polybrominated diphenyl ethers (PBDs), and bisphenols (Bouwmeester, Hollman et al. 2015). Microplastics accumulate in the food chain (in small fishes and larger mammals) (Boerger, Lattin et al. 2010, de Stephanis, Gimenez et al. 2013) and belong to the most serious pollutants worldwide. Strategies are needed to minimize existing environmental pollution for nearshore and riverine plastic collection (Sherman and van Sebille 2016). The implementation of zero waste strategies and waste management are needed to prevent an excessive generation of new microplastics (Eriksen, Lebreton et al. 2014). An improved waste recovery is crucial for a successful waste management. A microbial degradation of microplastic is possible by the secretion of specific polymer-degrading enzymatic and represents a promising strategy to convert plastic waste into biomass (Grima, Bellon-Maurel et al. 2000).

However, plastics are produced since the 1950´s (Geyer, Jambeck et al. 2017) and this very short time resulted in a limited evolutionary pressure for organisms to evolve sufficient enzymes for plastic degradation (Hopewell, Dvorak et al. 2009, Tokiwa, Calabia et al. 2009, Wei and Zimmermann 2017). Only a few plastics (e.g., PET and PUR) can undergo enzymatic degradation by fungi and bacteria (Howard 2002). PUR for instance is degraded by a hydrolytic cleavage of urethane bonds (Nakajima-Kambe, Shigeno-Akutsu et al. 1999). Enzymes like esterases and cutinases are reported to be capable of a hydrolytic cleavage of urethane bonds (Rowe and Howard 2002, Schmidt, Wei et al. 2017). However, the enzymatic degradation of polymers is slow and high local enzymes concentrations are needed on the polymer surface.

Naturally occurring polymers such as cellulose are degraded by specialized enzymes (e.g., cellulases) that bind via an adhesion promotor, the cellulose-binding domain (CBD). The CBD keeps the hydrolytic domain on the cellulose surface leading to an enhanced hydrolysis (Linder and Teeri 1997, Bolam, Ciruela et al. 1998). Comparable domains enhance enzymatically depolymerizing of chitin (Beintema 1994) and polyhydroxyalkanoate (Kasuya, Ohura et al. 1999).

Anchor peptides are natural occurring adhesive peptides, which efficiently bind to synthetic polymer surfaces (PP, PET, and PUR) at ambient temperature by forming a monolayer (Rübsam, Stomps et al. 2017, Rubsam, Weber et al. 2018). The anchor peptide

TA2 was fused to a bacterial cutinase (Tcur1278 from *Thermomonospora curvata*) capable of degrading polyester-polyurethane co-polymers (Impranil® DLN-SD, Covestro AG (Leverkusen, Germany)).

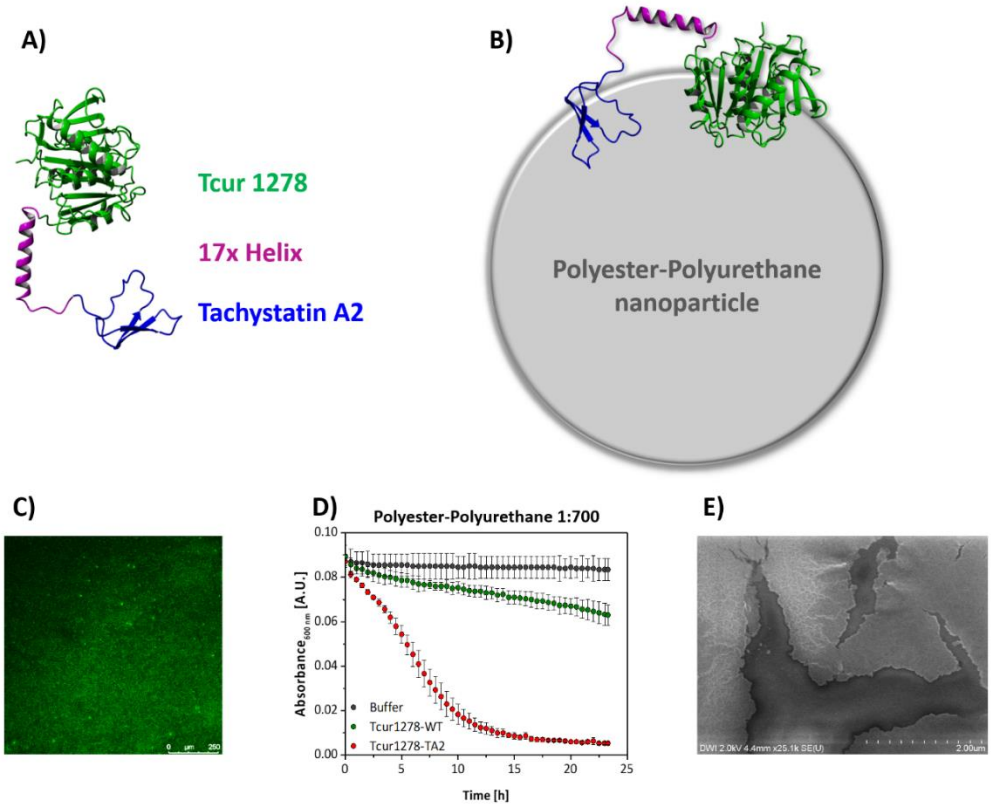

Figure 34: Polyester-polyurethane degradation by Tcur1278-TA2. A) Fusion of TA2 to the C-terminal end of the cutinase Tcur1278. **B)** TA2 enhances the binding of Tcur1278 to polyester-PUR. **C)** Confocal analysis of anchor peptide binding (TA2) to Impranil® DLN-SD. **D)** Degradation kinetics of Tcur1278 WT (green) and Tcur1278-TA2 (red). **E)** FE-SEM analysis of polyester-PUR film degradation by Tcur1278-TA2.

Figure 34 summarized the concept and the results of the anchor peptide promoted polyester-polyurethane degradation. The N-terminal Tcur1278 (Wei, Oeser et al. 2014) and the C-terminal anchor peptide TA2 (Osaki, Omotezako et al. 1999) were functionally separated by a 17x spacer helix (Arai, Ueda et al. 2001) (see Figure 34A). The binding of TA2 to polyester-polyurethane nanoparticles enables an enhanced polymer degradation by Tcur1278 (see Figure 34B). Anchor peptide binding (TA2 and LCI) to polyester-polyurethane films was monitored by confocal analysis (see Figure 34C). The polyester-polyurethane degradation performance by Tcur1278-TA2 was compared to Tcur1278-WT in a MTP-based assay and changes in particle size was determined by DLS (see Figure 34D).

A degradation of polyester-polyurethane films on a stainless steel support was visualize by FE-SEM analysis (see Figure 34E).

The degradation of polyester-polyurethane nanoparticles by Tcur1278-TA2 was accelerated the by a factor of 6.6 in comparison to Tcur1278-WT and the half-life of nanoparticles was reduced from 41.8 h to 6.2 h (6.7-fold) in a diluted polyester-polyurethane suspension (0.04 % w/v). FE-SEM analysis showed that Tcur1278-TA2 was able to degrade the polyester-polyurethane film within 40 h whereas a degradation by the Tcur1278-WT was not detectable. Degradation by Tcur1278-TA2 was achieved with a very low enzyme concentration (down to 0.6 nM) in the MTP-based assay as well as the degradation of polymer film. Key parameters for the establishment of sustainable microplastic degradation processes are low enzyme concentrations and applications at ambient temperature (e.g., in wastewater plants).

6 General discussion

Our daily life is accompanied by polymers and plastics. Polymers are produced and modified for uncountable applications in automotive industry, packaging, technical devices or medical applications. A broad applicability of polymers in medical science requires a high biocompatibility. The biocompatibility of a device is related to polymer surfaces since it is the point of interaction with the biological environment (Fabbri and Messori 2017). Polymer bulk properties were traditionally engineered to application conditions by chemical or physical surface functionalization (Penn and Wang 1994).

Surface functionalization with peptides offers a lot of attractive possibilities, such as a very coating high density or a coating of monolayers on target surfaces (Rübsam, Stomps et al. 2017). In comparison, chemical and physical coating technologies such as grafting are limited by a steric hindrance of attached polymer chains that are blocking available binding sites on the polymer surface (Raynor, Capadona et al. 2009). Peptides applied to a surface are monodispersed and can introduce multiple functionalities simultaneously (e.g., NH_2, COOH and OH). Coatings with peptides can be performed by industrially applied technologies such as dip coating and are suitable for the functionalization of sophisticated 3D structures (Jang, Bae et al. 2015, Rübsam, Stomps et al. 2017, Rubsam, Weber et al. 2018). Peptides are coated at ambient temperature and under solvent-free conditions, whereas chemical and physical technologies are often restrained by safety hazards or the generation of large volumes of solvent waste (Fabbri and Messori 2017).

The interest in peptides for therapeutic demands and for the generation of biocompatible material increased steadily during the last years due to their high activity per unit mass, great chemical and biological diversity, and low toxicity (Zhao, Xu et al. 2016). The global market for biomaterials was estimated to 88.4 billion US$ with a compound annual growth rate of 15 % in 2017 (Jaganathan, Balaji et al. 2015). An application of peptides for therapeutic purposes demands a reproducible production in high yields and at low costs. Peptides are either produced by chemical synthesis or recombinant production by transgenic organisms (Kyle, James et al. 2012).

The recombinant production of peptides enables to work with non-hazardous compounds and environmentally friendly raw materials. Especially long peptides (>35 aa)

(Kyle, James et al. 2012) and complex peptides with repetitive sequences can be produced in high monodispersity and in scalable amounts. Productions of 1 g peptide per 400 g raw material are reported (<120 US$), whereas in chemical synthesis, 10 kg raw material for 1 g of peptide are estimated (800-2000 US$) (Reddy 2017). In chemical synthesis, solid phase peptide synthesis (SPPS) is commonly applied. SPPS is based on the attachment of the C-terminal amino acid to a resin (e.g., 1-2 % divinylbenzene cross-linked polystyrene). The target peptide chain is elongated to the N-terminus (Jaradat 2018). During synthesis, the α-amino group and side chain have to be protected by an acid-sensitive tert-butoxycarbonyl (tBoc) group or a base-sensitive 9-fluorenylmethyloxycarbonyl (Fmoc) group (Nilsson, Soellner et al. 2005). The addition of every amino acid requires a protection, elongation and purification cycle. Consequently, the yield of produced peptides is decreasing with an increase in synthesized peptide length. Chemical peptide synthesis is ideal for a peptide length of 15 amino acids (Reddy 2017) and the introduction of non-natural amino acids (e.g., D-amino acids) or glycosylations. Longer peptide are often synthesized by convergent technologies (Seenaiah, Jbara et al. 2015). The production of suitable amounts of anchor peptides and especially biadhesive peptides (e.g., DS1-DZ-LCI: 134 aa) by chemical synthesis would be rather challenging and time consuming in comparison to a recombinant production. The expression host for the production of anchor peptides could be optimized. Even though a production of peptides shorter than 100 aa in *E. coli* is challenging it is the most commonly used production host in industry. The susceptibility of short peptides to degradation can be overcome by the introduction of a cleavable self-aggregating tag so that the peptides form active inclusion bodies (Zhao, Xu et al. 2016). Alternatively, *Corynebacterium glutamicum* is a useful host for the industrial production of heterologous proteins. It is commonly used for the production of amino acids due to an absence of many endogenous proteins and secreted proteases (Yim, Choi et al. 2016). The secretion pathway of *C. glutamicum* enables a simple purification of anchor peptides from the culture media.

7 Summary and conclusion

Biological surface functionalization of polymers is of growing importance for the generation of biocompatible devices. In an environmentally friendly and cost efficient way, multiple functionalities (e.g., NH_2-, COOH- or OH-groups) can be introduced onto a target surface. Adhesion promoters such as anchor peptides enable the generation of durable coatings for biologically inert polymers (e.g., PS, PP, and PCL) and metals (e.g., stainless steel) at very high densities. Industrial and medical applications require a reliable and stable anchor peptide binding under process conditions. A platform of anchor peptides and biadhesive peptides has been established that allowed an easy identification of target binders. Identified binders had to be optimized by directed evolution to application conditions. Therefore, a directed evolution protocol for short peptides (<100 aa) was developed to overcome shortcomings of conventional methods that normally are applied for the evolution of enzymes (~1000 aa).

A robust and generally applicable Peptide-Polymer evolution protocol (PeP*evo* protocol) was established that enabled for the first time a randomization of short peptide genes (*ta2*: 132 bp) with a very high mutation frequency. The high mutational load (59 mutations/kb) ensured a sufficient diversification of the target gene. Improved binding peptide variants were identified reliably applying the eGFP-based Assay for Better polymer Binding Anchor peptides (ABBA) (standard deviation of 10.6 %). The PeP*evo* protocol was validated in one round of directed evolution of Tachystatin A2 (44 amino acids) towards improved PS-binding in presence of the anionic surfactant LAS. Finally, PeP*evo* identified stronger PS-binders with an up to six-fold improved binding in the presence of 0.5 mM LAS.

A bottleneck in directed evolution is the screening throughput, which is normally magnitudes lower in comparison to the generated library diversity. Therefore, a whole-cell esterase A-based *E. coli* cell surface display technology was established. The presentation of improved polymer-binding anchor peptide variants on the cell surface of *E. coli* enabled an ultra-high-throughput screening (up to 10^7 variants) by a simple incubation of target materials with the culture broth. The PP-binding anchor peptide LCI was simultaneously saturated at five positions (Y29, D31, G35, E42, and D45) whereby

3.2 million peptide variants were generated. The *E. coli* cell surface display allowed an efficient analysis of the generated LCI diversity by screening in total approximately 10 million clones. A characterization of identified LCI variants revealed an up to 12-fold improvement in PP-binding strength in presence of 0.125 mM LAS. A peptide-mediated immobilization of whole-cells on a PP-film was visualized by ESEM analysis. The cell surface display technology represented a first ultra-high-throughput screening system to improve adhesion peptides.

The application of peptides to generate biocompatible materials is steadily increasing during the last years. Especially, in tissue culture, they are commonly utilized. However, most approaches rely on chemical conjugations of active peptides to a medical device. The high binding affinity of anchor peptides inspired the generation of fusion peptides that facilitated a simultaneous binding of two chemically different materials. Stainless steel (medical stents) and PCL (drug delivering micro-containers) were selected as target materials. Binding of anchor peptides to both components was analyzed using eGFP as reporter protein. Accordingly, biadhesive peptides were composed of one stainless steel binder and one PCL binder, functionally separated by a peptide-spacer. The biadhesive peptide Dermaseptin S1-Domain Z-LCI was able to immobilize kanamycin-loaded PCL micro-containers on stainless steel surfaces. Immobilization was visualized by confocal microscopy and FE-SEM analysis. The released kanamycin inhibited cell growth up to a cell density of 10^{-5} cfu/mL in a growth inhibitory halo-formation assay. The application of biadhesive peptides as adhesion promoters of stainless steel and PCL was the first proof-of-principle for the assembly of two chemically components at ambient conditions.

In addition to medical applications, anchor peptides are a versatile tool for environmental applications. The accumulation of microplastics in the environment is of severe global concerns. Therefore, efficient plastic degradation strategies have to be developed. Anchor peptides were used as adhesion promoters to enhance enzymatic degradation of polyester-polyurethane nanoparticles in highly diluted suspensions. The nanoparticles were depolymerized by the enzyme Tcur1278 (cutinase) in a MTP-based turbidity assay. The strong binding affinity of the anchor peptide Tachystatin A2 to polyester-polyurethane led to a fusion of the anchor peptide to Tcur1278 for an enhanced nanoparticle degradation. The enzymatic degradation kinetics of Tcur1278-TA2 in comparison to the Tcur1278-WT was monitored and the respective particle half-life was

determined. It could be shown, that the fusion of the adhesion promoter Tachystatin A2 improved both parameters up to six-fold. The effect of the anchor became more prominent with an increase of nanoparticle dilutions (until a dilution of 1:700). Degraded particles were analyzed by DLS measurements and it could be shown, that the anchor enabled a degradation of smaller particles (down to 0.8 nm). A FE-SEM analysis of a polyester-polyurethane film confirmed an enhanced degradation by the fusion enzyme Tcur1278-TA2.

In conclusion, anchor peptides have proven their high potential for a tailor-made functionalization of polymer and metal surfaces. The vast natural diversity of anchor peptides and the ability to adapt them to application conditions by the developed PeP*evo* protocol makes them a versatile tool for the generation of biohybrid materials. In combination with a two-step selection procedure it is likely that the developed anchor peptide engineering can be used to evolve selective adhesion promoters (e.g., binding on PP and not PS). Anchor peptide coatings can be applied as antimicrobial coatings for biomaterials, in plant health, or in nanomaterials. The platform of biadhesive peptides opens up a broad range of polymer and metal surfaces (e.g., platinum, gold, and zinc/titanium oxide) that can be functionalized. The immobilization technology can be extended to other medical materials like stents, implants or catheters.

The presentation of engineered adhesion promoters on a cell surface can be used to direct and immobilize polymer degrading organisms specifically to plastic particles. The usage of anchor peptides as fusion tags enables an enhanced immobilization of polymer-degrading enzymes on plastics to achieve an effective and controlled degradation. Both technologies might find applications in wastewater treatment technologies and in the development of sustainable biotechnological processes for conversion of plastics into valuable compounds.

IV Development of an anchor peptide platform

A general cloning platform was established to enable the cloning of eGFP-anchor peptide fusion constructs or biadhesive peptides using universal primers. Using this platform, a collection of > 60 eGFP-anchor peptides and >20 biadhesive peptides was generated within the Schwanebrg group. eGFP- anchor peptides and respective controls could be produced reproducibly according to validated protocols and their binding to selected surfaces (e.g., polymers, metal, textiles) can easlily be investigated. The reporter protein eGFP was used to detect and quantify anchor peptides on target surfaces. The fusion proteins consisted of an N-or C-terminal eGFP which was functionally separated by a stiff spacer helix (17 amino acids: AEAAAKEAAAKEAAAKA) (Arai, Ueda et al. 2001) and a TEV cleavage site (7 amino acids: ENLYFQG) (Kapust and Waugh 2000) from the C-terminal anchor peptide (see Figure 35). Anchor peptides and biadhesive peptides were purchased as synthetic genes (life Technologies/MWG, see Figure 35A-C) and were cloned into a pET28(+) backbone. Combination of general N- and C-anchor primers (see VIII. List of primers) allowed the construction of biadhesive peptides without the reporter eGFP (see Figure 35B):

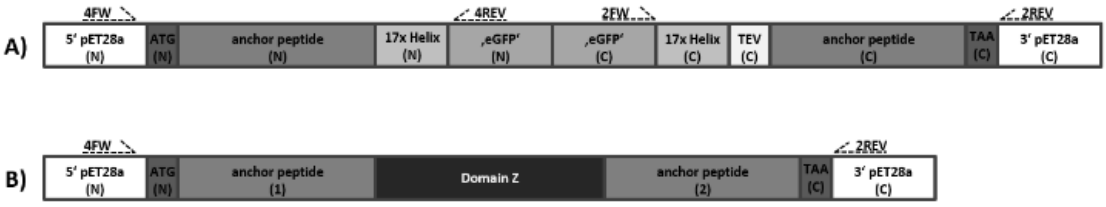

C) *GATCGAGATCTCGATCCCGCGA*AATTAATACGACTCACTATAGGGGAATTGTGAGCGGATAACAATTCCCCTCTAGAAATAATTTTGT
TTAACTTTAAGAAGGAGATATACC**ATG**PBP-SEQUENCEGCAGAAGCAGCAGCAAAAGAAGCCGCTGCCAAAGAAGCG*GCAGCG*
*AAAGCAATGGTGAGCAAGGCTGTACAAGGCAGAAGCAGCAG*CAAAAGAAGCCGCTGCCAAAGAAGCGGCAGCGAAAGCAGA
AAATCTGTATTTTCAGGGPBP-SEQUENCE**TAATAA**CACTGAGAT*CCGGCTGCTAAC*

Figure 35: Design of synthetic anchor peptides genes. A) Synthetic genes were designed in a way that, dependent on the primer pair used, N-anchor peptides (4FW+4ERV) or C-anchor peptides (2FW+2REV) can be amplified (see VIII. List of primers). **B)** Biadhesive peptides were cloned using the primer 4FW and 2REV. **C)** DNA sequence of synthetic genes. The gene is composed the N-anchor sequence (5') and the C-anchor sequence (3'). The N-anchor sequence starts with a 5' pET28(+) vector sequence (highlighted in purple) with a universal primer binding site (highlighted in purple, italic, bold), a start codon (ATG, highlighted in black) for transcription of N-anchor peptides followed by the codon optimized sequence of the respective anchor peptide (highlighted in blue, underlined), the sequence of the 17x Helix (highlighted in grey; primer binding site: italic, bold) and a 3' pET28(+) vector sequence (highlighted in purple, italic, bold). The C-anchor sequence starts with a 5' pET28(+) vector universal primer binding site sequence (highlighted in turquoise, italic, bold), the sequence of the 17x Helix (highlighted in grey; primer binding site: italic, bold), followed by

a TEV cleavage site (highlighted in orange) and the codon optimized sequence of the respective anchor peptide (X), two stop codons (TAATAA, highlighted in black) for termination of transcription and a 3' pET28(+) vector sequence (highlighted in turquoise) with a universal primer binding site (highlighted in turquoise, italic, bold).

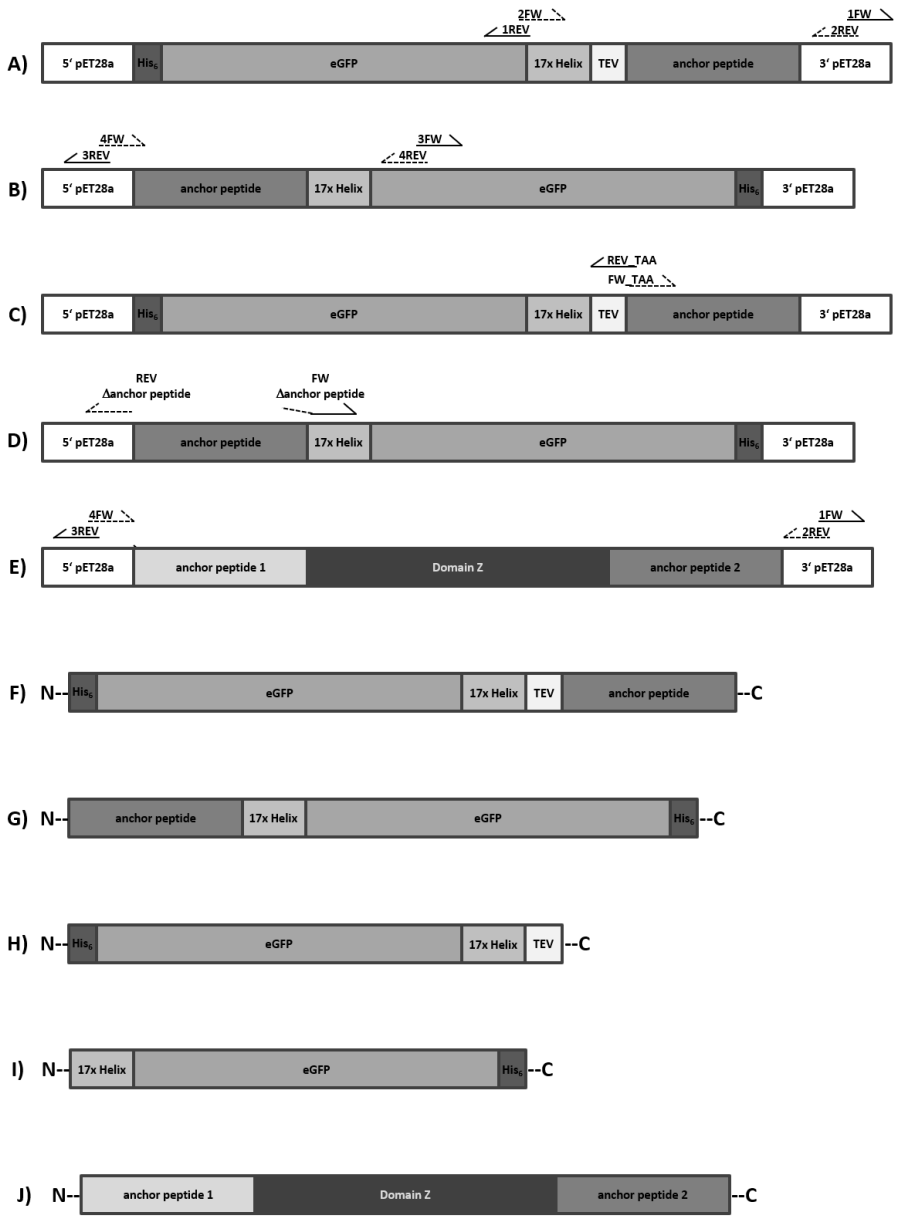

Figure 36: General cloning platform for anchor peptides. Anchor peptide fusion constructs were cloned in the pET28 a(+) backbone. They were fused to the 5'(N-anchor peptide) or the 3'end (C- anchor peptide) of the reporter gene eGFP. Functional separation was enabled by the stiff spacer helix 17x Helix. C-anchors were cloned with TEV cleavage site to cleave off anchor peptides from the reported eGFP. **A)** Generation of C-anchors: The backbone was amplified using 1FW and 1REV primers. Synthetic genes (17xHelix_TEV_ anchor peptide) were amplified using 2FW and 2REV primers. **B)** Generation of N-anchors: The backbone was amplified using 3FW and 3REV primers. Synthetic genes (anchor peptide_17xHelix) were amplified using 4FW and 4REV primers. **C)** Generation of C-anchor control: A C-anchor template was amplified with FW_TAA and REV_TAA primers to introduce a stop codon 3' of the TEV cleavage site. The anchor peptide will not be amplified. **D)** Generation of N-anchor control: The N-terminal anchor peptide was deleted by

amplifying an N-anchor construct with FWΔPBP and REV ΔPBP primers. **E)** Generation of biadhesive peptides: The backbone was amplified using 1FW and 3REV primers. Synthetic genes (anchor peptide1_Domain Z_ anchor peptide2) were amplified using 4FW and 2REV primers **F-J)** Translated fusion peptides: C-anchor peptide **(F)**, N-anchor peptide **(G)**, C-anchor control **(H)**, N-anchor control **(I)**, and biadhesive peptide **(J)**.

IV.I Methods

All used chemicals were purchased from Sigma-Aldrich Corp. (St. Louis, USA), AppliChem GmbH (Darmstadt, Germany), as well as Carl Roth GmbH (Karlsruhe, Germany) and had analytical-reagent grade or higher purity. Synthetic genes were obtained from GeneArt AG (Regensburg, Germany) or Eurofins Scientific SE (Ebersberg, Germany) and oligonucleotides were as well acquired from Eurofins Scientific SE (Ebersberg, Germany) in salt-free form. Enzymes were obtained from New England Biolabs GmbH (Frankfurt am Main, Germany). Plasmid extraction and PCR purification kits were purchased from Macherey-Nagel GmbH & Co. KG (Düren, Germany) and Qiagen GmbH (Hilden, Germany). The plasmid pET28a(+) (Novagen, Darmstadt, Germany) was used as expression vector. The *E. coli* strains DH5α (cloning host) and BL21-Gold (DE3) (host for protein expression) were purchased from Agilent Technologies (Santa Clara, USA).

IV.I.I Cloning of eGFP-anchor peptide fusion constructs

The synthetic gene *anchor peptide* (Eurofins MWG, Operon (Ebersberg, Germany)) was cloned in the pET28a(+)::eGFP backbone applying 'sequence independent phosphorothioate-based ligase-independent gene cloning' (PLICing) (Blanusa, Schenk et al. 2010).

Generation of C-anchor peptides: Target sequence (17xHelix-TEV-anchor peptide) and vector backbone (pET28a(+)::His_eGFP) were amplified in a PCR (Mastercycler® pro, Eppendorf, Germany) using the primer pairs 1FW+1REV and 2FW+2REV with complementary phosphorothioated nucleotides (PTOs) at the 5'-end (see Figure 36A) and Table 13).

Generation of N-anchor peptides: Target sequence (anchor peptide-17xHelix) and vector backbone (pET28a(+)::eGFP_His) were amplified using the primer pairs 3FW+3REV and 4FW+4REV with complementary phosphorothioated nucleotides (PTOs) at the 5'-end (see Figure 36B) and Table 13).

Generation of biadhesive peptides: Target sequence (anchor peptide1-DZ-anchor peptide2) and vector backbone (pET28a(+)) were amplified using the primer pairs 4FW+2REV and 1FW+3REV with complementary phosphorothioated nucleotides (PTOs) at the 5'-end (see Figure 36E and Table 13).

The PCR conditions for PLICed constructs are listed in Table 13 and primers are listed in VIII. List of primers. PCRs were performed using PfuS DNA polymerase (2.5 U) and deoxyribonucleotide triphosphates (dNTPs; 10 µM). The parental DNA was digested (20 U *Dpn*I, 16 h, 37°C) and purified (QIAquick PCR Purification Kit, QIAGEN, Hilden, Germany). Both PCR products were cleaved at the phosphorothioated nucleotides in an alkaline iodine solution (iodine (30 mM) in Tris/HCl buffer (50 mM, pH 9.0)) producing single-stranded overhangs (PCR cycler; 70°C, 10 min). The backbone mix and target sequence mix were united and hybridized (PCR cycler; 20°C, 5 min). After hybridization, the plasmid was transformed in chemically competent *E. coli* DH5α or BL21-Gold (DE3) cells.

Generation of controls: The **C-anchor control** was generated by introducing a stop codon (TAA) 3' of the TEV cleavage site using complementary primers FW_TAA and REV_TAA (20 µM each; see Figure 36C and Table 13) using pET28a(+)::eGFP-17xHelix-TEV-anchor peptide (25 ng) as a template. The **N-anchor control** was generated by deleting the N-terminal anchor peptide with overlapping primers FW-Δanchor peptide and REV-Δanchor peptide (20 µM each; see Figure 36D and Table 13) using pET28a(+)::anchor peptide -17xHelix-eGFP (25 ng) as a template. Both controls were amplified in a two-step-PCR. The PCR conditions for a two-step PCR are listed in Table 13. PCRs were performed using PfuS DNA polymerase (2.5 U) and dNTPs (10 µM). The parental DNA was digested (20 U *Dpn*I, 16 h, 37°C), purified (PCR clean-up gel extraction kit, Macherey-Nagel, Düren, Germany), and subsequently transformed into *E. coli* BL21-Gold (DE3). Successful cloning of all generated constructs was confirmed by sequencing (Eurofins Genomics GmbH, Ebersberg, Germany).

Table 12: PCR conditions to generate anchor peptides, biadhesive peptides, and respective controls.

Step	Temperature [°C]	Time [s]	Cycles [n]
Insert PCR - PLICing			
Initial denaturation	98	30	1
Denaturation	98	15	25
Annealing	55	30	25
Elongation	72	30	25
Final elongation	72	180	1
Storage	8	∞	

Backbone PCR - PLICing			
Initial denaturation	98	30	1
Denaturation	98	15	25
Annealing	55	30	25
Elongation	72	210	25
Final elongation	72	300	1
Storage	8	∞	

Step	Temperature [°C]	Time [s]	Cycles [n]
Two step PCR –Step 1			
Initial denaturation	98	30	1
Denaturation	98	15	5
Annealing	60	30	5
Elongation	72	210	5
Halt	8	∞	
Two step PCR –Step 2			
Initial denaturation	98	30	1
Denaturation	98	15	20
Annealing	62	30	20
Elongation	72	210	20
Final elongation	72	300	1
Storage	8	∞	

IV.I.II Cultivation of eGFP-anchor peptide constructs

Single colonies were transferred into cultivation tubes containing LB medium (5 mL; 10 g/L tryptone, 10 g/L NaCl, 5 g/L yeast extract) supplemented with kanamycin (50 µg/mL) and cultivated overnight (37°C, 200 rpm, 70 % humidity; Multitron Pro, Infors AG). After cultivation, glycerol (500 µL/1000 µL culture; 50 % (v/v)) was added and the glycerol stocks were stored at -80°C. Pre-cultures were inoculated from glycerol stocks with a sterile pipette tip into cultivation tubes containing LB medium +1 % Glc (5 mL; 10 g/L tryptone, 10 g/L NaCl, 5 g/L yeast extract + 1 % glucose (w/v)) supplemented with kanamycin (50 µg/mL) and cultivated overnight (37°C, 200 rpm, 70 % humidity; Multitron Pro, Infors AG). Main-cultures were inoculated in 100 mL or 1 L shaking flasks containing TB medium (10 mL or 250 mL; 12 g/L tryptone, 24 g/L yeast extract, 5 g/L glycerol, 17 mM KH_2PO_4 and 72 mM K_2HPO_4, supplemented with kanamycin (50 µg/mL)) with an OD_{600} of 0.025 and cultivated for 48 h (20°C, 200 rpm, 70 % humidity; Multitron Pro, Infors AG) according to (Rübsam, Stomps et al. 2017)

V. List of Figures

VI. List of Tables

VII. List of Abbreviations

aa	amino acid
ABBA	Assay for Better polymer Binding Anchor peptides
amp	ampicillin
AMP	antimicrobial peptide
Au	gold
B. subtilis	*Bacillus subtilis*
BCP	block copolymers
bp	base pair
BSA	bovine serum albumin
CFE	cell free extract
CFU	colony forming unit

CSD	Cell surface display
Da	Dalton
DE	directed evolution
DNA	deoxyribonucleic acid
dNTPs	deoxyribonucleotides
DS1	Dermaseptin S1
DZ	staphylococcal protein A domain Z
E. coli	*Escherichia coli*
eGFP	enhanced green fluorescent protein
Em	emission
epPCR	error prone polymerase chain reaction
ESEM	Environmental Scanning Electron Microscope
EtOH	EtOH
eV	electron-volts
Exc	excitation
FACS	Fluorescent-Activated Cell Sorting
FE-SEM	Field Emission Scanning Electron Microscopy
Glc	glucose
kan	kanamycin
LAS	sodium dodecylbenzenesulfonate
LB media	Luria-Bertani media
LCI	liquid chromatography peak I
MEGAWHOP	megaprimer PCR of whole plasmid
MTP	microtiter plate
OD	optical density
P. pastoris	*Pichia pastoris*
PBP	polymer binding anchor peptides
PCL	polycaprolactone
PCR	polymerase chain reaction
Pd	palladium
PEG	polyethylene glycol
PeP*evo*	Peptide-Polymer *evol*ution
peptesive	biadhesive peptide
pET22-EV	pET22 empty vector
pET28-EV	pET28 empty vector
PIB	polyisobutylene
PLGA	poly(lactic-co-glycolic acid)
PLICing	sequence independent phosphorothioate-based ligase-independent gene cloning
PLLA	poly(L-lactide)
PMMA	poly(methyl methacrylate)
PP	polypropylene
PPyCl	chlorine-doped polypyrrole
PS	polystyrene
PTFE	polytetrafluoroethylene
PTOs	phosphorothioated nucleotides
PVD	physical vapor deposition
RFU	relative flurescence units
rpm	revolutions per minute

SAM	self-assembled monolayer
SDM	site-directed mutagenesis
SDS-PAGE	sodium dodecyl sulfate polyacrylamide gel electrophoresis
SSM	site-saturation mutagenesis
TA2	Tachystatin A2
TB media	Terrific broth media
TEOS	tetramethoxysilane
TEV	Tobacco etch virus
THA	Thanatin
TPU	thermoplastic polyurethane
Triton X-100	octyl phenol ethoxylate
uHTS	ultra-high-throughput screening
WT	wild type

VIII. List of primers

Name	Sequence 5' → 3'
1FW*	ccg gct gct aac AAA GCC CGA AAG
1REV*	ctt gta cag cTC GTC CAT GCC G
2FW*	gct gta caa gGC AGA AGC AGC AG
2REV*	gtt agc agc cgg ATC TCA GTG
3FW*	ccg gct gct aac AAA GCC CGA AAG
3REV*	gag atc tcg atc CTC TAC GCC GGA C
4FW*	gat cga gat ctc GAT CCC GCG A
4REV*	gtt agc agc cgg ATC TCA GTG
FW-TAA	CTG TAT TTT CAG GGT TAA TGA GCA GGT TGC
REV-TAA	GCA ACC TGC TCA TTA ACC CTG AAA ATA CAG
FW-Δanchor peptide	CAT CAT CAT GGC AGA AGC AGC AGC AAA AG
REV-Δanchor peptide	GCT GCT TCT GCC ATG ATG ATG ATG GCT GCT GC
FW_epPCR_Tachystatin A2	GCG GAG AAC CTG TAC TTT CAG GGC
Rev_epPCR_Tachystatin A2	CGG GCT TTG TTA GCA GCC GGA TCT CAG TGT TAT CA
FW-CSD-pET22b*	gca gaa gca gca GCA AAA GAA G
REV-CSD-pET22b*	atg tat atc tcC TTC TTA AAG TTA AAC
FW-CSD-LCI*	gag ata tac atA TGA AAA AAA CCG CGA TTG
REV-CSD-LCI*	tgc tgc ttc tgc TTT GCG ATC
FW-CSD-control	GCA GAA GCA GCA GCA AAA GAA GCC GCT G
REV-CSD-control	CTG CTG CTT CTG CCG CGT TCG CCA CGG TC
FW-LCI-CSD-5SSMs**	TAT TGG GTG GGT ATT TAT **NNK** GTG TGG **NNK** CGC AAA G
REV-LCI-CSD-5SSMs**	CAC CCA ATA **MNN** TTT GCT GCT **MNN** ATA **MNN** TTT GCT TTT G
FW-LCI-CSD-LW1	TAT TGG GTG GGT ATT TAT **CAG** GTG TGG **TCT** CGC AAA TAA TAA CAC TG
REV-LCI-CSD-LW1	CAC CCA ATA **ATC** TTT GCT GCT **AGT** ATA **ACA** TTT GCT TTT G
FW-LCI-CSD-LW2	GGT TAT TGG GTG GGT ATT TAT **GGG** GTG TGG **GGG** CGC A
REV-LCI-CSD-LW2	CAC CCA ATA ACC TTT GCT GCT **CGC** ATA **AAC** TTT GCT TTT G
FW-LCI-CSD-LW3	GGT TAT TGG GTG GGT ATT TAT **GTG** GTG TGG **CAT** CGC A
REV-LCI-CSD-LW3	CAC CCA ATA ACC TTT GCT GCT GTC ATA GTA TTT GCT TTT G

**** Lower case letters indicate phosphorothioated nucleotides (PTOs)***

***** NNK and MNN indicate positions for site saturation mutagenesis***

IX. Amino acids

Name	One-letter code	Name	One-letter code
alanine	A	leucine	L
arginine	R	lysine	K
asparagine	N	methionine	M
aspartic acid	D	phenylalanine	F
cysteine	C	proline	P
glutamine	Q	serine	S
glutamic acid	E	threonine	T
glycine	G	tryptophan	W
histidine	H	tyrosine	Y
isoleucine	I	valine	V

X. List of proteins, peptides and spacers

Name	Sequence	Reference
eGFP	VSKGEELFTGVVPILVELDGDVNGHKFSVSGEGEGDATYGKLTLKFICTT GKLPVPWPTLVTTLTYGVQCFSRYPDHMKQHDFFKSAMPEGYVQERTI FFKDDGNYKTRAEVKFEGDTLVNRIELKGIDFKEDGNILGHKLEYNYNSH NVYIMADKQKNGIKVNFKIRHNIEDGSVQLADHYQQNTPIGDGPVLLP DNHYLSTQSALSKDPNEKRDHMVLLEFVTAAGITLGMDELYK	(Cormack, Valdivia et al. 1996)
Dermaseptin S1	GLWSTIKQKGKEAAIAAAKAAGQAALGAL	(Brand, Leite et al. 2002)
LCI	AIKLVQSPNGNFAASFVLDGTKWIFKSKYYDSSKGYWVGIYEVWDRK	(Gong, Wang et al. 2011)
Tachystatin A2	YSRCQLQGFNCVVRSYGLPTIPCCRGLTCRSYFPGSTYGRCQRY	(Osaki, Omotezako et al. 1999)
Thanatin	GSKKPVPIIYCNRRTGKCQRM	(Fehlbaum, Bulet et al. 1996)
17x Helix	AEAAAKEAAAKEAAAKA	(Arai, Ueda et al. 2001)
TEV cleavage site	ENLYFQG	(Kapust and Waugh 2000)
Domain Z	VDNKFNKEQQNAFYEILHLPNLNEEQRNAFIQSLKDDPSQSANLLAEAK KLNDAQAPK	(Tashiro, Tejero et al. 1997)
PS19	RAFIASRRIKRP	(Kumada, Tokunaga et al. 2006)
Tcur1278	SLRKSFGLLSATAALVAGLVAAPPAQAAANPYQRGPDPTESLLRAARGP FAVSEQSVSRLSVSGFGGGRIYYPTTTSQGTFGAIAISPGFTASWSSLAW LGPRLASHGFVVIGIETNTRLDQPDSRGRQLLAALDYLTQRSSVRNRVD ASRLAVAGHSMGGGGTLEAAKSRTSLKAAIPIAPWNLDKTWPEVRTPT LIIGGELDSIAPVATHSIPFYNSLTNAREKAYLELNNASHFFPQFSNDTMA KFMISWMKRFIDDDTRYDQFLCPPPRAIGDISDYRDTCPHT	(Wei, Oeser et al. 2014)

XI. Acknowledgement

The work of my PhD project was financed by Arbeitsgemeinschaft industrieller Forschungsvereinigungen (AiF; IGF-Vorhaben 18180 N). The AiF is kindly acknowledged for financial support.

I would like to thank Prof. Schwaneberg for giving me the opportunity to be part of his research group and for my scientific and personal development during the last years. Thank you for the very interesting project of anchor peptides and your scientific support and guidance during my PhD time. I thank Prof. Pich for his time and acceptance of being the second referee in my PhD committee. Thank you also for our nice and productive collaboration and support during manuscript preparation. I also thank PD Fabry and Prof. Schirawski for being part of my PhD committee.

A big thank you to Dr. Felix Jakob, who supervised my during my PhD time. It has been a pleasure to be part of your team. Thank you for all the support you gave me, for all discussions, guidance in preparation of presentations and manuscripts, fun coffee breaks and barbeques in your place. And for your strong nerves with all those girls in the basement. All of this makes you the probably best supervisor ever.

Thank you to the Biohybrid Systems division. I think we had a good and productive time in DWI. My colleagues made work enjoyable, so special thanks to Kristin, Catalina, Shohana, Letícia, Kati, Julia and Heidi. I liked the talks and discussions during coffee breaks and also in our free time (Kaiserwetter!). Thank you to all my students: Tim, Christina, Asma, Sebastian, Aldo and Kai.

I would like to thank all members of the Schwaneberg group I met along the way for the very nice time in Aachen. I learned a lot about how different people can be, working in a multinational atmosphere opened my mind a lot. I might want to visit some of you guys when you are back home!

I would really like to thank Kristin and Shohana. I collaborated with the two of them in projects (that resulted in nice publications ☺) and I could not wish for better project partners. We always worked well together, trying to complement the work of each other without any greed and complaints. We had a lot of fun.

Thank you to Sven Buschmann, Sabrina Mallmann, Thorsten Palmer, Khosrow Rahimi Harchegani and Stephan Rütten for the collaboration and performing experiments for me.

Sven prepared PCL micro-containers for me more than once and he was always very motivated to help me. Sabrina performed FE-SEM analysis for me (and Shohana), Khosrow Rahimi Harchegani and Stephan Rütten performed ESEM analysis. Thorsten performed DLS analysis for Shohana and me. All your effort improved my manuscripts a lot. I am very grateful for your support.

Thank you to David Schönauer, for giving me the opportunity to work for SeSaM for three month, the results we generated starting from there resulted in a nice publication.

The biggest thank you of all goes to my family, you always supported me. You made me do this, you made me believe in myself. My parents made me a person with an own opinion and a sense of justice, what is not always easy for others but I am very grateful for that. I thank my sister Luise (also for proof-reading) and my brother Jan for being such great siblings and for our family feeling. I thank my grand-mother, who always enlightened a candle in important moments and for: “If you have any questions regarding you PhD, just ask me. I think I can help!” I thank all my aunts, uncles and cousins, parents-in-law, and grandparents-in-law, who were part of the process and a big support.

Last but most importantly, I would like to thank my husband Florian. In the beginning of my PhD we had to take hard decisions about long distance relationships. Thank you for supporting me the whole time. Thank you for travelling 15 hours every weekend, just to visit me. I estimated that you spend roughly 2700-3000 hours in the train besides my own travelling time. I would also like to thank you for scientific discussion and proof-reading of this thesis.

XII. Curriculum vitae

Personal details

Name	Lina Apitius (née Weber)
Date and place of birth	September, 4th 1983 Mettingen, Germany

Professional experience and education:

Work positions:

Since 5/2014	**DWI-Leibniz Institute for Interactive Materials e.V.** **PhD student** Group Biotechnology/Univ.-Prof. Dr. Ulrich Schwaneberg Subgroup Biohybrid systems/ Dr. Felix Jakob ***Engineered adhesion peptides for functionalization of natural surfaces, polymers, and metal alloys***
11/2013-4/2014	**DWI-Leibniz Institute for Interactive Materials e.V.** **Scientific co-worker** Group Biotechnology/Univ.-Prof. Dr. Ulrich Schwaneberg Subgroup Biohybrid systems/ Dr. Felix Jakob ***Engineering of a protease towards a higher stability and improved washing performance using random and focused mutagenesis methods***

Education:

4/2011-6/2013	**RWTH Aachen University, Germany** Major subjects: Medical and Industrial Biotechnology Degree: Master of Science in Molecular and Applied Biotechnology
9/2006-3/2011	**University of Applied Science Emden-Leer, Germany** Major subjects: Cell culture techniques, Toxicology, Engineering Degree: Bachelor of Science (Engineer) in Biotechnology
9/2009-4/2010	**Athlone Institute of Technology,** Co. Westmeath, Ireland Major subjects: Pathology, Pharmacology, Analytical Toxicology Degree: Bachelor of Science in Toxicology
9/2003-7/2005	**Biological-technical assistant** „Die Schule“, Berufsbildende Schule, Osnabrück

School education:

1994-2003	**Gymnasium Dionysianum, Rheine, Germany**

XIII. Declaration

I hereby declare that all information in this document has been obtained and presented in accordance with academic rules and ethical conduct. I also declare that, as required by these rules and conduct, I have fully cited and referenced all material and results that are not original to this work.

_____

Aachen, 2019/02/26

XIV. Author contributions

Rübsam K*, **Weber L***, Jakob F, and Schwaneberg U (2018). "Directed evolution of polypropylene and polystyrene binding peptides." Biotechnol Bioeng 115(2): 321-330.

The manuscript has been published by Dr. Kristin Rübsam and Lina Apitius with a shared first authorship (*). The developed PeP*evo* protocol for a directed evolution of anchor peptides was established in cooperation. Lina Apitius performed the directed evolution campaign of Tachystatin A2 towards improved PS binding in presence of LAS, whereas the directed evolution campaign of LCI towards improved PP binding in presence of Triton-X100 was performed by Dr. Kristin Rübsam. Both contributed equally to the evaluation of the establishment of the protocol, manuscript preparation, and writing.

Aachen, 2019/02/26

_____

Lina Apitius

_____

Dr. Kristin Rübsam

_____

Dr. Felix Jakob

_____

Prof. Dr. Ulrich Schwaneberg

Islam S*, **Apitius L***, Jakob F and Schwaneberg U (2019). "Targeting microplastic particles in the void of diluted suspensions." Environment International 123: 428-435.

The manuscript has been published by Shohana Islam and Lina Apitius with a shared first authorship. The technology of enzymes (cutinases) fused to anchor peptides for enhanced microplastic degradation was jointly developed in a collaborative effort. Lina Apitius contributed to the binding tests of anchor peptides on surfaces. Shohana Islam contributed to the generation of enzyme and enzyme-anchor fusion constructs. Both contributed equally to the evaluation of the microplastic degradation performance, manuscript preparation, and writing. A detailed chapter is implemented in Shohana Islam´s PhD thesis and Lina Apitius will in her thesis only include a short description. Parts of this chapter were submitted by the authors to the journal of RSC Chemical Science.

Aachen, 2019/02/26

_____

Lina Apitius

_____

Shohana Islam

_____

Dr. Felix Jakob

_____

Prof. Dr. Ulrich Schwaneberg

XV. References

Allabashi, R., M. Arkas, G. Hörmann and D. Tsiourvas (2007). "Removal of some organic pollutants in water employing ceramic membranes impregnated with cross-linked silylated dendritic and cyclodextrin polymers." Water Research **41**(2): 476-486.

Alves, P., S. Pinto, J.-P. Kaiser, A. Bruinink, H. C. de Sousa and M. H. Gil (2011). "Surface grafting of a thermoplastic polyurethane with methacrylic acid by previous plasma surface activation and by ultraviolet irradiation to reduce cell adhesion." Colloids and Surfaces B: Biointerfaces **82**(2): 371-377.

Arai, R., H. Ueda, A. Kitayama, N. Kamiya and T. Nagamune (2001). "Design of the linkers which effectively separate domains of a bifunctional fusion protein." Protein Engineering **14**(8): 529-532.

Arnold, F. H. (1998). "Design by Directed Evolution." Accounts of Chemical Research **31**(3): 125-131.

Asatekin, A., M. C. Barr, S. H. Baxamusa, K. K. S. Lau, W. Tenhaeff, J. Xu and K. K. Gleason (2010). "Designing polymer surfaces via vapor deposition." Materials Today **13**(5): 26-33.

Atrah, H. I. (1994). "Fibrin glue." BMJ : British Medical Journal **308**(6934): 933-934.

Auta, H. S., C. U. Emenike and S. H. Fauziah (2017). "Screening of Bacillus strains isolated from mangrove ecosystems in Peninsular Malaysia for microplastic degradation." Environmental Pollution **231**(Pt 2): 1552-1559.

Ayyub, O. B., J. W. Sekowski, T.-I. Yang, X. Zhang, R. M. Briber and P. Kofinas (2011). "Color changing block copolymer films for chemical sensing of simple sugars." Biosensors and Bioelectronics **28**(1): 349-354.

Bacakova, M., J. Musilkova, T. Riedel, D. Stranska, E. Brynda, M. Zaloudkova and L. Bacakova (2016). "The potential applications of fibrin-coated electrospun polylactide nanofibers in skin tissue engineering." International Journal of Nanomedicine **11**: 771-789.

Bailey, R. J., R. Geurts, D. J. Stokes, F. de Jong and A. H. Barber (2013). "Evaluating focused ion beam induced damage in soft materials." Micron **50**: 51-56.

Balaji, A., S. K. Jaganathan, M. V. Vellayappan, A. A. John, A. P. Subramanian, M. SelvaKumar, H. Mohandas, S. R. M and E. Supriyanto (2015). "Prospects of common biomolecules as coating substances for polymeric biomaterials." RSC Advances **5**(85): 69660-69679.

Barnes, D. K. A., F. Galgani, R. C. Thompson and M. Barlaz (2009). "Accumulation and fragmentation of plastic debris in global environments." Philosophical Transactions of the Royal Society B: Biological Sciences **364**(1526): 1985-1998.

Bechinger, B. (2001). "Membrane insertion and orientation of polyalanine peptides: a (15)N solid-state NMR spectroscopy investigation." Biophysical Journal **81**(4): 2251-2256.

Bechinger, B. and S. U. Gorr (2017). "Antimicrobial Peptides: Mechanisms of Action and Resistance." Journal of Dental Research **96**(3): 254-260.

Becker, S., A. Michalczyk, S. Wilhelm, K. E. Jaeger and H. Kolmar (2007). "Ultrahigh-throughput screening to identify E. coli cells expressing functionally active enzymes on their surface." Chembiochem **8**(8): 943-949.

Becker, S., S. Theile, N. Heppeler, A. Michalczyk, A. Wentzel, S. Wilhelm, K. E. Jaeger and H. Kolmar (2005). "A generic system for the Escherichia coli cell-surface display of lipolytic enzymes." FEBS Letters **579**(5): 1177-1182.

Beintema, J. J. (1994). "Structural features of plant chitinases and chitin-binding proteins." FEBS Letters **350**(2-3): 159-163.

Benatuil, L., J. M. Perez, J. Belk and C. M. Hsieh (2010). "An improved yeast transformation method for the generation of very large human antibody libraries." Protein Engineering, Design and Selection **23**(4): 155-159.

Bidlingmaier, S., Y. Su and B. Liu (2015). Combining Phage and Yeast Cell Surface Antibody Display to Identify Novel Cell Type-Selective Internalizing Human Monoclonal Antibodies. Yeast Surface Display: Methods, Protocols, and Applications. B. Liu. New York, NY, Springer New York**:** 51-63.

Blanusa, M., A. Schenk, H. Sadeghi, J. Marienhagen and U. Schwaneberg (2010). "Phosphorothioate-based ligase-independent gene cloning (PLICing): An enzyme-free and sequence-independent cloning method." Analytical Biochemistry **406**(2): 141-146.

Boder, E. T., M. Raeeszadeh-Sarmazdeh and J. V. Price (2012). "Engineering antibodies by yeast display." Archives of Biochemistry and Biophysics **526**(2): 99-106.

Boder, E. T. and K. D. Wittrup (1997). "Yeast surface display for screening combinatorial polypeptide libraries." Nature Biotechnology **15**(6): 553-557.

Boerger, C. M., G. L. Lattin, S. L. Moore and C. J. Moore (2010). "Plastic ingestion by planktivorous fishes in the North Pacific Central Gyre." Marine Pollution Bulletin **60**(12): 2275-2278.

Bolam, D. N., A. Ciruela, S. McQueen-Mason, P. Simpson, M. P. Williamson, J. E. Rixon, A. Boraston, G. P. Hazlewood and H. J. Gilbert (1998). "Pseudomonas cellulose-binding domains mediate their effects by increasing enzyme substrate proximity." Biochemical Journal **331 (Pt 3)**: 775-781.

Boulares-Pender, A., A. Prager-Duschke, C. Elsner and M. R. Buchmeiser (2009). "Surface-functionalization of plasma-treated polystyrene by hyperbranched polymers and use in biological applications." Journal of Applied Polymer Science **112**(5): 2701-2709.

Bouwmeester, H., P. C. Hollman and R. J. Peters (2015). "Potential Health Impact of Environmentally Released Micro- and Nanoplastics in the Human Food

Production Chain: Experiences from Nanotoxicology." Environmental Science & Technology **49**(15): 8932-8947.

Bowley, D. R., A. F. Labrijn, M. B. Zwick and D. R. Burton (2007). "Antigen selection from an HIV-1 immune antibody library displayed on yeast yields many novel antibodies compared to selection from the same library displayed on phage." Protein Engineering, Design and Selection **20**(2): 81-90.

Boyer, C., A. Granville, P. Davis Thomas and V. Bulmus (2009). "Modification of RAFT-polymers via thiol-ene reactions: A general route to functional polymers and new architectures." Journal of Polymer Science Part A: Polymer Chemistry **47**(15): 3773-3794.

Brand, G. D., J. R. Leite, L. P. Silva, S. Albuquerque, M. V. Prates, R. B. Azevedo, V. Carregaro, J. S. Silva, V. C. Sa, R. A. Brandao and C. Bloch, Jr. (2002). "Dermaseptins from Phyllomedusa oreades and Phyllomedusa distincta. Anti-Trypanosoma cruzi activity without cytotoxicity to mammalian cells." Journal of Biological Chemistry **277**(51): 49332-49340.

Brogden, K. A. (2005). "Antimicrobial peptides: pore formers or metabolic inhibitors in bacteria?" Nature Reviews Microbiology **3**(3): 238-250.

Browne, M. A., P. Crump, S. J. Niven, E. Teuten, A. Tonkin, T. Galloway and R. Thompson (2011). "Accumulation of Microplastic on Shorelines Woldwide: Sources and Sinks." Environmental Science & Technology **45**(21): 9175-9179.

Bulet, P., R. Stocklin and L. Menin (2004). "Anti-microbial peptides: from invertebrates to vertebrates." Immunological Reviews **198**: 169-184.

Cacciari, I., P. Quatrini, G. Zirletta, E. Mincione, V. Vinciguerra, P. Lupattelli and G. Giovannozzi Sermanni (1993). "Isotactic polypropylene biodegradation by a microbial community: physicochemical characterization of metabolites produced." Applied and Environmental Microbiology **59**(11): 3695-3700.

Cadwell, R. C. and G. F. Joyce (1992). "Randomization of genes by PCR mutagenesis." PCR methods and applications **2**(1): 28-33.

Care, A., P. L. Bergquist and A. Sunna (2015). "Solid-binding peptides: smart tools for nanobiotechnology." Trends in Biotechnology **33**(5): 259-268.

Carley James, F. and P. T. Kitze (1980). "Corona-discharge treatment of polymeric films, II: Chemical studies." Polymer Engineering & Science **20**(5): 330-338.

Cetinel, S., W. Z. Shen, M. Aminpour, P. Bhomkar, F. Wang, E. R. Borujeny, K. Sharma, N. Nayebi and C. Montemagno (2018). "Biomining of MoS2 with Peptide-based Smart Biomaterials." Scientific Reports **8**(1): 3374.

Chakraborty, T., I. Chakraborty and S. Ghosh (2011). "The methods of determination of critical micellar concentrations of the amphiphilic systems in aqueous medium." Arabian Journal of Chemistry **4**(3): 265-270.

Chan, C.-M. (1999). Surface treatment of polypropylene by corona discharge and flame. Polypropylene: An A-Z reference. J. Karger-Kocsis. Dordrecht, Springer Netherlands**:** 800-805.

Chan, C. M., T. M. Ko and H. Hiraoka (1996). "Polymer surface modification by plasmas and photons." Surface Science Reports **24**(1-2): 3-54.

Chaudhury, M. K. (1995). "Self-assembled monolayers on polymer surfaces." Biosensors and Bioelectronics **10**(9): 785-788.

Chen, W., T. C. Habraken, W. E. Hennink and R. J. Kok (2015). "Polymer-Free Drug-Eluting Stents: An Overview of Coating Strategies and Comparison with Polymer-Coated Drug-Eluting Stents." Bioconjugate Chemistry **26**(7): 1277-1288.

Chen, W. and T. J. McCarthy (1998). "Chemical Surface Modification of Poly(ethylene terephthalate)." Macromolecules **31**(11): 3648-3655.

Chen, X., J. Li, H. Sun, S. Li, T. Chen, G. Liu and P. Dyson (2017). "High-level heterologous production and Functional Secretion by recombinant Pichia pastoris of the shortest proline-rich antibacterial honeybee peptide Apidaecin." Scientific Reports **7**(1): 14543.

Cheng, F., L. Zhu and U. Schwaneberg (2015). "Directed evolution 2.0: improving and deciphering enzyme properties." Chemical Communications **51**(48): 9760-9772.

Chiralt, A., C. González-Martínez, M. Vargas and L. Atarés (2018). 18 - Edible films and coatings from proteins. Proteins in Food Processing (Second Edition). R. Y. Yada, Woodhead Publishing**:** 477-500.

Cho, D.-W., J.-S. Lee, J. Jang, J. W. Jung, J. H. Park and F. Pati (2015). Stereolithography-based 3D printing. Organ Printing, Morgan & Claypool Publishers**:** 2-1-2-6.

Cho, G. S. and J. W. Szostak (2006). "Directed Evolution of ATP Binding Proteins from a Zinc Finger Domain by Using mRNA Display." Chemistry & Biology **13**(2): 139-147.

Choi, H., N. Rangarajan and J. C. Weisshaar (2016). "Lights, Camera, Action! Antimicrobial Peptide Mechanisms Imaged in Space and Time." Trends in Microbiology **24**(2): 111-122.

Cirino, P. C., K. M. Mayer and D. Umeno (2003). "Generating mutant libraries using error-prone PCR." Methods in Molecular Biology **231**: 3-9.

Clauser, J., K. Gester, U. Steinseifer and S. J. Sonntag (2016). 10 - Regulating blood cell adhesion via surface modification of polyurethanes. Advances in Polyurethane Biomaterials. S. L. Cooper and J. Guan, Woodhead Publishing**:** 287-318.

Cormack, B. P., R. H. Valdivia and S. Falkow (1996). "FACS-optimized mutants of the green fluorescent protein (GFP)." Gene **173**(1): 33-38.

Cotten, S. W., J. Zou, R. Wang, B.-c. Huang and R. Liu (2012). "mRNA Display Based Selections Using Synthetic Peptide and Natural Protein Libraries." Methods in molecular biology (Clifton, N.J.) **805**: 287-297.

Coulthard, P., M. Esposito, H. V. Worthington, M. van der Elst, O. J. van Waes and J. Darcey (2010). "Tissue adhesives for closure of surgical incisions." Cochrane Database Syst Rev(5): Cd004287.

Croll, T. I., A. J. O'Connor, G. W. Stevens and J. J. Cooper-White (2004). "Controllable Surface Modification of Poly(lactic-co-glycolic acid) (PLGA) by Hydrolysis or

Aminolysis I: Physical, Chemical, and Theoretical Aspects." Biomacromolecules **5**(2): 463-473.

Database, N. C. f. B. I. P. C. "CID=441374." Retrieved June 19, 2018, from https://pubchem.ncbi.nlm.nih.gov/compound/441374.

de Stephanis, R., J. Gimenez, E. Carpinelli, C. Gutierrez-Exposito and A. Canadas (2013). "As main meal for sperm whales: plastics debris." Mar Pollut Bull **69**(1-2): 206-214.

Dennig, A., A. V. Shivange, J. Marienhagen and U. Schwaneberg (2011). "OmniChange: the sequence independent method for simultaneous site-saturation of five codons." PLoS One **6**(10): e26222.

Desmet, T., R. Morent, N. De Geyter, C. Leys, E. Schacht and P. Dubruel (2009). "Nonthermal plasma technology as a versatile strategy for polymeric biomaterials surface modification: a review." Biomacromolecules **10**(9): 2351-2378.

Ederth, T., T. Ekblad, M. E. Pettitt, S. L. Conlan, C.-X. Du, M. E. Callow, J. A. Callow, R. Mutton, A. S. Clare, F. D'Souza, G. Donnelly, A. Bruin, P. R. Willemsen, X. J. Su, S. Wang, Q. Zhao, M. Hederos, P. Konradsson and B. Liedberg (2011). "Resistance of Galactoside-Terminated Alkanethiol Self-Assembled Monolayers to Marine Fouling Organisms." ACS Applied Materials & Interfaces **3**(10): 3890-3901.

Ensari, Y., G. V. Dhoke, M. D. Davari, A. J. Ruff and U. Schwaneberg (2018). "A Comparative Reengineering Study of cpADH5 through Iterative and Simultaneous Multisite Saturation Mutagenesis." Chembiochem.

Eriksen, M., L. C. M. Lebreton, H. S. Carson, M. Thiel, C. J. Moore, J. C. Borerro, F. Galgani, P. G. Ryan and J. Reisser (2014). "Plastic Pollution in the World's Oceans: More than 5 Trillion Plastic Pieces Weighing over 250,000 Tons Afloat at Sea." PLOS ONE **9**(12): e111913.

Fabbri, P. and M. Messori (2017). 5 - Surface Modification of Polymers: Chemical, Physical, and Biological Routes. Modification of Polymer Properties. C. F. Jasso-Gastinel and J. M. Kenny, William Andrew Publishing**:** 109-130.

Fan, L., J. Sun, M. Zhou, J. Zhou, X. Lao, H. Zheng and H. Xu (2016). "DRAMP: a comprehensive data repository of antimicrobial peptides." Scientific Reports **6**: 24482.

Farris, S., S. Pozzoli, P. Biagioni, L. Duó, S. Mancinelli and L. Piergiovanni (2010). "The fundamentals of flame treatment for the surface activation of polyolefin polymers – A review." Polymer **51**(16): 3591-3605.

Fehlbaum, P., P. Bulet, S. Chernysh, J. P. Briand, J. P. Roussel, L. Letellier, C. Hetru and J. A. Hoffmann (1996). "Structure-activity analysis of thanatin, a 21-residue inducible insect defense peptide with sequence homology to frog skin antimicrobial peptides." Proc Natl Acad Sci U S A **93**(3): 1221-1225.

Frauenkron-Machedjou, V. J., A. Fulton, J. Zhao, L. Weber, K.-E. Jaeger, U. Schwaneberg and L. Zhu (2018). "Exploring the full natural diversity of single amino acid

exchange reveals that 40–60% of BSLA positions improve organic solvents resistance." Bioresources and Bioprocessing **5**(1): 2.

Galan, A., L. Comor, A. Horvatic, J. Kules, N. Guillemin, V. Mrljak and M. Bhide (2016). "Library-based display technologies: where do we stand?" Molecular BioSystems **12**(8): 2342-2358.

Geyer, R., J. R. Jambeck and K. L. Law (2017). "Production, use, and fate of all plastics ever made." Science Advances **3**(7).

Glassman, I. and R. A. Yetter (2008). Chapter 4 - Flame Phenomena in Premixed Combustible Gases. Combustion (Fourth Edition). I. Glassman and R. A. Yetter. Burlington, Academic Press**:** 147-260.

Gong, W., J. Wang, Z. Chen, B. Xia and G. Lu (2011). "Solution structure of LCI, a novel antimicrobial peptide from Bacillus subtilis." Biochemistry **50**(18): 3621-3627.

Grima, S., V. Bellon-Maurel, P. Feuilloley and F. Silvestre (2000). "Aerobic Biodegradation of Polymers in Solid-State Conditions: A Review of Environmental and Physicochemical Parameter Settings in Laboratory Simulations." Journal of Polymers and the Environment **8**(4): 183-195.

Grimm, A. R., D. F. Sauer, T. Polen, L. Zhu, T. Hayashi, J. Okuda and U. Schwaneberg (2018). "A Whole Cell E. coli Display Platform for Artificial Metalloenzymes: Poly(phenylacetylene) Production with a Rhodium–Nitrobindin Metalloprotein." ACS Catalysis **8**(3): 2611-2614.

Guven, G., R. Prodanovic and U. Schwaneberg (2010). "Protein Engineering - An Option for Enzymatic Biofuel Cell Design." Electroanalysis **22**(7-8): 765-775.

Ha, N.-Y., H. M. Shin, P. Sharma, H. A. Cho, C.-K. Min, H.-i. Kim, N. T. H. Yen, J.-S. Kang, I.-S. Kim, M.-S. Choi, Y. K. Kim and N.-H. Cho (2016). "Generation of protective immunity against Orientia tsutsugamushi infection by immunization with a zinc oxide nanoparticle combined with ScaA antigen." Journal of Nanobiotechnology **14**(1): 76.

Han, Z., Y. Wang and X. Duan (2017). "Biofunctional polyelectrolytes assembling on biosensors – A versatile surface coating method for protein detections." Analytica Chimica Acta **964**: 170-177.

Henderson, I. R., F. Navarro-Garcia, M. Desvaux, R. C. Fernandez and D. Ala'Aldeen (2004). "Type V Protein Secretion Pathway: the Autotransporter Story." Microbiology and Molecular Biology Reviews **68**(4): 692-744.

Hernandez, K. and R. Fernandez-Lafuente (2011). "Control of protein immobilization: Coupling immobilization and site-directed mutagenesis to improve biocatalyst or biosensor performance." Enzyme Microb Tech **48**(2): 107-122.

Ho, B. T., T. K. Roberts and S. Lucas (2018). "An overview on biodegradation of polystyrene and modified polystyrene: the microbial approach." Crit Rev Biotechnol **38**(2): 308-320.

Hopewell, J., R. Dvorak and E. Kosior (2009). "Plastics recycling: challenges and opportunities." Philosophical Transactions of the Royal Society B: Biological Sciences **364**(1526): 2115-2126.

Hopewell, J., R. Dvorak and E. Kosior (2009). "Plastics recycling: challenges and opportunities." Philosophical transactions of the Royal Society of London. Series B, Biological sciences **364**(1526): 2115-2126.

Howard, G. T. (2002). "Biodegradation of polyurethane: a review." International Biodeterioration & Biodegradation **49**(4): 245-252.

Imanaka, H., D. Yamadzumi, K. Yanagita, N. Ishida, K. Nakanishi and K. Imamura (2016). "The use of a proteinaceous “cushion” with a polystyrene-binding peptide tag to control the orientation and function of a target peptide adsorbed to a hydrophilic polystyrene surface." Biotechnology Progress **32**(2): 527-534.

Ivar do Sul, J. A. and M. F. Costa (2014). "The present and future of microplastic pollution in the marine environment." Environ Pollut **185**: 352-364.

Jaganathan, S. K., A. Balaji, M. V. Vellayappan, A. P. Subramanian, A. A. John, M. K. Asokan and E. Supriyanto (2015). "Review: Radiation-induced surface modification of polymers for biomaterial application." Journal of Materials Science **50**(5): 2007-2018.

Jakob, F., C. Lehmann, R. Martinez and U. Schwaneberg (2013). "Increasing protein production by directed vector backbone evolution." AMB Express **3**(39): 1-9.

Jang, E. J., I. H. Bae, D. S. Park, S. Y. Lee, K. S. Lim, J. K. Park, J. W. Shim, D. S. Sim and M. H. Jeong (2015). "Effect of a novel peptide, WKYMVm- and sirolimus-coated stent on re-endothelialization and anti-restenosis." J Mater Sci Mater Med **26**(10): 251.

Jaradat, D. s. M. M. (2018). "Thirteen decades of peptide synthesis: key developments in solid phase peptide synthesis and amide bond formation utilized in peptide ligation." Amino Acids **50**(1): 39-68.

John, T., A. Rajpurkar, G. Smith, M. Fairfax and J. Triest (2007). "Antibiotic pretreatment of hydrogel ureteral stent." J Endourol **21**(10): 1211-1216.

Jonkheijm, P., D. Weinrich, H. Schroder, C. M. Niemeyer and H. Waldmann (2008). "Chemical Strategies for Generating Protein Biochips." Angew Chem Int Edit **47**(50): 9618-9647.

Jordan, A. M., V. Viswanath, S.-E. Kim, J. K. Pokorski and L. T. J. Korley (2016). "Processing and surface modification of polymer nanofibers for biological scaffolds: a review." Journal of Materials Chemistry B **4**(36): 5958-5974.

Jose, J., D. Betscheider and D. Zangen (2005). "Bacterial surface display library screening by target enzyme labeling: Identification of new human cathepsin G inhibitors." Anal Biochem **346**(2): 258-267.

Kapust, R. B. and D. S. Waugh (2000). "Controlled intracellular processing of fusion proteins by TEV protease." Protein Expr Purif **19**(2): 312-318.

Kasuya, K., T. Ohura, K. Masuda and Y. Doi (1999). "Substrate and binding specificities of bacterial polyhydroxybutyrate depolymerases." International journal of biological macromolecules **24**(4): 329-336.

Keane, P. F., M. C. Bonner, S. R. Johnston, A. Zafar and S. P. Gorman (1994). "Characterization of biofilm and encrustation on ureteric stents in vivo." Br J Urol **73**(6): 687-691.

Khosa, S., R. Scholz, C. Schwarz, M. Trilling, H. Hengel, K. E. Jaeger, S. H. J. Smits and L. Schmitt (2018). "An A/U-Rich Enhancer Region Is Required for High-Level Protein Secretion through the HlyA Type I Secretion System." Appl Environ Microbiol **84**(1).

Kim, J.-H., M. S. Kang, M. Eltohamy, T.-H. Kim and H.-W. Kim (2016). "Dynamic Mechanical and Nanofibrous Topological Combinatory Cues Designed for Periodontal Ligament Engineering." PLoS ONE **11**(3): e0149967.

Klermund, L., S. T. Poschenrieder and K. Castiglione (2016). "Simple surface functionalization of polymersomes using non-antibacterial peptide anchors." J Nanobiotechnol **14**(48): 1-12.

Kloskowski, A., M. Pilarczyk, W. Chrzanowski and J. Namieśnik (2010). "Sol-Gel Technique—A Versatile Tool for Adsorbent Preparation." Critical Reviews in Analytical Chemistry **40**(3): 172-186.

Ko, R., P. A. Cadieux, J. L. Dalsin, B. P. Lee, C. N. Elwood and H. Razvi (2008). "First prize: Novel uropathogen-resistant coatings inspired by marine mussels." J Endourol **22**(6): 1153-1160.

Konning, D. and H. Kolmar (2018). "Beyond antibody engineering: directed evolution of alternative binding scaffolds and enzymes using yeast surface display." Microb Cell Fact **17**(1): 32.

Kord Forooshani, P. and B. P. Lee (2017). "Recent approaches in designing bioadhesive materials inspired by mussel adhesive protein." J Polym Sci A Polym Chem **55**(1): 9-33.

Korfer, G., C. Pitzler, L. Vojcic, R. Martinez and U. Schwaneberg (2016). "In vitro flow cytometry-based screening platform for cellulase engineering." Sci Rep **6**(26128).

Kumada, Y., D. Kuroki, H. Yasui, T. Ohse and M. Kishimoto (2010). "Characterization of polystyrene-binding peptides (PS-tags) for site-specific immobilization of proteins." J Biosci Bioeng **109**(6): 583-587.

Kumada, Y., Y. Tokunaga, H. Imanaka, K. Imamura, T. Sakiyama, S. Katoh and K. Nakanishi (2006). "Screening and characterization of affinity peptide tags specific to polystyrene supports for the orientated immobilization of proteins." Biotechnol Prog **22**(2): 401-405.

Kunkel, T. A. (1985). "Rapid and efficient site-specific mutagenesis without phenotypic selection." Proc Natl Acad Sci U S A **82**(2): 488-492.

Kwon, B. G., K. Saido, K. Koizumi, H. Sato, N. Ogawa, S. Y. Chung, T. Kusui, Y. Kodera and K. Kogure (2014). "Regional distribution of styrene analogues generated from

polystyrene degradation along the coastlines of the North-East Pacific Ocean and Hawaii." Environ Pollut **188**: 45-49.

Kyle, S., K. A. R. James and M. J. McPherson (2012). "Recombinant production of the therapeutic peptide lunasin." Microbial Cell Factories **11**: 28-28.

Labet, M. and W. Thielemans (2009). "Synthesis of polycaprolactone: a review." Chem Soc Rev **38**(12): 3484-3504.

Laemmli, U. K. (1970). "Cleavage of structural proteins during the assembly of the head of bacteriophage T4." Nature **227**(5259): 680-685.

Laemmli, U. K. (1970). "Cleavage of Structural Proteins during the Assembly of the Head of Bacteriophage T4." Nature **227**: 680.

Lee, S. Y., J. H. Choi and Z. Xu (2003). "Microbial cell-surface display." Trends in Biotechnology **21**(1): 45-52.

Liang Alvin, A. W., M. Tanaka and M. Okochi (2017). "Characterization of particulate matter binding peptides screened from phage display." Journal of Bioscience and Bioengineering **123**(5): 621-624.

Lin, J. J., P. P. Ghoroghchian, Y. Zhang and D. A. Hammer (2006). "Adhesion of Antibody-Functionalized Polymersomes." Langmuir **22**(9): 3975-3979.

Linder, M. and T. T. Teeri (1997). "The roles and function of cellulose-binding domains." Journal of Biotechnology **57**(1): 15-28.

Liu, Z., S. Ma, S. Duan, D. Xuliang, Y. Sun, X. Zhang, X. Xu, B. Guan, C. Wang, M. Hu, X. Qi, X. Zhang and P. Gao (2016). "Modification of Titanium Substrates with Chimeric Peptides Comprising Antimicrobial and Titanium-Binding Motifs Connected by Linkers To Inhibit Biofilm Formation." ACS Appl Mater Interfaces **8**(8): 5124-5136.

Lo, K. H., M. C. Chen, R. M. Ho and H. W. Sung (2009). "Pore-filling nanoporous templates from degradable block copolymers for nanoscale drug delivery." ACS Nano **3**(9): 2660-2666.

Lulsdorf, N., C. Pitzler, M. Biggel, R. Martinez, L. Vojcic and U. Schwaneberg (2015). "A flow cytometer-based whole cell screening toolbox for directed hydrolase evolution through fluorescent hydrogels." Chem Commun (Camb) **51**(41): 8679-8682.

Lutz, S. (2010). "Beyond directed evolution - semi-rational protein engineering and design." Current opinion in biotechnology **21**(6): 734-743.

MacDonald, C., R. Morrow, A. S. Weiss and M. M. M. Bilek (2008). "Covalent attachment of functional protein to polymer surfaces: a novel one-step dry process." Journal of the Royal Society Interface **5**(23): 663-669.

Mäkelä, M. R., N. Donofrio and R. P. de Vries (2014). "Plant biomass degradation by fungi." Fungal Genetics and Biology **72**: 2-9.

Makhlouf, A. S. H. (2011). 1 - Current and advanced coating technologies for industrial applications. Nanocoatings and Ultra-Thin Films. A. S. H. Makhlouf and I. Tiginyanu, Woodhead Publishing**:** 3-23.

Malanovic, N. and K. Lohner (2016). "Gram-positive bacterial cell envelopes: The impact on the activity of antimicrobial peptides." Biochimica et Biophysica Acta (BBA) - Biomembranes **1858**(5): 936-946.

Marchand, C., K. Krajewski, H.-F. Lee, S. Antony, A. A. Johnson, R. Amin, P. Roller, M. Kvaratskhelia and Y. Pommier (2006). "Covalent binding of the natural antimicrobial peptide indolicidin to DNA abasic sites." Nucleic Acids Research **34**(18): 5157-5165.

Marienhagen, J., A. Dennig and U. Schwaneberg (2012). "Phosphorothioate-based DNA recombination: an enzyme-free method for the combinatorial assembly of multiple DNA fragments." Biotechniques **52**(5).

Matsuno, H., J. Sekine, H. Yajima and T. Serizawa (2008). "Biological selection of peptides for poly(l-lactide) substrates." Langmuir **24**(13): 6399-6403.

Matsuzaki, K., O. Murase, N. Fujii and K. Miyajima (1996). "An antimicrobial peptide, magainin 2, induced rapid flip-flop of phospholipids coupled with pore formation and peptide translocation." Biochemistry **35**(35): 11361-11368.

Mattheakis, L. C., R. R. Bhatt and W. J. Dower (1994). "An in vitro polysome display system for identifying ligands from very large peptide libraries." Proc Natl Acad Sci U S A **91**(19): 9022-9026.

McKeen, L. W. (2014). Handbook of Polymer Applications in Medicine and Medical Devices, Elsevier

Meurer, R. A., S. Kemper, S. Knopp, T. Eichert, F. Jakob, H. E. Goldbach, U. Schwaneberg and A. Pich (2017). "Biofunctional Microgel-Based Fertilizers for Controlled Foliar Delivery of Nutrients to Plants." Angew Chem Int Ed Engl **56**(26): 7380-7386.

Meyers, S. R., D. J. Kenan, X. Khoo and M. W. Grinstaff (2011). "Bioactive stent surface coating that promotes endothelialization while preventing platelet adhesion." Biomacromolecules **12**(3): 533-539.

Milner, S. T. (1991). "Polymer brushes." Science **251**(4996): 905-914.

Minardi, D., R. Ghiselli, O. Cirioni, A. Giacometti, W. Kamysz, F. Orlando, C. Silvestri, G. Parri, E. Kamysz, G. Scalise, V. Saba and M. Giovanni (2007). "The antimicrobial peptide Tachyplesin III coated alone and in combination with intraperitoneal piperacillin-tazobactam prevents ureteral stent Pseudomonas infection in a rat subcutaneous pouch model." Peptides **28**(12): 2293-2298.

Mishra, B. and G. Wang (2012). "Ab Initio Design of Potent Anti-MRSA Peptides Based on Database Filtering Technology." Journal of the American Chemical Society **134**(30): 12426-12429.

Miyazaki, K. (2011). "MEGAWHOP cloning: a method of creating random mutagenesis libraries via megaprimer PCR of whole plasmids." Methods Enzymol **498**: 399-406.

Miyazaki, K. and F. H. Arnold (1999). "Exploring nonnatural evolutionary pathways by saturation mutagenesis: rapid improvement of protein function." J Mol Evol **49**(6): 716-720.

Moens, J. and G. Smets (1957). "Alkaline and acid hydrolysis of polyvinylamides." Journal of Polymer Science **23**(104): 931-948.

Molina-Espeja, P., J. Vina-Gonzalez, B. J. Gomez-Fernandez, J. Martin-Diaz, E. Garcia-Ruiz and M. Alcalde (2016). "Beyond the outer limits of nature by directed evolution." Biotechnol Adv **34**(5): 754-767.

Mor, R. and A. Sivan (2008). "Biofilm formation and partial biodegradation of polystyrene by the actinomycete Rhodococcus ruber." Biodegradation **19**(6): 851-858.

Moritomi, S., T. Watanabe and S. Kanzaki (2010). Polypropylene Compounds for Automoive Applications**:** 1-16.

Morra, M. (2000). "On the molecular basis of fouling resistance." J Biomater Sci Polym Ed **11**(6): 547-569.

Myles, A., D. Haberlin, L. Esteban-Tejeda, M. D. Angione, M. P. Browne, M. K. Hoque, T. K. Doyle, E. M. Scanlan and P. E. Colavita (2018). "Bioinspired Aryldiazonium Carbohydrate Coatings: Reduced Adhesion of Foulants at Polymer and Stainless Steel Surfaces in a Marine Environment." ACS Sustainable Chemistry & Engineering **6**(1): 1141-1151.

Nakajima-Kambe, T., Y. Shigeno-Akutsu, N. Nomura, F. Onuma and T. Nakahara (1999). "Microbial degradation of polyurethane, polyester polyurethanes and polyether polyurethanes." Applied Microbiology and Biotechnology **51**(2): 134-140.

Nguyen, L. T., E. F. Haney and H. J. Vogel (2011). "The expanding scope of antimicrobial peptide structures and their modes of action." Trends Biotechnol **29**(9): 464-472.

Nguyen, P. Q., Z. Botyanszki, P. K. Tay and N. S. Joshi (2014). "Programmable biofilm-based materials from engineered curli nanofibres." Nat Commun **5**: 4945.

Nilsson, B. L., M. B. Soellner and R. T. Raines (2005). "Chemical Synthesis of Proteins." Annual review of biophysics and biomolecular structure **34**: 91-118.

Noor, M., T. Dworeck, A. Schenk, P. Shinde, M. Fioroni and U. Schwaneberg (2012). "Polymersome surface decoration by an EGFP fusion protein employing Cecropin A as peptide "anchor"." J Biotechnol **157**(1): 31-37.

Noren, K. A. and C. J. Noren (2001). "Construction of High-Complexity Combinatorial Phage Display Peptide Libraries." Methods **23**(2): 169-178.

Noronha, C. M., I. Otsuka, C. Bouilhac, C. Rochas, P. L. M. Barreto and R. Borsali (2017). "Self-assembly of maltoheptaose-b-PMMA block copolymer systems: 10nm Resolution in thin film and bulk states." Carbohydrate Polymers **170**: 15-22.

Osaki, T., M. Omotezako, R. Nagayama, M. Hirata, S. Iwanaga, J. Kasahara, J. Hattori, I. Ito, H. Sugiyama and S. Kawabata (1999). "Horseshoe crab hemocyte-derived antimicrobial polypeptides, tachystatins, with sequence similarity to spider neurotoxins." J Biol Chem **274**(37): 26172-26178.

Otzen, D. (2011). "Protein-surfactant interactions: A tale of many states." Bba-Proteins Proteom **1814**(5): 562-591.

Pathak, V. M. and Navneet (2017). "Review on the current status of polymer degradation: a microbial approach." Bioresources and Bioprocessing **4**(1): 15.

Penn, L. S. and H. Wang (1994). "Chemical modification of polymer surfaces: A Review." Polym Adv Technol **5**(12): 809-817.

Peschel, A. and H. G. Sahl (2006). "The co-evolution of host cationic antimicrobial peptides and microbial resistance." Nat Rev Microbiol **4**(7): 529-536.

Pitzler, C., G. Wirtz, L. Vojcic, S. Hiltl, A. Boker, R. Martinez and U. Schwaneberg (2014). "A fluorescent hydrogel-based flow cytometry high-throughput screening platform for hydrolytic enzymes." Chem Biol **21**(12): 1733-1742.

Pitzler, C., G. Wirtz, L. Vojcic, S. Hiltl, A. Böker, R. Martinez and U. Schwaneberg (2014). "A Fluorescent Hydrogel-Based Flow Cytometry High-Throughput Screening Platform for Hydrolytic Enzymes." Chemistry & Biology **21**(12): 1733-1742.

Qiang, X., K. Sun, L. Xing, Y. Xu, H. Wang, Z. Zhou, J. Zhang, F. Zhang, B. Caliskan, M. Wang and Z. Qiu (2017). "Discovery of a polystyrene binding peptide isolated from phage display library and its application in peptide immobilization." Scientific Reports **7**: 2673.

Rasila, T. S., M. I. Pajunen and H. Savilahti (2009). "Critical evaluation of random mutagenesis by error-prone polymerase chain reaction protocols, Escherichia coli mutator strain, and hydroxylamine treatment." Anal Biochem **388**(1): 71-80.

Raynor, J. E., J. R. Capadona, D. M. Collard, T. A. Petrie and A. J. García (2009). "Polymer brushes and self-assembled monolayers: Versatile platforms to control cell adhesion to biomaterials (Review)." Biointerphases **4**(2): FA3-FA16.

Reddy, J. (2017). Recombinant Peptide Synthesis.

Reetz, M. T. and J. D. Carballeira (2007). "Iterative saturation mutagenesis (ISM) for rapid directed evolution of functional enzymes." Nat Protoc **2**(4): 891-903.

Reetz, M. T., J. D. Carballeira, J. Peyralans, H. Hobenreich, A. Maichele and A. Vogel (2006). "Expanding the substrate scope of enzymes: combining mutations obtained by CASTing." Chemistry **12**(23): 6031-6038.

Rokitskaya, T. I., N. I. Kolodkin, E. A. Kotova and Y. N. Antonenko (2011). "Indolicidin action on membrane permeability: carrier mechanism versus pore formation." Biochim Biophys Acta **1808**(1): 91-97.

Romero, P. A. and F. H. Arnold (2009). "Exploring protein fitness landscapes by directed evolution." Nat Rev Mol Cell Biol **10**(12): 866-876.

Rosano, G. L. and E. A. Ceccarelli (2014). "Recombinant protein expression in Escherichia coli: advances and challenges." Front Microbiol **5**: 172.

Rowe, L. and G. T. Howard (2002). "Growth of Bacillus subtilis on polyurethane and the purification and characterization of a polyurethanase-lipase enzyme." International Biodeterioration & Biodegradation **50**(1): 33-40.

Ruan, C.-M., T. Bayer, S. Meth and C. N. Sukenik (2002). "Creation and characterization of n-alkylthiol and n-alkylamine self-assembled monolayers on 316L stainless steel." Thin Solid Films **419**(1): 95-104.

Rübsam, K., D. M. Davari, F. Jakob and U. Schwaneberg (2018). "KnowVolution of the Polymer-Binding Peptide LCI for Improved Polypropylene Binding." Polymers **10**(4).

Rübsam, K., B. Stomps, A. Böker, F. Jakob and U. Schwaneberg (2017). "Anchor peptides: A green and versatile method for polypropylene functionalization." Polymer **116**: 124-132.

Rubsam, K., L. Weber, F. Jakob and U. Schwaneberg (2018). "Directed evolution of polypropylene and polystyrene binding peptides." Biotechnol Bioeng **115**(2): 321-330.

Ruckenstein, E. and I. V. Rao (1986). "Effect of solvent on the stability of mixtures of sterically stabilized dispersions and free polymers." Colloids and Surfaces **17**(3): 185-205.

Ruff, A. J., A. Dennig and U. Schwaneberg (2013). "To get what we aim for--progress in diversity generation methods." Febs j **280**(13): 2961-2978.

Salema, V. and L. A. Fernandez (2017). "Escherichia coli surface display for the selection of nanobodies." Microb Biotechnol **10**(6): 1468-1484.

Samuelsson, E., T. Moks, B. Nilsson and M. Uhlen (1994). "Enhanced in vitro refolding of insulin-like growth factor I using a solubilizing fusion partner." Biochemistry **33**(14): 4207-4211.

Sangermano, M., I. Roppolo and M. Messori (2015). "CHAPTER 7 UV-Cured Functional Coatings." Photocured Materials: 121-133.

Sanghvi, A. B., K. P. Miller, A. M. Belcher and C. E. Schmidt (2005). "Biomaterials functionalization using a novel peptide that selectively binds to a conducting polymer." Nat Mater **4**(6): 496-502.

Sani, M. A. and F. Separovic (2016). "How Membrane-Active Peptides Get into Lipid Membranes." Acc Chem Res **49**(6): 1130-1138.

Schagger, H. (2006). "Tricine-SDS-PAGE." Nat Protoc **1**(1): 16-22.

Schmidt-Dannert, C. and F. H. Arnold (1999). "Directed evolution of industrial enzymes." Trends Biotechnol **17**(4): 135-136.

Schmidt, J., R. Wei, T. Oeser, A. L. Dedavid e Silva, D. Breite, A. Schulze and W. Zimmermann (2017). "Degradation of Polyester Polyurethane by Bacterial Polyester Hydrolases." Polymers **9**(2).

Schottner, G. (2001). "Hybrid Sol−Gel-Derived Polymers: Applications of Multifunctional Materials." Chemistry of Materials **13**(10): 3422-3435.

Seenaiah, M., M. Jbara, S. M. Mali and A. Brik (2015). "Convergent versus sequential protein synthesis: the case of ubiquitinated and glycosylated H2B." Angew Chem Int Ed Engl **54**(42): 12374-12378.

Seker, U. O. and H. V. Demir (2011). "Material binding peptides for nanotechnology." Molecules **16**(2): 1426-1451.

Seker, U. O. S., B. Wilson, J. L. Kulp, J. S. Evans, C. Tamerler and M. Sarikaya (2014). "Thermodynamics of Engineered Gold Binding Peptides: Establishing the Structure–Activity Relationships." Biomacromolecules **15**(7): 2369-2377.

Selvakumar, N. and H. C. Barshilia (2012). "Review of physical vapor deposited (PVD) spectrally selective coatings for mid- and high-temperature solar thermal applications." Solar Energy Materials and Solar Cells **98**: 1-23.

Serizawa, T., T. Sawada and H. Matsuno (2007). "Highly specific affinities of short peptides against synthetic polymers." Langmuir **23**(22): 11127-11133.

Serizawa, T., P. Techawanitchai and H. Matsuno (2007). "Isolation of peptides that can recognize syndiotactic polystyrene." Chembiochem **8**(9): 989-993.

Shah, A. A., F. Hasan, A. Hameed and S. Ahmed (2008). "Biological degradation of plastics: a comprehensive review." Biotechnol Adv **26**(3): 246-265.

Shah, A. A., F. Hasan, A. Hameed and S. Ahmed (2008). "Biological degradation of plastics: A comprehensive review." Biotechnology Advances **26**(3): 246-265.

Shai, Y. (1999). "Mechanism of the binding, insertion and destabilization of phospholipid bilayer membranes by alpha-helical antimicrobial and cell non-selective membrane-lytic peptides." Biochim Biophys Acta **1462**(1-2): 55-70.

Sheldon, R. A. and P. C. Pereira (2017). "Biocatalysis engineering: the big picture." Chem Soc Rev **46**(10): 2678-2691.

Sherman, P. and E. van Sebille (2016). "Modeling marine surface microplastic transport to assess optimal removal locations." Environmental Research Letters **11**(1): 014006.

Shikiya, Y., S. Tomita, T. Arakawa and K. Shiraki (2013). "Arginine Inhibits Adsorption of Proteins on Polystyrene Surface." PLOS ONE **8**(8): e70762.

Shivange, A. V., J. Marienhagen, H. Mundhada, A. Schenk and U. Schwaneberg (2009). "Advances in generating functional diversity for directed protein evolution." Curr Opin Chem Biol **13**(1): 19-25.

Shivange, A. V., D. Roccatano and U. Schwaneberg (2016). "Iterative key-residues interrogation of a phytase with thermostability increasing substitutions identified in directed evolution." Appl Microbiol Biotechnol **100**(1): 227-242.

Sim, D. S. and M. H. Jeong (2017). "Development of Novel Drug-Eluting Stents for Acute Myocardial Infarction." Chonnam Med J **53**(3): 187-195.

Smith, G. P. (1985). "Filamentous fusion phage: novel expression vectors that display cloned antigens on the virion surface." Science **228**(4705): 1315-1317.

Smith, G. P. and J. K. Scott (1993). [15] Libraries of peptides and proteins displayed on filamentous phage. Methods in Enzymology, Academic Press. **217:** 228-257.

Soehnlein, O., S. Wantha, S. Simsekyilmaz, Y. Doring, R. T. Megens, S. F. Mause, M. Drechsler, R. Smeets, S. Weinandy, F. Schreiber, T. Gries, S. Jockenhoevel, M. Moller, S. Vijayan, M. A. van Zandvoort, B. Agerberth, C. T. Pham, R. L. Gallo, T. M. Hackeng, E. A. Liehn, A. Zernecke, D. Klee and C. Weber (2011). "Neutrophil-

derived cathelicidin protects from neointimal hyperplasia." Sci Transl Med **3**(103): 103ra198.

Steiner, H., D. Andreu and R. B. Merrifield (1988). "Binding and action of cecropin and cecropin analogues: antibacterial peptides from insects." BBA **939**(2): 260-266.

Steiner, H., D. Hultmark, A. Engstrom, H. Bennich and H. G. Boman (1981). "Sequence and specificity of two antibacterial proteins involved in insect immunity." Nature **292**(5820): 246-248.

Stemmer, W. P. (1994). "Rapid evolution of a protein in vitro by DNA shuffling." Nature **370**(6488): 389-391.

Sun, H. and S. Önneby (2006). "Facile polyester surface functionalization via hydrolysis and cell-recognizing peptide attachment." Polymer International **55**(11): 1336-1340.

Sunde, M., A. H. Y. Kwan, M. D. Templeton, R. E. Beever and J. P. Mackay (2008). "Structural analysis of hydrophobins." Micron **39**(7): 773-784.

Tadros, T. (2013). Critical Micelle Concentration. Encyclopedia of Colloid and Interface Science. T. Tadros. Berlin, Heidelberg, Springer Berlin Heidelberg**:** 209-210.

Tanaka, K., M. Kasahara and H. Usui (2000). "Preparation of ITO electrode on the organic layer by sputtering." Electronics and Communications in Japan (Part II: Electronics) **83**(4): 23-30.

Tashiro, M., R. Tejero, D. E. Zimmerman, B. Celda, B. Nilsson and G. T. Montelione (1997). "High-resolution solution NMR structure of the Z domain of staphylococcal protein A." J Mol Biol **272**(4): 573-590.

Tawfik, D. S. and A. D. Griffiths (1998). "Man-made cell-like compartments for molecular evolution." Nat Biotechnol **16**(7): 652-656.

Tee, K. L. and U. Schwaneberg (2007). "Directed evolution of oxygenases: Screening systems, success stories and challenges." Comb Chem High T Scr **10**(3): 197-217.

Tee, K. L. and U. Schwaneberg (2007). "Directed evolution of oxygenases: screening systems, success stories and challenges." Comb Chem High Throughput Screen **10**(3): 197-217.

Togashi, T., N. Yokoo, M. Umetsu, S. Ohara, T. Naka, S. Takami, H. Abe, I. Kumagai and T. Adschiri (2011). "Material-binding peptide application—ZnO crystal structure control by means of a ZnO-binding peptide." Journal of Bioscience and Bioengineering **111**(2): 140-145.

Tokiwa, Y., P. B. Calabia, U. C. Ugwu and S. Aiba (2009). "Biodegradability of Plastics." International Journal of Molecular Sciences **10**(9).

Ulery, B. D., L. S. Nair and C. T. Laurencin (2011). "Biomedical Applications of Biodegradable Polymers." J Polym Sci B Polym Phys **49**(12): 832-864.

Upton, C. and J. T. Buckley (1995). "A new family of lipolytic enzymes?" Trends Biochem Sci **20**(5): 178-179.

Valo, H. K., P. H. Laaksonen, L. J. Peltonen, M. B. Linder, J. T. Hirvonen and T. J. Laaksonen (2010). "Multifunctional Hydrophobin: Toward Functional Coatings for Drug Nanoparticles." ACS Nano **4**(3): 1750-1758.

van Bloois, E., R. T. Winter, H. Kolmar and M. W. Fraaije (2011). "Decorating microbes: surface display of proteins on Escherichia coli." Trends Biotechnol **29**(2): 79-86.

Vojcic, L., C. Pitzler, G. Korfer, F. Jakob, R. Martinez, K. H. Maurer and U. Schwaneberg (2015). "Advances in protease engineering for laundry detergents." New Biotechnol **32**(6): 629-634.

Wakabayashi, N., Y. Yano, K. Kawano and K. Matsuzaki (2017). "A pH-dependent charge reversal peptide for cancer targeting." Eur Biophys J **46**(2): 121-127.

Wang, G., X. Li and Z. Wang (2016). "APD3: the antimicrobial peptide database as a tool for research and education." Nucleic Acids Research **44**(D1): D1087-D1093.

Wang, W. and B. A. Malcolm (1999). "Two-stage PCR protocol allowing introduction of multiple mutations, deletions and insertions using QuikChange Site-Directed Mutagenesis." Biotechniques **26**(4): 680-682.

Wei, Q., Y. Xu and Y. Wang (2009). 3 - Textile surface functionalization by physical vapor deposition (PVD). Surface Modification of Textiles. Q. Wei, Woodhead Publishing**:** 58-90.

Wei, R., T. Oeser, J. Then, N. Kühn, M. Barth, J. Schmidt and W. Zimmermann (2014). "Functional characterization and structural modeling of synthetic polyester-degrading hydrolases from Thermomonospora curvata." AMB Express **4**: 44-44.

Wei, R. and W. Zimmermann (2017). "Microbial enzymes for the recycling of recalcitrant petroleum-based plastics: how far are we?" Microb Biotechnol **10**(6): 1308-1322.

Wilhelm, S., F. Rosenau, H. Kolmar and K. E. Jaeger (2011). "Autotransporters with GDSL passenger domains: molecular physiology and biotechnological applications." Chembiochem **12**(10): 1476-1485.

Wilhelm, S., J. Tommassen and K. E. Jaeger (1999). "A novel lipolytic enzyme located in the outer membrane of Pseudomonas aeruginosa." J Bacteriol **181**(22): 6977-6986.

Wimley, W. C. (2010). "Describing the Mechanism of Antimicrobial Peptide Action with the Interfacial Activity Model." ACS chemical biology **5**(10): 905-917.

Winter, M., R. Ries, C. Kleiner, D. Bischoff, A. H. Luippold, T. Bretschneider and F. H. Buttner (2018). "Automated MALDI Target Preparation Concept: Providing Ultra-High-Throughput Mass Spectrometry-Based Screening for Drug Discovery." SLAS Technol: 2472630318791981.

Wong, T. S., K. L. Tee, B. Hauer and U. Schwaneberg (2004). "Sequence saturation mutagenesis (SeSaM): a novel method for directed evolution." Nucleic Acids Res **32**(3): e26.

Wong, T. S., D. Zhurina and U. Schwaneberg (2006). "The diversity challenge in directed protein evolution." Comb Chem High Throughput Screen **9**(4): 271-288.

Wu, C.-H., I. J. Liu, R.-M. Lu and H.-C. Wu (2016). "Advancement and applications of peptide phage display technology in biomedical science." Journal of Biomedical Science **23**: 8.

Xu, J., J. He, D. Fan, X. Wang and Y. Yang (2006). "Aminolysis of Polymers with Thiocarbonylthio Termini Prepared by RAFT Polymerization: The Difference between Polystyrene and Polymethacrylates." Macromolecules **39**(25): 8616-8624.

Yamaguchi, S., T. Hong, A. Waring, R. I. Lehrer and M. Hong (2002). "Solid-state NMR investigations of peptide-lipid interaction and orientation of a beta-sheet antimicrobial peptide, protegrin." Biochemistry **41**(31): 9852-9862.

Yaman, N., E. Ozdogan, N. Seventekin and H. Ayhan (2009). "Plasma treatment of polypropylene fabric for improved dyeability with soluble textile dyestuff." Appl Surf Sci **255**(15): 6764-6770.

Yang, J., A. J. Ruff, M. Arlt and U. Schwaneberg (2017). "Casting epPCR (cepPCR): A simple random mutagenesis method to generate high quality mutant libraries." Biotechnol Bioeng **9999**.

Yang, L., T. A. Harroun, T. M. Weiss, L. Ding and H. W. Huang (2001). "Barrel-stave model or toroidal model? A case study on melittin pores." Biophys J **81**(3): 1475-1485.

Yang, L., S. Whiteside, P. A. Cadieux and J. D. Denstedt (2015). "Ureteral stent technology: Drug-eluting stents and stent coatings." Asian Journal of Urology **2**(4): 194-201.

Yim, S. S., J. W. Choi, R. J. Lee, Y. J. Lee, S. H. Lee, S. Y. Kim and K. J. Jeong (2016). "Development of a new platform for secretory production of recombinant proteins in Corynebacterium glutamicum." Biotechnol Bioeng **113**(1): 163-172.

Yoshida, S., K. Hagiwara, T. Hasebe and A. Hotta (2013). "Surface modification of polymers by plasma treatments for the enhancement of biocompatibility and controlled drug release." Surface and Coatings Technology **233**: 99-107.

Yu, S., J. Geng, P. Zhou, J. Wang, X. Chen and J. Hu (2008). "New hydroxyapatite monolithic column for DNA extraction and its application in the purification of Bacillus subtilis crude lysate." J Chromatogr A **1183**(1-2): 29-37.

Zalasiewicz, J., C. N. Waters, J. A. Ivar do Sul, P. L. Corcoran, A. D. Barnosky, A. Cearreta, M. Edgeworth, A. Gałuszka, C. Jeandel, R. Leinfelder, J. R. McNeill, W. Steffen, C. Summerhayes, M. Wagreich, M. Williams, A. P. Wolfe and Y. Yonan (2016). "The geological cycle of plastics and their use as a stratigraphic indicator of the Anthropocene." Anthropocene **13**: 4-17.

Zernia, S., R. Frank, R. H. J. Weiße, H. G. Jahnke, K. Bellmann-Sickert, A. Prager, B. Abel, N. Sträter, A. Robitzki and A. G. Beck-Sickinger (2018). "Surface-Binding Peptide Facilitates Electricity-Driven NADPH-Free Cytochrome P450 Catalysis." ChemCatChem **10**(3): 525-530.

Zernia, S., F. Ott, K. Bellmann-Sickert, R. Frank, M. Klenner, H. G. Jahnke, A. Prager, B. Abel, A. Robitzki and A. G. Beck-Sickinger (2016). "Peptide-mediated specific

immobilization of catalytically active cytochrome P450 BM3 variant." Bioconjugate Chem **27**(4): 1090-1097.

Zhang, H., G. Liu, X. Zeng, Y. Wu, C. Yang, L. Mei, Z. Wang and L. Huang (2015). "Fabrication of genistein-loaded biodegradable TPGS-b-PCL nanoparticles for improved therapeutic effects in cervical cancer cells." Int J Nanomedicine **10**: 2461-2473.

Zhang, Y., F. Zheng, T. Yang, W. Zhou, Y. Liu, N. Man, L. Zhang, N. Jin, Q. Dou, Y. Zhang, Z. Li and L. P. Wen (2012). "Tuning the autophagy-inducing activity of lanthanide-based nanocrystals through specific surface-coating peptides." Nat Mater **11**(9): 817-826.

Zhao, H., L. Giver, Z. Shao, J. A. Affholter and F. H. Arnold (1998). "Molecular evolution by staggered extension process (StEP) in vitro recombination." Nat Biotechnol **16**(3): 258-261.

Zhao, J., T. Kardashliev, A. Joelle Ruff, M. Bocola and U. Schwaneberg (2014). "Lessons from diversity of directed evolution experiments by an analysis of 3,000 mutations." Biotechnol Bioeng **111**(12): 2380-2389.

Zhao, Q., W. Xu, L. Xing and Z. Lin (2016). "Recombinant production of medium- to large-sized peptides in Escherichia coli using a cleavable self-aggregating tag." Microbial Cell Factories **15**: 136.

Zheng, Y., E. K. Yanful and A. S. Bassi (2005). "A review of plastic waste biodegradation." Crit Rev Biotechnol **25**(4): 243-250.

Zhu, Y., Z. Mao and C. Gao (2013). "Aminolysis-based surface modification of polyesters for biomedical applications." RSC Advances **3**(8): 2509-2519.

Zou, Z., D. M. Mate, K. Rubsam, F. Jakob and U. Schwaneberg (2018). "Sortase-Mediated High-Throughput Screening Platform for Directed Enzyme Evolution." ACS Comb Sci.

Zuo, R., D. Ornek and T. K. Wood (2005). "Aluminum- and mild steel-binding peptides from phage display." Appl Microbiol Biotechnol **68**(4): 505-509.